CHEMICAL REVIEWS

Review

The Use of Calixarenes in Metal-Based Catalysis

Damien M. Homden, and Carl Redshaw

More About This Article

Additional resources and features associated with this article are available within the HTML version:

- Supporting Information
- Access to high resolution figures
- Links to articles and content related to this article
- Copyright permission to reproduce figures and/or text from this article

View the Full Text HTML

The Use of Calixarenes in Metal-Based Catalysis

Damien M. Homden and Carl Redshaw*

Energy Materials Laboratory, School of Chemical Sciences and Pharmacy, University of East Anglia, Norwich, NR4 7TJ, United Kingdom

Contents

1. Introduction

The condensation of formaldehyde with *p*-alkylphenols under alkaline conditions, a reaction dating back to the days of Baeyer and Zinke, affords initially linear polyphenols, which, once a certain temperature is achieved, yield cyclic oligomeric phenolic compounds (Scheme 1).[1,2] One-step, multigram synthetic procedures have now been developed, which by varying either the temperature or amount of base used in the preparation, readily afford the tetrameric, hexameric, and octameric phenolic ring systems, bridged by methylene ($-CH_2-$) spacers.[3] Ring systems with up to 20 phenolic residues are now known, although methods of preparation for these higher members, and for those with an odd number of phenolic residues, are usually low yielding. The smaller members of the family adopt a cone-shaped structure, hence the name calix[*n*]arene coined by Gutsche, from the Greek "calix" meaning vase, where *n* denotes the number of phenolic residues.[4] Such a bowl shape results in the formation of a hydrophobic, electron-rich cavity, which is well-suited to the formation of inclusion complexes, particularly cations.[5] The synthetic methodology has also been adapted to allow for the incorporation of bridging groups other than methylene, such as dimethyleneoxa ($-CH_2OCH_2-$), thia ($-S-$), and aza [$-CH_2N(R)CH_2-$] bridged calixarenes,[6] and these additional donors can provide extra binding sites.

Organic derivatization of calix[*n*]arenes is now a well-established area.[7−11] Much elegant work has been conducted on both the phenolic (lower) rim and the non-phenolic (upper) rim by groups such as those of Shinkai and Ungaro,[8,9] and this class of molecule has now found application in a number of areas, including medical diagnostics, fluorescent probes, phase-transfer agents, separation chemistry (e.g., C_{60} vs C_{70}), and nanochemistry and are showing promise as ion-channel blockers and as anticancer agents.[10] Chemical modification of both rims has also paved the way for numerous calixarene-based anion receptors.[11] Both sulfonato- and acyl-calix[*n*]arenes are emerging as useful building blocks for the construction of supramolecular

* Corresponding author (e-mail, carl.redshaw@uea.ac.uk).

Damien Homden, originally from Wadhurst, East Sussex, received his M.Chem. (Honors, 2004) and Ph.D. (2008, with Carl Redshaw) from the University of East Anglia (Norwich, United Kingdom). Following a stint in a postdoctoral position working under the supervision of Prof. Chris Pickett, also at the University of East Anglia, Norwich, he has begun training as a science teacher.


Carl Redshaw entered university after a promising career with Hull City was cut short by injury. He received his B.Sc. (Honors 1985) and Ph.D. (1989, with John Errington) degrees from Newcastle University. He was a Robert A. Welch Fellow at the University of Texas, Austin (1989−1990), and a postdoctoral fellow with the late Professor Sir G. Wilkinson at Imperial College, London (1990−1992), and at the IRC Durham (1993−1995). He then returned to Imperial College in 1995 with Vernon Gibson. In 1998, he was awarded a Leverhulme Fellowship and moved to the University of East Anglia in 1999, where he was appointed as a lecturer in Inorganic Chemistry and was promoted to Senior Lecturer in 2007. His research interests include calixarene coordination chemistry, main group macrocyclic chemistry, and the use of metal reagents in medicine, particularly in the battle against cancer.

structures, and a number of intruiging molecular capsules have been structurally identified.[12]

In comparison, since the first reports in the mid-1980s, the coordination chemistry of calix[*n*]arenes was initially sluggish; however, in the past decade, research on metallocalixarenes has intensified,[13−21] and numerous new metal-containing structural motifs have now been characterized. The parent calixarenes are able to bind metals in various positions as illustrated in Figure 1, while the introduction of the aforementioned donor linker groups can lead to further bonding at the metal; for example, thia type bridges can bind in a κ^3 mode via sulfur and two oxygen atoms.

This growth in calixarene coordination chemistry has in turn led to an increasing number of reports concerning the use of calix[*n*]arenes as ancillary ligands in the metal-containing components of catalysts in a variety of transformations.[20a] For example, Floriani recognized that for

Scheme 1. Formation and Nomenclature of Calix[*n*]arenes (R = Alkyl)
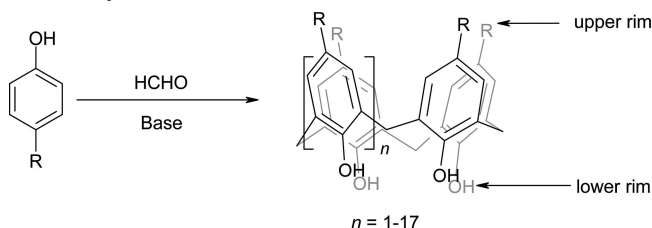
the calix[4]arene ligand system, the four oxygen donors preorganized in a quasi-planar geometry offered an ideal opportunity for modeling oxo surfaces and heterogeneous catalysts.[20b] Chart 1 gives the reader an insight into the variety/distribution of metal-based transformations that have benefited from the addition of a calixarene in one form or another.

The conformational flexibility, presence of cavities, and ability to coordinate simultaneously numerous metal centers are proving extremely good attributes, although it should be emphasized that the bulk of the work carried out to date (and reported herein) has been conducted on the easily prepared, and hence comparatively cheap, calix[4]arene system, which upon metalation tends to retain the cone conformation, binding to only one metal center. This is illustrated in Chart 2, where it is clear that around 75% of the work conducted to date involves the calix[4]arene ligand system and, in particular, the *p-tert*-butyl derivative.

Furthermore, in many of the systems described herein, the catalyst (or metallocalixarene) is formed in situ or the calixarene plays a "tertiary" role, such that the addition of calixarene is beneficial to the outcome of the catalytic process, while not forming an integral part of the catalyst. In this review, we discuss the literature over the last 10 years or so, grouping the results in terms of the position of the metal ("bound" to the calixarene) in the periodic table and with subgroups for the particular catalytic process for which the "metallocalixarene" has been employed. The benefits produced by the use of calixarenes, such as those highlighted in Table 1, are emphasized throughout. Resorcinarene-based catalytic systems,[22] calixarene-containing polymers,[23] nor stoichiometric C−C bond formation reactions[24] are discussed herein.

2. Alkali Metals

2.1. Sodium

Water-soluble calixarenes **1** (Chart 3) have been screened as catalysts in nucleophilic substitutions of alkyl and aryla-
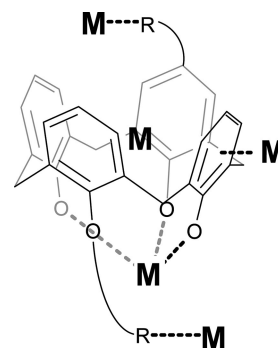
Figure 1. Potential metal binding sites in a calix[4]arene ligand system (R = assorted functionality).[13−21]

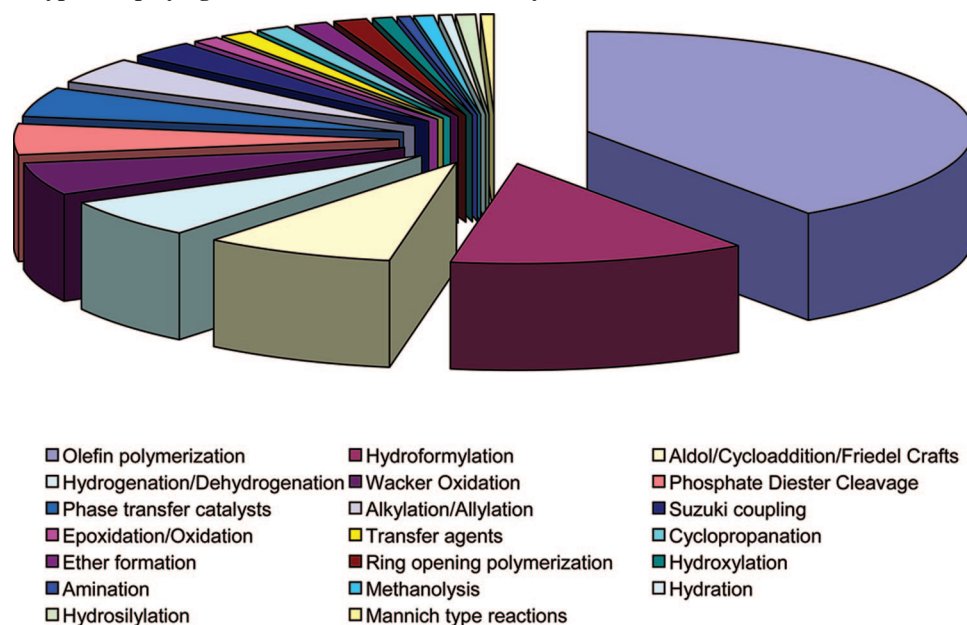**Chart 1. Reaction Types Employing Calixarene-Based Metal Catalysts**

□ Olefin polymerization   ■ Hydroformylation   □ Aldol/Cycloaddition/Friedel Crafts
□ Hydrogenation/Dehydrogenation   ■ Wacker Oxidation   ■ Phosphate Diester Cleavage
■ Phase transfer catalysts   □ Alkylation/Allylation   ■ Suzuki coupling
■ Epoxidation/Oxidation   □ Transfer agents   □ Cyclopropanation
■ Ether formation   ■ Ring opening polymerization   ■ Hydroxylation
■ Amination   ■ Methanolysis   □ Hydration
□ Hydrosilylation   □ Mannich type reactions

Chart 2. Breakdown of Calixarene Types Employed in Metal-Based Catalysis

□ Calix[4]arene
■ Calix[6]arene
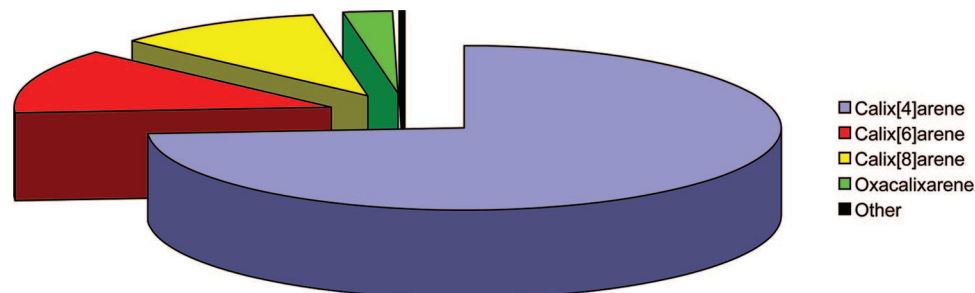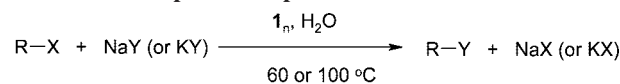□ Calix[8]arene
■ Oxacalixarene
■ Other

Table 1. Advantages Associated with the Use of Calixarene Ligands

available to calixarenes	benefit
easily and cheaply prepared	multigram quantities
readily functionalized	solubility control (including water)
can incorporate chirality	enantio-discrimination
cavity	substrate recognition
multiple binding sites	cooperative effects
can be fixed to solid supports	heterogeneous catalysis

Chart 3. Water-Soluble Trimethylammoniomethyl Calix[n]arene Methyl Ethers, TAC$_n$M (1) and (p-Methoxybenzyl)trimethylammonium Chloride (A)
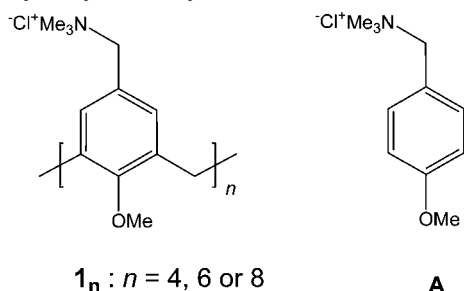
1$_n$: n = 4, 6 or 8   **A**

lkylhalides of the type illustrated in Scheme 2 (see also Table 2), using simple nucleophiles such as NaCN. The beneficial effect of having the calixarene present was clearly evidenced by the results of runs 1 and 5, where the yield of 1-cyanooctane formed increased from 6 to 83%. Use of the calix[6]arene-based ligand set proved to be more efficient than the use of the more established inverse phase-transfer

Scheme 2. Nucleophilic Substitution of Alkyl and Arylalkyl Halides with Simple Nucleophiles in Water

$$R-X \ + \ NaY \ (or \ KY) \xrightarrow[\text{60 or 100 °C}]{\textbf{1}_n, H_2O} R-Y \ + \ NaX \ (or \ KX)$$

R = C$_8$H$_{17}$, PhCH$_2$CH$_2$, Bn, 2-naphthylmethyl
X = Cl, Br, I
Y = CN, SCN, I
n = 4, 6, 8

catalyst β-cyclodextrin (see runs 3, 9, 12, and 19). The comparative efficiency within the calix[n]arene-based series was found to be highly dependent upon the substrate size and/or shape. Typically, no difference was observed for benzyl bromide reactions, whereas for 1-bromooctane and 2-(bromomethyl)napthylene, the activities were found to increase in the order $\textbf{1}_{[4]} < \textbf{1}_{[6]} = \textbf{1}_{[8]}$ and $\textbf{1}_{[4]} \leq \textbf{1}_{[6]} < \textbf{1}_{[8]}$, respectively. Such observations were suggestive of the calix[n]arene cavity acting as an inverse phase-transfer catalyst,[25] and as little as 0.05 mol % of $\textbf{1}_{[6]}$ (run 14) was sufficient to produce the observed yield. Replacement of calixarene by the noncyclic analogue **A** (run 2) produced no acceleration effect.

Such trimethylammoniomethyl-containing ligands **1** (Chart 3) were also shown to catalyze the alkylation of phenylacetone with alkyl halides in a NaOH solution (Scheme 3 and Table 3), with an increase in product yield from negligible to 85%.[26] For n = 4, 6, and 8, all reactions produced superior yields (e.g., run 6) to reactions where the calix[n]arene ligand was absent (run 1) or where β-cyclodextrin was used (run

Table 2. Nucleophilic Substitution of Alkyl and Arylalkyl Halides with Simple Nucleophiles[a]

| run	catalyst	substrate	nucleophile	T (°C)	time (h)	yield[b] (%)
1	none	$C_8H_{17}Br$	NaCN	100	6	6
2	**A**[c]	$C_8H_{17}Br$	NaCN	100	6	3
3	β-CD	$C_8H_{17}Br$	NaCN	100	6	20
4	**1**[4]	$C_8H_{17}Br$	NaCN	100	6	61
5	**1**[6]	$C_8H_{17}Br$	NaCN	100	6	83
6	**1**[8]	$C_8H_{17}Br$	NaCN	100	6	85
7	**1**[6]	$C_8H_{17}I$	NaCN	100	6	91
8	none	$PhCH_2CH_2Br$	NaCN	100	6	23
9	β-CD	$PhCH_2CH_2Br$	NaCN	100	6	45
10	**1**[4]	BnBr	NaCN	100	6	83
11	none	BnBr	NaCN	60	2	1
12	β-CD	BnBr	NaCN	60	2	55
13	**1**[6]	BnBr	NaCN	60	2	85
14	**1**[6][d]	BnBr	NaCN	60	2	72
15	**1**[6]	BnBr	KCN	60	2	88
16	**1**[6]	BnBr	KI	60	2	78
17	**1**[4]	BnCl	NaCN	60	12	67[e]
18	none	2-naphthylCH_2Br	NaCN	60	2	0
19	β-CD	2-naphthylCH_2Br	NaCN	60	2	8
20	**1**[4]	2-naphthylCH_2Br	NaCN	60	2	47
21	**1**[6]	2-naphthylCH_2Br	NaCN	60	2	55
22	**1**[8]	2-naphthylCH_2Br	NaCN	60	2	82

[a] Conditions: catalyst (0.5 mol %), substrate (4.6 mmol), nucleophile (10 mmol), and water (5 mL); stirring speed, 1300 rpm. In the reaction of 2-(bromomethyl)naphthalene, dipropyl ether (1 mL) was used (entries 18–22). [b] On the basis of substrate. Refers to GC yield (entries 1–7 and 11–17) or isolated yield (entries 8–10 and 18–22). [c] Catalyst: 3.0 mol % used. [d] Catalyst: 0.05 mol % used. [e] By-product: benzyl alcohol (8%).

Scheme 3. Alkylation of Phenylacetone with RX [R = $CH_3(CH_2)_7$, $Cl(CH_2)_4$, $Br(CH_2)_4$, $CH_2=CH(CH_2)_3$, o-$C_6H_{11}CH_2$, 4-t-$BuC_6H_4CH_2$, 4-$BrC_6H_4CH_2$, or 2-$C_{10}H_7CH_2$]
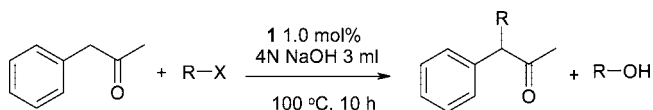
Table 3. C-Alkylation of Phenylacetone Using 1

run	catalyst	R–X	isolated yield (%)	
			ketone	alcohol
1	none	$CH_3(CH_2)_7Br$	trace	trace
2	β-CD[a]	$CH_3(CH_2)_7Br$	14	trace
3	TBAB[b]	$CH_3(CH_2)_7Br$	76 (+trace)[c]	17
4	TBAB[b,c]	$CH_3(CH_2)_7Br$	73 (+5)[d]	8
5	HTPB[e]	$CH_3(CH_2)_7Br$	71 (+8)[d]	2
6	TAC4M	$CH_3(CH_2)_7Br$	86	6
7	TAC4M	$CH_3(CH_2)_7Cl$	12	trace
8	TAC4M	$CH_3(CH_2)_7I$	84	4
9	TAC4M	$Cl(CH_2)_4Br$	65[f]	(9)[g]
10	TAC4M	$Br(CH_2)_4Br$	8 (+63)[h]	(trace)[g]
11	TAC4M	$CH_2=CH(CH_2)_3Br$	75	0
12	TAC4M[i]	o-$C_6H_{11}CH_2Br$	91	0
13	TAC4M[i]	4-t-$BuC_6H_4CH_2Br$	94	trace
14	TAC4M[j]	4-$BrC_8H_4CH_2Br$	92	0
15	TAC4M[j]	2-$C_{10}H_7CH_2Br$	87	0

[a] β-Cyclodextrin. [b] Tetrabutylammonium bromide, 4.0 mol %. [c] Dibutyl ether (3 mL) was used as the solvent. [d] 2-Methyl-3-oxa-1-phenyl-1-undecene was also formed as O-alkylated product. [e] Hexadecyltributylphosphonium bromide, 4.0 mol %. [f] 7-Chloro-3-phenyl-2-heptanone was formed selectively. [g] 7-Hydroxy-3-phenyl-2-heptanone. [h] 1-(1-Phenylcyclopentyl)ethanone. [i] Reaction time, 20 h. [j] Reaction temperature, 60 °C.

2) as the phase-transfer catalyst. The use of such calix[n]arenes also proved to be superior to the use of tetrabutylammonium bromide (run 4) and hexadecyltributylphosphonium bromide (run 5), with improvements observed for alkylation/

Scheme 4. C-Alkylation of Methylene Substrates Using 1 (for R[1] and R[2], see Table 4)
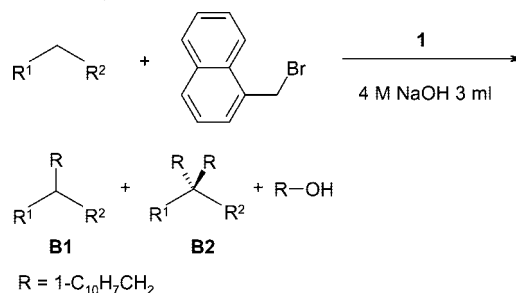
hydrolysis and C-/O-alkylation selectivities. The observed order of reactivity for use of the alkyl halides R–X was I ≈ Br ≫ Cl (runs 6–8), while runs 9 and 10 illustrated the difference in the reactivity between alkyl bromide/chloride.

Various methylene-containing substrates (see Scheme 4 and Table 4) were subjected to alkylation using **1** as catalyst. In the case of 2,4-pentanedione and benzoylacetonitrile (runs 3 and 4), aqueous 2 N NaOH was sufficient to generate the required carbo-anions.[26] Advantages over conventional phase-transfer catalysis were highlighted by runs 6, 8, and 14, where monoalkylated products were formed with excellent selectivities. An interfacial mechanism whereby the calix[n]arene formed a host–guest complex with the carbanion generated at the solvent interface by nucleophilic attack was proposed to explain the observed alkylation activities of **1**[4] < **1**[6] < **1**[8] for the 1-naphthylacetonitrile system.

Ligand systems **1** also proved useful for O-alkylation reactions of alcohols and phenols with alkyl halides (Scheme 5 and Table 5). Vastly increased yields were observed when **1** was present (e.g., run 1 vs run 3), and other advantages included product selectivity and separation. In the case of the calix[4]arene system, the catalytic efficiency increased with increasing size (and solubility in water) of the alcohol (runs 1–4) until hexanol (run 5), the latter being too large to be accommodated in the calix[4]arene cavity. Results for O-alkylation were consistent with a similar mechanism to that operating in the C-alkylation reactions, that is, a host–guest complex comprising the calix[n]arene and an alkoxide anion formed at the interface. Overall, the efficiency of the catalyst systems **1** was dictated by the size and/or shape of the acidic substrate but not by the alkyl halide.

The ability of the trioxadecyl calix[6]arene ligand **2** (Figure 2), a so-called "octapus type" calixarene, to complex sodium ions provided a catalytic system comparable to the well-established phase-transfer catalysts benzyltrimethylammonium chloride and 18-crown-6 for the catalytic condensation of alkali metal carboxylates with alkyl halides to form esters.[27–29] Typically, sodium acetate and 4-nitrobenzyl bromide, in the presence of a catalytic amount of **2**, at 40 °C in CH_2Cl_2, CH_2Cl_2/H_2O, benzene, or dioxane, over 24 h led, following workup, to 4-nitrobenzyl acetate. In CH_2Cl_2/H_2O (20:1), 12% of product was obtained, although far better results were obtained using potassium acetate (see section 2.2). In the absence of **2**, only trace product was formed.

The water-soluble calixarenes of the type **3** (Figure 3) have been shown to regio-selectively catalyze the hydrolysis of ribonucleoside 2′,3′-cyclic phosphates under acidic conditions (pH 2, see scheme 6).[30] All reactions (Table 6) showed first-order kinetics, with both regioselectivity and reaction rate increasing with enhanced calixarene concentration. In the case of calix[4]arene, the substrate was thought to be held just above the cavity by electrostatic interactions, and in turn,

Table 4. *C*-Alkylation of Methylene Compounds Using 1

				isolated yield (%)		
run	$R^1-CH_2-R^2$ (mmol)	catalyst (mol %)	conditions (°C/h)	**B1**	**B2**	alcohol
1	$CH_3COCH_2COCH_3$ (12.0)[a]	none	60, 0.5	11 (+trace)[b]	0	0
2	$CH_3COCH_2COCH_3$ (12.0)[a]	TAC$_6$M (1.0)	60, 0.5	50 (+2)[b]	trace	0
3	$CH_3COCH_2COCH_3$ (12.0)[b]	TAC$_6$M (1.0)	60, 2	88 (+3)[b]	3	0
4	$C_6H_5COCH_2CN$ (12.0)[a]	TAC$_6$M (1.0)	60, 2	82	12	(trace)[c]
5	$C_6H_5COCH_2CN$ (4.8)[a]	TAC$_6$M (1.0)	60, 2	69	22	(trace)[c]
6	$C_6H_5CH_2CN$ (12.0)	TAC$_4$M (1.0)	70, 10	90	8	0
7	$C_6H_5CH_2CN$ (4.8)	TAC$_4$M (1.0)	70, 10	68	19	13
8	$2\text{-}ClC_6H_4CH_2CN$ (4.8)	TAC$_4$M (1.0)	60, 10	84	0	0
9	$C_6H_4\text{-}1,2\text{-}(\text{-}CH{=}CH\text{-}CH_2\text{-})$ (4.8)	TAC$_4$M (1.0)	70, 10	74[d]	trace[e]	4 (+6)[c]
10	$1\text{-}C_{10}H_7CH_2CN$ (4.8)[f]	none	70, 2	21	0	0
11	$1\text{-}C_{10}H_7CH_2CN$ (4.8)[f]	TAC$_4$M (1.5)	70, 2	58	0	trace
12	$1\text{-}C_{10}H_7CH_2CN$ (4.8)[f]	TAC$_6$M (1.0)	70, 2	66	0	trace
13	$1\text{-}C_{10}H_7CH_2CN$ (4.8)[f]	TAC$_8$M (0.75)	70, 2	78	0	trace
14	$1\text{-}C_{10}H_7CH_2CN$ (4.8)[f]	TAC$_6$M (1.0)	70, 5	91	0	trace

[a] Aqueous NaOH (2 N) was used in the place of 4 N aqueous NaOH. [b] 6-(1-Napthyl)-2,4-hexanedione was isolated as a mixture with 3-(4-napthylmethyl)-2,4-pentanedione. [c] Bis-(1-napthylethyl) ether. [d] 3-(1-Napthylmethyl)indene. [e] 1,3-Bis-(1-napthylmethyl)indene. [f] Dipropyl ether (3 mL) was used as a solvent.

Scheme 5. *O*-Alkylation of Alcohols/Phenols Using 1 (for R³ and R, See Table 5)

$$R^3-OH + R-X \xrightarrow[\text{4 M NaOH 3 ml}]{\textbf{1}} R^3-O-R + R-O-R + R-OH$$
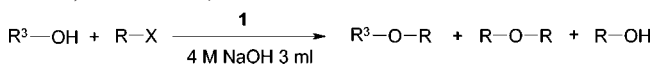
this led to chemical differentiation of certain P–O bonds within the substrate. Calix[6 and 8]arenes were less effective, and this was thought to be due to the increased conformational flexibility of these larger ligands. The need for a calixarene type structure to bring about the observed regioselective catalysis was demonstrated by conducting similar experiments using the monomeric analogue 4-hydroxybenzenesulfonic acid and observing only 1/28 of the effect achieved by using the calix[4]arene.

Interestingly, calixarenes can be used to slow reactions down; for example, during the alkaline hydrolysis of *m*- and *p*-substituted phenyl benzoates (Scheme 7) were found to inhibit activity.[31] Strictly speaking, this system is metal-free, with only a sodium carbonate buffer present to maintain a pH of 9.2; however, we have included it here to illustrate the potential for inhibition applications of calixarenes in other metal-based systems. Substitution of the lower rim hydroxyls for acetyl groups prevented such inhibition; however, the presence of only one hydroxyl group was enough for full inhibition to return. The conformation of the calixarene was also important, with a partial cone conformer (**4g**) having
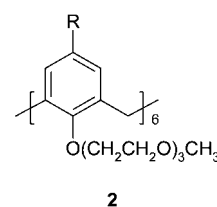
Figure 2. Trioxadecyl calix[6]arene **2** (R = *tert*-butyl).

Scheme 6. Regioselective Cleavage of Ribonucleoside 2′,3′-Cyclic Phosphates Using 3
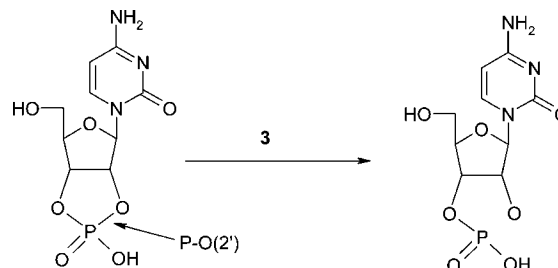
no effect upon phenol yield. It was suggested that the released phenoxide ion resided within the cavity and was hydrogen bonded to a hydroxyl group at the lower rim and, thereby, was released only slowly. The largest inhibition was observed for the calix[8]arene ligand system, where 1:2 complexes

Table 5. *O*-Alkylation of Alcohols/Phenols Using 1

					isolated yield (%)		
run	R^3-OH (mmol)	R–X (4.0 mmol)	catalyst (mol %)	conditions	R^3-O-R	$R-O-R$	ROH
1	$CH_3(CH_2)_5OH$ (12.0)	$4\text{-}t\text{-}BuC_6H_4CH_2Br$	none	60, 3	22	trace	trace
2	$CH_3(CH_2)_5OH$ (12.0)	$4\text{-}t\text{-}BuC_6H_4CH_2Br$	CTAB[a] (0.5)	60, 3	56	12	5
3	$CH_3(CH_2)_5OH$ (12.0)	$4\text{-}t\text{-}BuC_6H_4CH_2Br$	TAC$_6$M (0.5)	60, 3	75	trace	3
4	$CH_3(CH_2)_5OH$ (12.0)	$4\text{-}BrC_6H_4CH_2Br$	TAC$_6$M (0.5)	60, 2	87	0	3
5	$CH_3(CH_2)_5OH$ (12.0)	$Cl(CH_2)_4Br$	TAC$_4$M (1.0)	100, 8	79[b] (+8)[c]	0	0
6	$CH_3(CH_2)_5OH$ (12.0)	$CH_3(CH_2)_5CHBrCH_3$	TAC$_4$M (1.0)	100, 10	17	0	6 (+6)[d]
7	$CH_2{=}CHCH_2OH$ 12.0)	$4\text{-}t\text{-}BuC_6H_4CH_2Br$	TAC$_4$M (0.5)	60, 2	86	4	5
8	$CH_3CHOMe(CH_2)_2OH$ (12.0)	$4\text{-}t\text{-}BuC_6H_4CH_2Br$	TAC$_4$M (0.5)	60, 3	78	4	6
9	C_6H_5OH (4.8)[e]	$4\text{-}t\text{-}BuC_6H_4CH_2Br$	TAC$_4$M (0.5)	60, 7	82 (+trace)[f]	0	8
10	$4\text{-}MeC_6H_4OH$ (4.8)[e]	$4\text{-}t\text{-}BuC_6H_4CH_2Br$	TAC$_6$M (1.0)	60, 7	82 (+9)[g]	0	trace
11	$C_6H_5CH_2OH$ (12.0)	$CH_3(CH_2)_7Br$	TAC$_4$M (1.0)	100, 2	83	0	3
12	$C_6H_4\text{-}1,4\text{-}(\text{-}CH_2OH)_2$ (8.0)	$CH_3(CH_2)_7Br$	HTPB[h] (1.0)	100, 2	21 (+47)[i]	trace	13
13	$C_6H_4\text{-}1,4\text{-}(\text{-}CH_2OH)_2$ (8.0)	$CH_3(CH_2)_7Br$	TAC$_6$M (1.0)	100, 2	49 (+12)[i]	trace	21

[a] Acetyltrimethylammonium bromide (hexadecyltrimethylammonium bromide). [b] 1-Butoxy-4-chlorobutane. [c] 1,4-Dibutoxybutane. [d] 2-Octene. [e] Aqueous NaOH (1 N) was used in the place of 4 N NaOH. [f] 2-(4-*tert*-Butylbenzyl)phenol. [g] 2-(4-*tert*-Butylbenzyl)-4-methylphenol. [h] Hexadecyltributylphosphonium bromide. [i] 1,4-Bis(hexyloxymethyl)benzene.

Table 6. Regioselectivity and Reaction Rate for the Hydrolysis of Ribonucleoside 2′,3′-Cyclic Phosphates by the Use of Water-Soluble Calixarenes 3[a]

2′,3′-cyclic phosphate substrate	water-soluble calixarene	reaction rate (10^{-3} min^{-1})	regioselectivity (3′/2′)
cytidine	calix[4]arene	16	2.7
		2.2[b]	3.5[b]
	calix[6]arene	8.9	1.7
	calix[8]arene	9.3	1.6
	none	2.9	1.5
		0.14[b]	1.8[b]
adenosine	calix[4]arene	8.9	2.0
	none	3.3	1.7
guanosine	calix[4]arene	6.4	2.0
	none	3.0	1.9
uridine	calix[4]arene	5.4	1.6
	none	5.3	1.6

[a] pH 2, 30 °C; [calixarene] = 0.01 mol dm^{-3}. [b] pH 2, 4 °C.

were formed with phenoxide ion. Use of open chain phenols such as **C** did not affect the yield of the released phenol.

2.2. Potassium

Nomura et al.[32] investigated dichlorocarbene generation from CHCl$_3$ and solid KOH in CH$_2$Cl$_2$, catalyzed by **2**, a 1,4-*anti* calix[6]arene bearing 3,6,9-trioxadecyl substituents at the lower rim (conformation shown in Figure 4), calix[4, 5, 6, and 8]arenes of the type **4** (Chart 4; see also Figure 2 and Scheme 8). When compared against the *tert*-butylphenol monomer, calixarene **2** was found to generate the dichlorocarbene with a higher level of efficiency, suggesting that the calix[6]arene ligand was the source of the rate enhancement. Comparable yields to that of 18-crown-6 were observed for **2**; however, the ease of recycling of **2**, aged samples of which exhibited similar activities to that of a fresh sample, gave the catalyst a more practical advantage. A dependency upon alkali metal cations present in the reaction was also observed,

with potassium ions producing increased activities over those observed using sodium or lithium. Rate enhancement to that of the monomer was therefore attributed to the binding capability of **2**, which has a higher selectivity for potassium cations, and this "inclusion complex" was thought to be the active form of the catalyst.
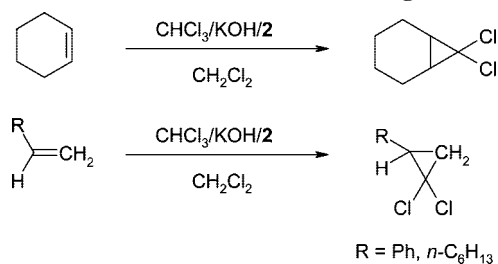
In the presence of catalytic quantities of **2**, oxidation of alkenes and alkynes with 3 equiv of KMnO$_4$ in CH$_2$Cl$_2$ or CH$_2$Cl$_2$−water (10:1) gave the corresponding carboxylic acids in high yields (ca. 80%); without **2** as a catalyst, corresponding yields fell to <10%.[33] The efficiency of the reactions was highly solvent-dependent, with the use of benzene leading to far inferior yields due to solvent effects upon the complexing ability of **2** toward K$^+$. Again, with respect to 18-crown-6, **2** gave comparable yields; however, because of the higher solubility of 18-crown-6 over that of **2**, it was discovered that **2** could be more easily and efficiently recycled, making it a more cost-effective system. Primary alcohols were oxidized to carboxylic acids in quantitative yields, whereas oxidation of secondary alcohols was dependent upon the structure of the alcohol concerned, such that the corresponding yield of ketone formation followed the trend aromatic > alicyclic > aliphatic. Catalysis of this reaction by **2** was found to have a strong dependency upon water content of the reaction media, where increased water content led to lower yields of the desired product.

In the presence of KOH, **2** catalyzed the reaction between benzyl bromide and phenol with 100% conversion within 2 h, indicating the higher selectivity of the calixarene for potassium ions; in the presence of Na$^+$ under analogous conditions, yields of 6% were observed (see also section 4.8).[29]

Ligand **2** (see Figures 2 and 4) has also been shown to catalyze the formation of an ether and bisphenoxymethanes, from 2,4-disubstituted phenols **D1**−**D3** (Scheme 9), in the presence of KOH.[29] The reaction worked best for **D1** affording the product in quantitative yield over 24 h. For

Scheme 7. Alkaline Hydrolysis of *p*- and *m*-Substituted Phenyl Benzoates at pH 9.2

for R$_1$ = NO$_2$, R$_2$ = H
R$_1$ = Me, R$_2$ = H
R$_1$ = H, R$_2$ = Me
R$_1$ = Cl, R$_2$ = H
R$_1$ = *tert*-butyl, R$_2$ = H
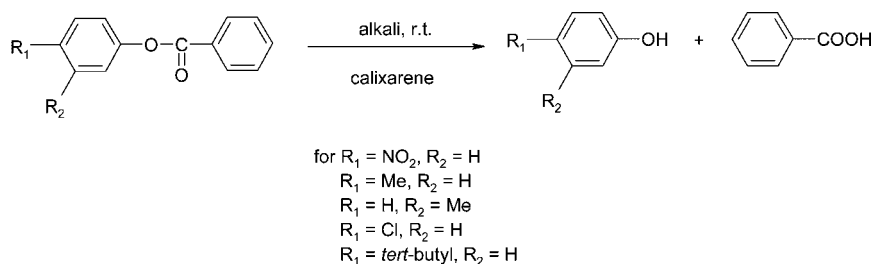
Chart 4. Alkylated Calix[*n*]arenes 4a−h and the Open Chain Analogue C
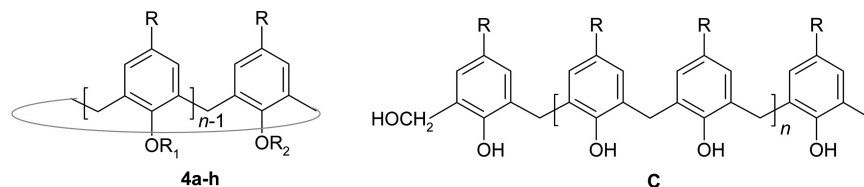
4a R = *tert*-butyl, R$_1$ = R$_2$ = H, n = 4
b R = *tert*-butyl, R$_1$ = R$_2$ = H, n = 8
c R = (CH$_3$)$_2$CCH$_2$C(CH$_3$)$_3$, R$_1$ = R$_2$ = H, n = 6
d R = Me, R$_1$ = R$_2$ = H, n = 5
e R = *tert*-butyl, R$_1$ = R$_2$ = COCH$_3$, n = 8
f R = *tert*-butyl, R$_1$ = COC$_6$H$_5$, R$_2$ = H, n = 4 (cone conformation)
g R = *tert*-butyl, R$_1$ = COC$_6$H$_5$, R$_2$ = H, n = 4 (partial cone conformation)
h R = *tert*-butyl, n = 2
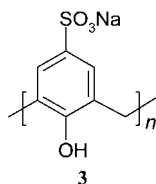
Figure 3. Water-soluble calix[*n*]arenes **3**.
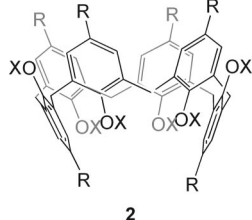
Figure 4. View of **2** highlighting 1,4-*anti* conformation (R = *tert*-butyl, X = $(CH_2CH_2O)_3CH_3$).

Scheme 8. Dichlorocarbene Generation Using 2

R = Ph, *n*-C_6H_{13}

Scheme 9. Bisphenoxymethane Formation

X = Y = H
X = H, Y = Cl
X = Y = Cl

D1, X = Y = H
D2, X = H, Y = Cl
D3, X = Y = Cl

R = H
CH_2OOH
CH_3
n-C_6H_{13}
n-$C_{12}H_{25}$
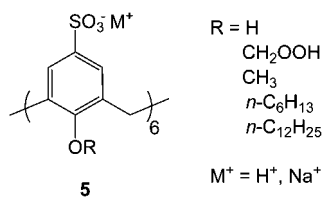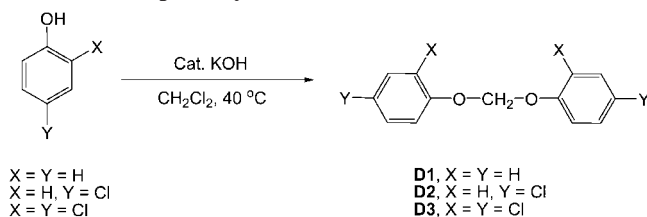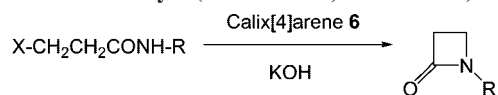
M^+ = H^+, Na^+ or NH_4^+

Figure 5. Hexasulfonated calix[6]arenes.

Scheme 10. Synthesis of 1-Arylazetidin-2-ones Using 6 as a Phase-Transfer Catalyst (for X and R, See Table 7)

D2, much greater reaction times were required (96−144 h), and best results were obtained in wet dichloromethane (which is presumably the source of the CH_2 bridge). In the case of **D3**, only benzyltrimethylammonium chloride (and not **2**) catalyzed the reaction.

Hexasulfonated derivatives of the type **5** (Figure 5), which are derivatives of **3** (*n* = 6, Figure 3), have shown potential in the acid-catalyzed hydration of *N*-benzyl-1,4-dihydronico-tinamide.[34,35] It was found that the use of the calix[4 and 8]arene analogues led to a drop in catalytic activity, due to restriction within (in the case of calix[4]arene) or deformation of the central calixarene cavity (in the case of calix[8]arene).
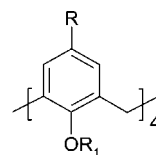
Figure 6. Calixarenes **6** (R_1 = CH_2CONEt_2 and R = *tert*-butyl).

Table 7. Yields of 1-Arylazetidin-2-ones Using 6

	% yield		
	calix[4]arene		18-crown-6
R	X = Br	X = Cl	X = Br
4-I-C_6H_4	68	61	57
4-Cl-C_6H_4	73	35	73
4-F-C_6H_4	65	49	42
4-MeO-C_6H_4	90	70	42
4-Br-C_6H_4	63	34	64
Ph	69	40	50
4-Me-C_6H_4	61	57	72
1-naphthyl	60	35	69 (X = Cl)
4-I-C_6H_4	76	65	71 (X = Cl)

Chart 5. Compounds E1 and E2

R = OMe, Cl

E1   **E2**
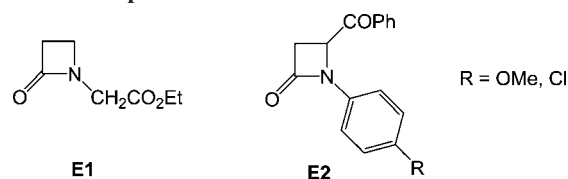
Scheme 11. Williamson Ether Synthesis
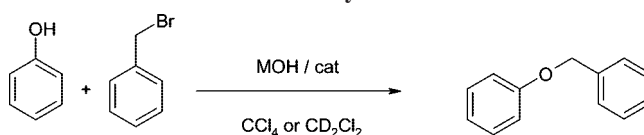
Chart 6. Calixarene Analogue 7 and the Calixarenes 2 and 8

7

R = *tert*-butyl
R_1 = -$(CH_2CH_2O)_3CH_3$

n = 6 **2**
n = 4 **8**
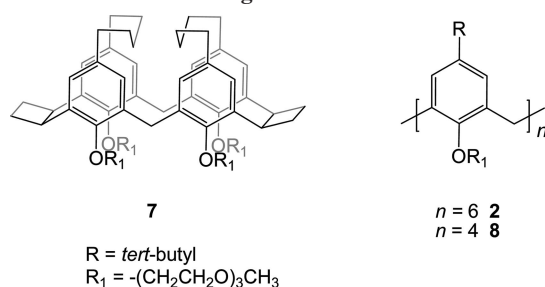
In the case of the calix[6]arene systems containing acidic protons, rate constants were some 426−1220 times greater than those displayed by their noncyclic analogues.

Normura et al. have also used such ligand systems as catalysts in the reaction of alkali-metal carboxylates with alkyl halides (see also section 2.1). The reaction worked well in dichloromethane or acetonitrile but not so well in less polar solvents; for example, there was no reaction in benzene. Indeed, in CH_2Cl_2 at 40 °C, the yield of 4-nitrobenzyl acetate was quantitative. In the case of potassium acetate, the presence of water proved detrimental to the observed catalytic activity.[36]

The dehydrohalogenation of 3-halopropionamides (halo = chloro or bromo) to afford *N*-substituted azetidin-2-ones (Scheme 10) can be catalyzed by the tetra-amide **6** (Figure 6).[37] In a number of cases (Table 7), yields were greater than observed when using an 18-crown-6 catalyst, and **6**

Table 8. Rate Constant of the Reaction between Phenoxide and Benzyl Bromide[a]

base (MOH)	solvent	k (10^7 s^{-1})			
		none	7	8	2
NaOH	CCl$_4$	4.2	62	50	67
KOH	CCl$_4$	6.1	79	56	70
RbOH	CCl$_4$	5.6	160	60	180
NaOH	CD$_2$Cl$_2$	8.4	120	90	140
NaOH	saturated CD$_2$Cl$_2$[b]	17	590	120	390
KOH	CD$_2$Cl$_2$	15	520	480	600
RbOH	CD$_2$Cl$_2$	18	760	420	990
CsOH	CD$_2$Cl$_2$	28	320	220	710

[a] Phenol:benzyl bromide:base:catalyst = 1:1:3.5:0.029 (molar ratio); phenol, 0.45 mol dm^{-3}; temperature, 32 ± 1 °C. [b] Saturated with D$_2$O.

Scheme 12. Finkelstein Reaction of Octyl Bromide (for X and Y, See Table 9)

$$CH_3(CH_2)_7\text{-}X \xrightarrow[\text{CD}_3\text{COCD}_3 \text{ or CD}_3\text{CN}]{\text{MY / cat}} CH_3(CH_2)_7\text{-}Y$$

Table 9. Rate Constant of the Finkelstein Reaction[a]

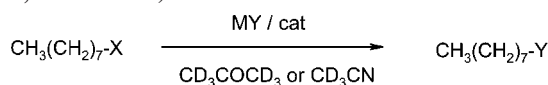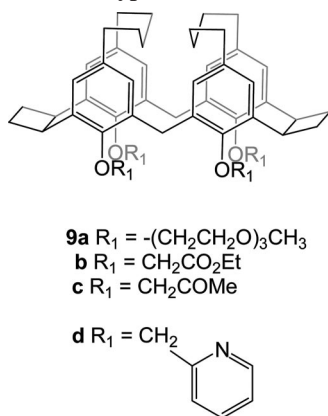| substrate n-C$_8$H$_7$X	reagent (MY)	solvent	temperature (°C)	k (10^7 s^{-1})			
				none	7	8	2
n-C$_8$H$_7$Br	KI	CD$_3$COCD$_3$	50	27	42	28	31
	RbI	CD$_3$COCD$_3$	50	22	41	24	24
	CsI	CD$_3$COCD$_3$	50	14	24	18	20
	KI	CD$_3$CN	50		39	20	28
	RbI	CD$_3$CN	50		36	17	25
	CsI	CD$_3$CN	50		31	14	20
n-C$_8$H$_7$I	KBr	CD$_3$CN	75	9.2	15	12	13
	RbBr	CD$_3$CN	75		14	10	11
	CsBr	CD$_3$CN	75		12	8.0	9.7

[a] Substrate:reagent:catalyst = 1:5:0.05 (molar ratio); substrate, 0.24 mol dm^{-3}.

Chart 7. Ethers of the Type 9

9a R$_1$ = -(CH$_2$CH$_2$O)$_3$CH$_3$
b R$_1$ = CH$_2$CO$_2$Et
c R$_1$ = CH$_2$COMe

d R$_1$ = CH$_2$ (2-pyridyl)

could be used at lower concentrations (0.025 M cf. 0.05 M for 18-crown-6). Best results were obtained using KOH as the base as opposed to NaOH. The compounds **E1** and **E2** (Chart 5) were also available using this procedure.

An octahydroxylated calix[8]arene ligand system has been used, in the presence of diphenylmethylpotassium as deprotoning agent, to trigger the anionic polymerization of ethylene oxide. Better control (PDI < 1.2) over the starred products was achieved using THF as solvent,[38] which allowed for the synthesis of well-defined eight-arm polyethyleneoxide stars with tunable molar mass. In DMSO, the initiating alkoxides had a tendency to aggregate, which proved problematic.

Chart 8. Oligo(ethylene glycol) Calixarenes 2′ and 10 and Reference Compound F [R$_1$ = (CH$_2$CH$_2$O)$_n$Me, R$_2$ = (CH$_2$CH$_2$O)$_3$Me), R$_3$ = tert-Butyl, and R$_4$ = tert-Octyl]
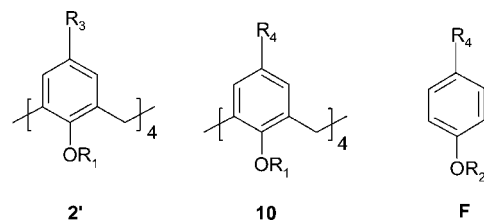
Table 10. Extraction % of Alkali Metal Picrates in CH$_2$Cl$_2$ at 25 °C[a]

calixarene	ex %			
	M$^+$ = Li$^+$	Na$^+$	K$^+$	Cs$^+$
cone-**2**/($n = 1$)	27.6	74.8	27.7	6.2
partial cone-**10** ($n = 1$)	0	15.3	63.9	70.3
cone-**10** ($n = 1$)	29.2	100	77.2	51.2
cone-**10** ($n = 2$)	27.5	89.8	80.8	58.1
cone-**10** ($n = 3$)	34.4	91.2	69.8	66.0
F	8.4	7.5	12.4	0

[a] The aqueous phase (5 mL) contains M$^+$Pic$^-$ (2.50×10^{-4} M), MOH (0.10 M), and MCl (0.50 M). The organic phase (5 mL) contains calixarene ionophores (2.5×10^{-3} M).

11
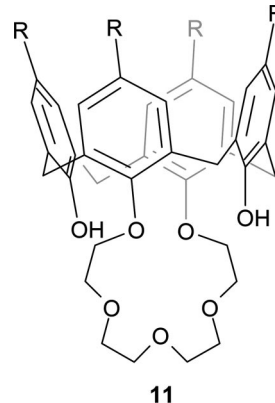
Figure 7. Calix[4]-crown-5 (R = tert-butyl).

Scheme 13. Formation of p-Nitrobenzyl Butyrate

$$C_3H_7COONa + O_2N\text{—}C_6H_4\text{—}CH_2Br \longrightarrow$$

$$O_2N\text{—}C_6H_4\text{—}CH_2OCOC_3H_7$$
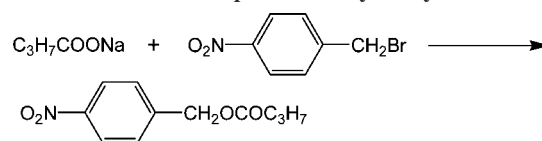
Scheme 14. Simplified Possible Mechanism for Nucleophilic Catalysis of Acyl Transfer Via 11

Ac = acetate
'cat' = catalyst generated from BaBr$_2$ and **11** (1:1)
'cat'Ac = acylated intermediate
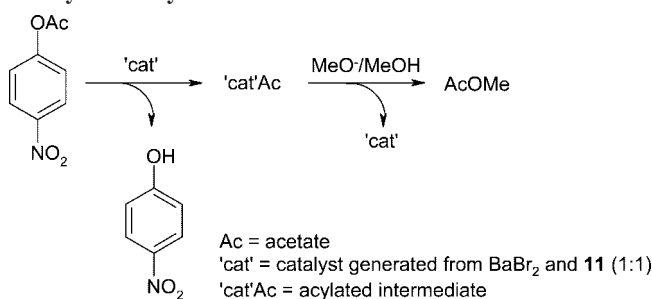
The calixarene analogue **7**, bearing triethyleneglycol groups at the lower rim, has shown catalytic activity in the Williamson ether synthesis (Scheme 11 and Chart 6).[39] Data for the reaction between phenoxide and benzyl bromide (Table 8) revealed, in the nonpolar solvent CCl$_4$, an increased

X = Y = OH
X = OH, Y = OAc
X = Y = O⁻
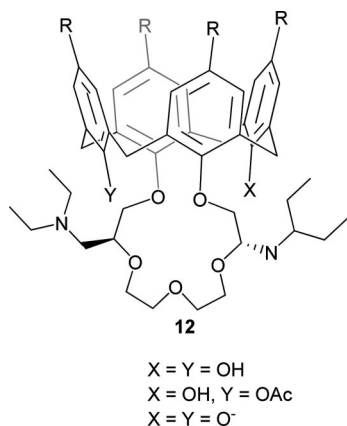
Figure 8. Calix[4]-crown-5 complex **12** bearing diethylaminomethyl arms (R = *tert*-butyl).

rate constant when larger ions were used; that is, the highest rate was observed for the RbOH system. Results using **7** were compared with those obtained using the calixarenes **8** and **2**. For **2**, a similar affinity for larger ions was observed. Use of the more polar solvent CD_2Cl_2 led to enhanced activity, as did the addition of a small amount of water. The order of catalytic activity for the ether synthesis was **8** < **7** ≤ **2**.

The same three ligand systems were also screened in the Finkelstein reaction of octyl bromide (Scheme 12). The use of these ligands (Table 9), particularly ligand **7**, led to an almost 2-fold increase in activity.

We note that Birch reduction of **7** followed by treatment with RX and NaH afforded the ethers **9** (Chart 7), which act as ionophores for alkali metals, transition metals, and lanthanides.[40]

Calix[4]arenes **10** functionalized at the upper rim with *tert*-octyl groups and the lower rim with OCH_2CH_2OMe groups (Chart 8) were shown to be effective extraction agents and phase-transfer catalysts.[41] For the extraction of alkali-metal ions with picrate ion in dichloromethane (Table 10), it was shown that increasing the length of the ethyleneglycol chain was not beneficial and was indeed detrimental to workup due to the nature of the emulsions formed. On the upper rim, the presence of *tert*-octyl groups over *tert*-butyl groups led to the best Na⁺ selectivity; however, the introduction of *tert*-octyl groups produced a second conformational isomer, a partial cone, which exhibited K⁺ or Cs⁺ selectivity. These ligands systems were employed as phase-transfer catalysts in the formation of *p*-nitrobenzyl butyrate as shown in Scheme 13. For the system employing *tert*-octyl/OCH_2-

CH_2OMe groups, catalytic activity comparable with dicyclohexyl-18-crown-6 was observed, with results for the other ligand systems mimicking those observed for the metal extraction work. Noncyclic **F** showed no catalytic activity.

These studies prompted Shinkai et al. to highlight a number of the benefits of calixarene-based catalysts over crown ether-based systems, including (i) the ease and scale-up ability of lipophilic calixarene chemistry, (ii) lipophilic calixarene as easily handled solids (lipophilic crown ethers are often oily), and (iii) superior metal selectivity.

3. Alkaline Earth Metals (Barium)

In the presence of 1 mol equiv of $BaBr_2$, the catalytic activity of proligand **11** (Figure 7) was found to increase with respect to the methanolysis of *p*-nitrophenyl acetate,[42] a result of the barium complexing with the free phenolic moieties of the calixarene to form an activated ionized intermediate.

The intermediate was thought to aid methoxide attack upon the substrate, as well as forming a deionized complex, which acted as an in-built electrophilic catalyst favoring the nucleophilic addition of the acyl group to the calixarene moiety (see Scheme 14).[43] The ionized form had previously been shown to undergo methoxide ion attack from methanol up to 10^6 times faster than the monoacylated non barium containing derivative of **11**. The work was extended to include several crown ethers derived from *p-tert*-butyl-calix[4]arene; however, the resulting barium(II) salts possessed poor catalytic properties.[44] This barium(II) complex has also been used in the methanolysis of a series of aryl acetates.[45] The scope of the catalyst was restricted to acetate esters with reactivities ranging from phenyl acetate to *p*-nitrophenyl acetate; maximum efficiency was achieved using *p*-chlorophenyl acetate. Use of the related calix-crown ligand **12** (Figure 8), bearing two diethylaminomethyl arms at the polyether bridge, did not afford an improvement in observed activity.

Dinuclear barium(II) complexes of calix[4]arenes bearing two aza[18] crown-6 units at vicinal (1,2-) **13** or diagonal (1,3-) **14** positions (Chart 9) were screened as catalysts for acyl transfer.[46] Results were suggestive of cooperative effects, with the vicinal derivative out-performing the diagonal regioisomer. For the esters screened (**G1**−**G4** in Chart 10), the distance between the carboxylate and the ester carbonyl was shown to influence the catalytic ester cleavage. However, despite the relationship between ester size and metal-to-metal distance, other factors must also be influenc-

Chart 9. Aza[18]crown-6 Calix[4]arenes (R = *n*-Propyl)

13

14
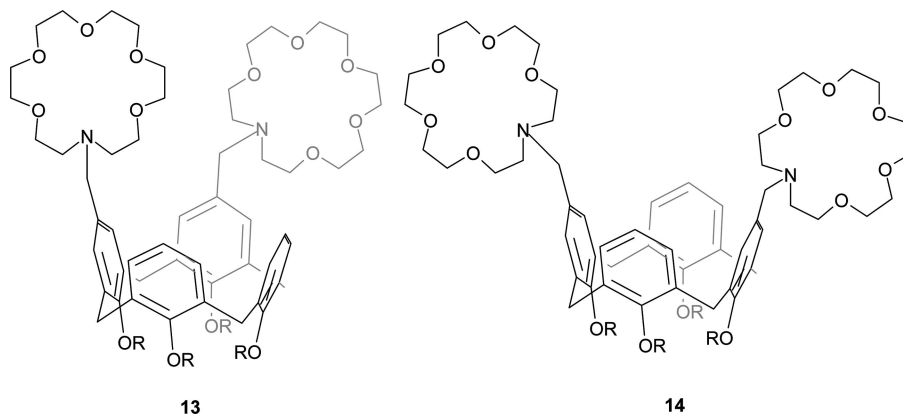
Chart 10. Esters G1 to G4

G1   G2   G3   G4
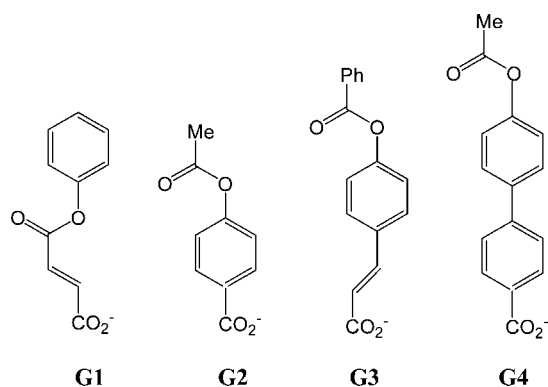
ing the catalytic activity given the observed better performance of the vicinal system **13**.

4. Early Transition Metals

4.1. Scandium

A complex formed from the interaction of scandium isopropoxide and p-tert-butylcalix[6]areneH$_6$ (using a reaction ratio of 1.33: 1) in toluene has been used as a single component initiator for the ring-opening polymerization of 2,2-dimethyltrimethylene carbonate under mild conditions.[47] The resulting poly(2,2-dimethyltrimethylene carbonate) had an average molecular weight of 33700 and a PDI of 1.21. The polymerization rate was first order with respect to both the monomer and the initiator concentrations. ^{1}H NMR measurements on the polymer suggested that the monomer ring opened via acyl oxygen bond cleavage; highly polar solvents were found to be detrimental to the ring-opening polymerization.

4.2. Titanium

4.2.1. Olefin Polymerization

The interaction of group IV metallocene complexes and methylaluminoxane (MAO) has provided much insight into the active species of the metallocene catalysts in α-olefin polymerization.[48,49] ^{1}H NMR spectroscopic investigations carried out by Proto et al. into the nature of the Ti/MAO cationic alkyl intermediate using **15**, originally prepared by Floriani and co-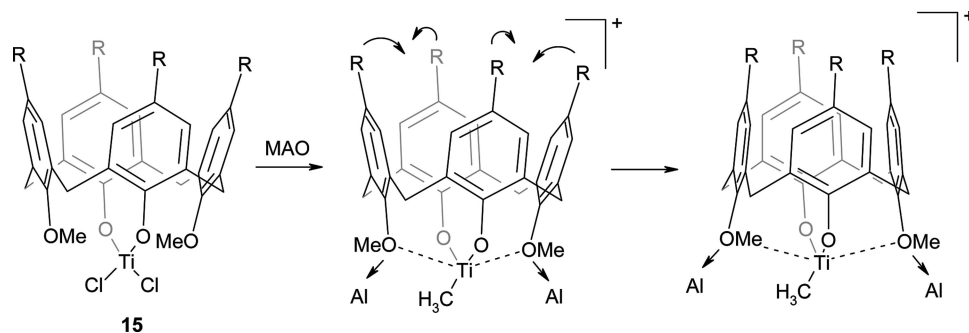workers,[50] suggested that upon formation of the complex, a conformational change occurs in the calixarene, indicated below (Scheme 15) by the arrows, which helped to stabilize the metal center.[51] Following the introduction of ethylene into the system, moderate activities for polymerization were observed (ca. 100 g/mmol h bar); the

corresponding B(C$_6$F$_5$)$_3$/1,3-dimethoxy-p-tert-butylcalix[4]-arene[Zr(CH$_2$Ph)$_2$] system[52] was found to be inactive as a catalyst, an observation explained by the steric crowding of the metal center by the calixarene-bound methoxy groups.

Increasing the length of the alkoxide substituent on the calix[4]arene lower rim from Me in the debutylated analogue of **15** to n-Pr was found by Frediani et al. to produce complex **16** (Figure 9),[53] which, when screened, afforded not only ultrahigh molecular weight polyethylene ($M_n = 4 \times 10^6$ g mol^{-1}) but also demonstrated high thermal stability with activities of ca. 2000 g/mmol h bar, which were observed at temperatures as high as 120 °C. At these elevated temperatures, the catalyst also demonstrated single-site catalysis (PDI 1.3−1.5) and obeyed first-order kinetics. The thermal stability was attributed to the two pendant n-Pr groups, which help to stabilize/protect any reactive intermediates from deactivation processes. As for the Proto system, the active species was determined by NMR spectroscopy to be a titanium methyl cation.

Calix[4]arenes bearing a bridging phosphorus group in a 1,2-alternate conformation or cone conformation **17−20** (Chart 11) and those bearing silicon groups in a 1,2-alternate conformation (**21** and **22**, Chart 12) have been used to support the TiCl$_2$ fragment.[54] Subsequent reactions of the sulfur systems with the appropriate dialkylmagnesium reagents R$_2$Mg·THF (R = Me or CH$_2$Ph) gave the corresponding dialkyl complex, which could be further reacted on a 1:1 molar ratio with [Ph$_3$C]OTf (Tf = CF$_3$SO$_3$) to afford the complexes [Ti(DMSC)(OTf)R] (DMSC = dimethyl sulfur calix[4]arene) **23** (R = Me) and **24** (R = CH$_2$Ph). Attempts to generate a cationic alkyl species, analogous to the chain propagating species found in Ziegler−Natta metallocene catalysis using [(Et$_2$O)$_2$H]BAr$_4$ (Ar = (CF$_3$)$_2$C$_6$H$_3$), were hindered due to side reactions, which caused decomposition of the dimethylsilyl calix[4]arene. However, alkyl abstraction using [Ph$_3$C]BAr$_4$ was facile when carried out in the presence of acetonitrile. At 25 °C, with 500 equiv of MAO, low activities were observed (<100 g/mmol h bar); the highest activity was exhibited by **17**, as the cone conformation provided an open face for the polymerization reaction to occur, while the coordinating phosphorus helped to stabilize the cationic center. The same catalyst also demonstrated the ability to oligomerize 1-hexene under similar reaction conditions. The observation of only modest activities here was attributed to a number of factors including (i) a low equilibrium concentration of the active species and (ii) possible interaction of MAO with the bridging phosphorus or sulfur.

The reaction of p-tert-butylcalix[n]areneH$_n$ (n = 4, 6, and 8) with n/2 equivalents of TiCl$_4$ produced catalysts, which,

Scheme 15. Proposed Conformational Change of Calix[4]arene during Complex Formation (R = tert-Butyl and Al = "Coordinated" MAO)
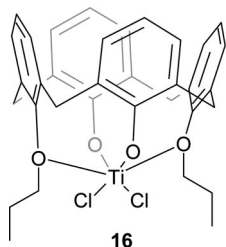

15

Figure 9. Di-*n*-propyl-substituted titanium calix[4]arene complex **16**.

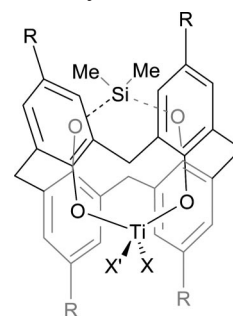upon activation with MAO, were highly active for ethylene polymerization, producing ultrahigh molecular weight polyethylene ($M_w > 5000000$ for the calix[6]arene derivative).[55] Under analogous conditions, all catalysts also displayed very good activities (6000−8000 g/mmol h) for styrene polymerization, with the calix[4 and 6]arene-based procatalysts affording over 90% syndiotactic polystyrene. It should be noted that the calix[8]arene-based procatalyst was active but did not yield syndiotactic polymer.

The use of alkoxysilanes as external electron donors in the manufacturing of isotactic polypropylene (*i*-PP) has been shown to increase the fraction of stereoregular polymer produced during the polymerization reaction.[56] In light of this, Kemp et al. investigated a range of substituted hydroxy-, methoxy-, and silyl- bearing calix[4 and 5]arenes as external electron donors in the TiCl$_4$/TMA polymerization of propylene and found that in the presence of the calixarenes, the yield of *i*-PP formed increased significantly (the xylene-soluble fraction fell from 30% with no calixarene present to 8−17% when present).

A calix[4]arene titanium system of unknown structure has been screened for the polymerization of ethylene in the presence of a variety of cocatalysts. The catalytic activity of the system was found to decrease in the following cocatalyst order AlEt$_3$ > Al(*i*Bu)$_3$ > AlEt$_2$Cl > Al(*i*Bu)$_2$Cl. In the case of Al(*i*Bu)$_3$, polyethylene with a molecular weight of 9.4×10^5 was obtained, with a catalytic activity for the system of 60.7 g/mmol h bar (35 °C, Al:Ti = 20).[57]

In the patent literature,[58] catalytic systems comprising titanium (usually added as TiCl$_4$), a halogen-containing magnesium compound, and an aluminum/silicon additive have been utilized for the synthesis of polyethylene. The claimed additive contained a *p-tert*-butylcalix[4, 6 or 8]arene/Me$_3$Al mixture. It is also noteworthy here that hydroxyl-depleted calix[4, 6 or 8]arenes have been utilized in olefin polymerization. The catalyst system incorporated transition metals from group 3 through to group 10 (elements of the lanthanide and actinide series were also claimed) chelated by the "calixarene" and a cocatalyst, which was either an alkylaluminum complex or an acid salt containing a noncoordinating anion (typically of boron).[59] The olefin polymerization was conducted over a wide temperature range (−30 to ca. 280 °C). The hydroxyl-depleted calix[4, 6 or 8]arenes were generated via established procedures using phosphorylating agents to convert a number of the phenolic OH groups to phosphate esters,[60] followed by subsequent cleavage with alkali metals, releasing the calixarene upon quenching.

Chart 12. Dimethylsilyl-bridged Titanium Calix[4]arene Complexes (R = *tert*-Butyl)

X=X'=Me	**21**
X=X'=CH$_2$Ph	**22**
X=Me, X'=CF$_3$SO$_3$	**23**
X=CH$_2$Ph, X'=CF$_3$SO$_3$	**24**

4.2.2. Aldol/Cycloaddition/Friedal Crafts Reactions

Treatment of *p-tert*-butylthiacalix[4]areneH$_4$ with TiCl$_4$ in dichloromethane produced two Ti(IV) complexes, both bearing two metal centers and bound through OSO motifs (Chart 13). In one case, the Ti atoms were found to be *syn*-(**25**), while in the other an *anti*-(**26**) arrangement was assigned by ^{1}H NMR spectroscopy; product **26** was essentially insoluble in the reaction solvent.[61] The *syn*-conformation was later structurally characterized by single crystal X-ray diffraction and found to include a bridging water molecule. Because of the highly oxophilic nature of **25**, it was evaluated as a potential catalyst in the Mukaiyama-aldol reaction of aromatic aldehydes with silyl enol ethers (Scheme 16 and Table 11). High yields were obtained for a variety of aldehydes, indicating a double-activation of the aldehyde by **25**, whereby the close proximity of the two metal centers allowed the complex to act as a bidentate Lewis acid.

The same procatalysts have been shown by Morohashi et al.[62] to catalyze the [2 + 2 + 2] cycloaddition of terminal alkynes with high regioselectivity (Scheme 17 and Table 12). The reaction of ethynylbenzene with **25**/Na produced a mixture of 1,3,5- and 1,2,4-triphenylbenzene in a ratio of 77:23 in a 65% yield. The use of the *anti*-complex **26**/Na increased the selectivity to 85:15 and the overall yield to

Chart 11. Phosphorus-Bearing Titanium Calix[4]arene Complexes (R = *tert*-Butyl)
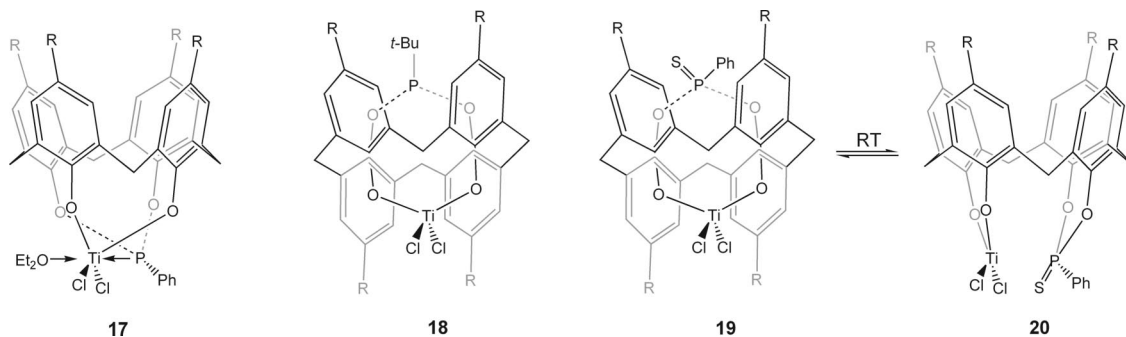
Chart 13. Titanium Thiacalix[4]arene and Calix[4]arene Complexes (R = *tert*-Butyl)

25   **26**   **27**
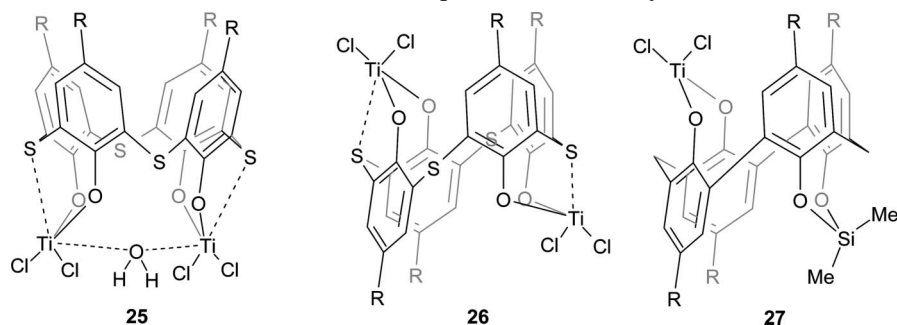
Scheme 16. Reaction of Aldehydes with Silyl Enol Ethers in the Presence of 25 or 26 (for R^1, See Table 11)

R^2 = Ph
R^2 = S*t*-Bu
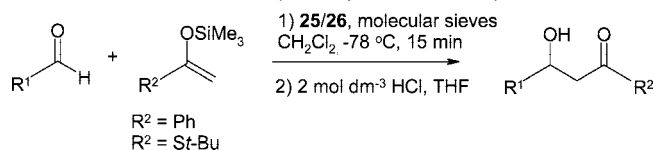
Table 11. Yields from the Reaction of Silyl Enol Ethers in the Presence of 25 or 26

entry	aldehyde (R′CHO)	silyl enol ether	Lewis acid (mol%)	yield (%)
1	benzaldehyde	5	**25** (5.0)	93
2	benzaldehyde	5	**26** (5.0)	2
3	benzaldehyde	5	TiCl$_4$ (10.0)	36
4^a	benzaldehyde	5	**25** (5.0)	6
5^b	benzaldehyde	5	**25** (5.0)	61
6	4-chlorobenzaldehyde	5	**25** (5.0)	85
7	4-methylbenzaldehyde	5	**25** (5.0)	88
8	2-methylbenzaldehyde	5	**25** (5.0)	57
9^c	2-methylbenzaldehyde	5	**25** (5.0)	77
10	2,6-dimethylbenzaldehyde	5	**25** (5.0)	30
11	1-naphthaldehyde	5	**25** (5.0)	50
12^c	1-naphthaldehyde	5	**25** (5.0)	87
13	2-naphthaldehyde	5	**25** (5.0)	91
14	cinnamaldehyde	5	**25** (5.0)	87
15	3-phenylpropanal	5	**25** (5.0)	0
16	benzaldehyde	6	**25** (5.0)	95
17	4-chlorobenzaldehyde	6	**25** (5.0)	93
18	4-methylbenzaldehyde	6	**25** (5.0)	97
19	1-naphthaldehyde	6	**25** (5.0)	95
20	2-naphthaldehyde	6	**25** (5.0)	92

^{a} Reaction conducted at 0 °C for 2 h. ^{b} Molecular sieves not added. ^{c} Reaction conducted at −78 °C for 2 h.

Scheme 17. [2 + 2 + 2] Cycloaddition of Terminal Alkynes (R = Ph)

Table 12. [2 + 2 + 2] Cycloaddition of Terminal Alkynes by 26

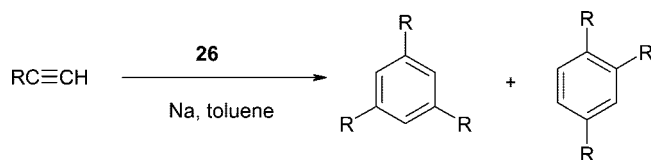| alkyne	temperature (°C)	time (h)	yield (%)	1,3,5-isomer: 1,2,4-isomer
4-MeC$_6$H$_4$C≡H	23	3.5	95	95:5
4-CF$_3$C$_6$H$_4$C≡CH	23	15	0	
4-CF$_3$C$_6$H$_4$C≡CH	80	15	0	
BuC≡CH	23	15	0	
BuC≡CH	80	15	0	
4-CF$_3$C$_6$H$_4$C≡CH^a	23	3.5	30	~100:0
PrC≡CH^a	23	15	73	75:25
BuC≡CH^a	23	15	73	78:22
OctC≡CH^a	23	15	71	95:5
Me$_3$SiC≡CH^a	50	15	14	100:0
*t*BuC≡CH^a	50	15	0	
PhC≡CH^a	23	20	0	

^{a} Sodium phenylacetylide was added.

Chart 14. Disiloxane-Bridged Calix[4]arenes 28 and 29 (R = *tert*-Butyl)

X = S   **28**
X = CH$_2$ **29**
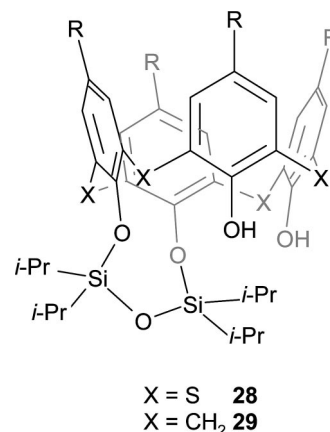
alkynes, required pretreatment of the dichloride procatalyst with sodium phenylacetylide as, even at elevated temperatures, it was postulated that the dichloride species prevented the formation of a key titanacyclopentadiene intermediate. This method, however, gave the corresponding 1,3,5-trisubstituted benzenes in good yield with varying degrees of regioselectivity.

Furthermore, the TiCl$_2$/SiX$_2$ bearing calix[4]arenes **30**−**33** (Chart 15) also catalyzed alkyne cycloaddition in the presence of magnesium (or excess sodium) with terminal alkynes following similar trends to that of **25** and **26**.[64] Additionally, cycloaddition of internal alkynes was found to rely heavily upon the steric factors of the substituent groups. A 1,2,4-substitution pattern was found to be the preference for unsymmetrical internal alkyne cycloaddition; however, the ratio of 1,2,4- to 1,3,5-substitution was found to fall with decreasing steric bulk of the substituents, although never below 3:1. Structural analysis of a η^6-arene ring-bound

95%. The related monometallic complex **27** exhibited a change in regioisomers of 1:99 in favor of the 1,2,4-isomer. The disiloxane bridged calixarenes **28** and **29** (Chart 14) have been used to investigate the origin of such regioselectivity.[63] Upon treatment with TiCl$_4$ in situ, **28** was found to be comparable with **26** (both exhibiting yields between 93 and 95% with a ratio of 85:15 for **26** and 83:17 for **28**), whereas **29**, although requiring higher reaction temperatures, favored the 1,2,4-product as with **27** (1,2,4-selectivity 99:1 for both). Cycloaddition of various terminal alkynes indicated that 1-ethynyl-4-(trifluoromethyl)benzene, as well as aliphatic

Chart 15. Silicon-Bearing Titanium Calix[4]arene Complexes 30−34

R = t-Bu, X = Et   **30**
R = H, X = Me   **31**
R = Me, X = Me   **32**
R = t-Bu, X = Ph   **33**

R = t-Bu   **34**
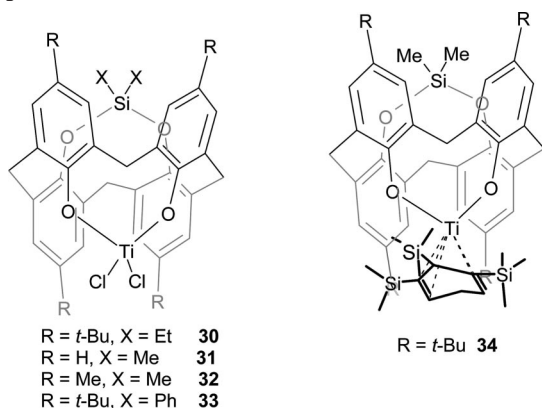
Scheme 18. Aldol Condensation of Chans' Diene (R = p-NO$_2$−C$_6$H$_4$)
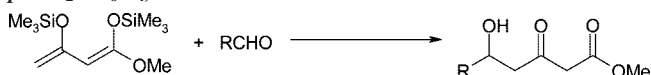
Table 13. Aldol Reaction of Benzaldehyde with Chans' Diene Promoted by 35−41[a]

calix[n]arene	yield (%)
p-$tert$-butylcalix[4]arene	77
p-$tert$-butylcalix[6]arene	96
p-$tert$-butylcalix[8]arene	56
Ti(Oi-Pr)$_4$	4
35	95
36	10
37	17
38	
39	69
40	44
41	58[b]

[a] Conditions: molecular sieves, THF, −78 °C, 2 h, 25 °C (16 h). [b] Toluene used as the solvent.

Ti/Me$_2$Si-bridged calix[4]arene complex **34** indicated that rather than the expected Ti(II) η^6-arene complex, significant Ti(IV) character was seen with loss of aromaticity in the arene, suggestive of a strong contribution from a cyclohexadiene dianion type system.[63] Better still, **34** can be described as a 7-titanonorbornadiene complex, for which first-order dependence with an associative mechanism for the [2 + 2 + 2] cycloaddition of Me$_3$SiC≡CH was observed.
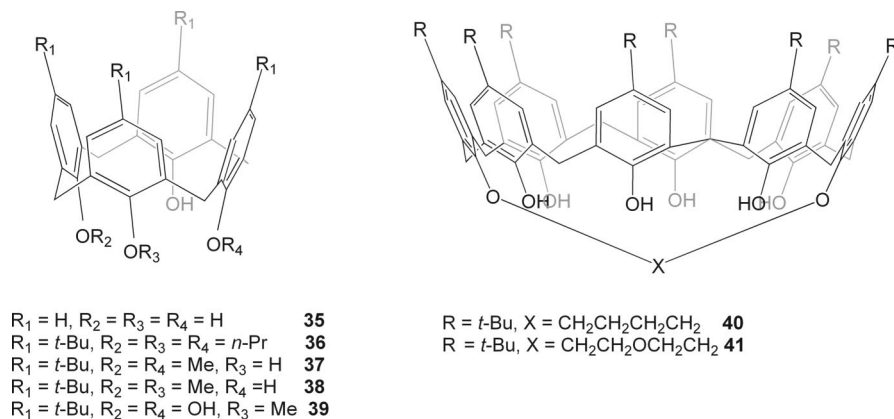
The aldol condensation of Chans' diene (Scheme 18) has been found to be a powerful preparative tool used in total synthesis of complex molecules.[65−68] Systems of the type Ti(Oi-Pr)$_4$/p-$tert$-butylcalix[4, 6, and 8]areneH$_{4,6,8}$ were found to catalyze the reaction between Chans' diene and benzaldehyde in 77, 96, and 56% yields, respectively.[69] In all cases, superior activities were observed to that of Ti(Oi-Pr)$_4$ (4%), indicating that the calixarene/titanium complex successfully acted as a Lewis acid, enhancing the reactivity of the aldehyde toward Chans' diene. In light of these results, a series of substituted calix[4 and 8]arenes **35−41** (Chart 16 and Table 13) were tested as potential ligands; it was found that **35**/Ti(Oi-Pr)$_4$ promoted the aldol reaction of benzaldehyde with Chans' diene with a 95% yield; this was attributed to the increased solubility of the calix[4]arene in THF. Similar aldol reactions carried out using **36−41** indicated that a minimum of three phenolic OH's were required to strongly bind to the Ti(IV) center, with **39−41** giving the highest yields. The yields observed when using **40** and **41** were found to be only comparable to that of the parent calix[8]areneH$_8$ ligand, thought to be a result of problems associated with solubility.[69]

Further success was achieved using various differently substituted aldehydes affording products in moderate to excellent yields over 18 h (40% for p-nitrobenzaldehyde rising to 99% for benzaldehyde).[70] In these systems, there was evidence of a relationship between the number of free phenolic (nonalkylated) groups present and the observed catalytic activity. At least three free phenolic groups were deemed necessary to attain decent activity, and this was thought to be due to enhanced coordination to the titanium(IV) center.

Use of a number of known and well-characterized (single crystal X-ray diffraction) titanium calix[4]arenes, such as **42** and **43** (Chart 17),[50,71] in the aldol condensation of Chans' silyloxydiene with a range of aldehydes, revealed that **36** exhibited the best catalytic efficiency. Incorporation of a second chloride at titanium (as in **15**, see Scheme 13) led to a further decrease in catalytic efficiency.

Under analogous conditions, Ti/**44** (Chart 18) gave high yields (80%) of the desired adduct, namely, 5-hydroxy-5-(4-nitro-phenyl)-3-oxo-pentanoic methyl ester **H** with high catalytic loading (16 mol %) but displayed almost no enantioselectivity (7%).[72] Complexes Ti/**45−47** also gave low yields with little to no enantioselectivity. A lowering of the reaction temperature to −20 °C aided overall enantioselectivity (27%); however, any further decrease of the temperature afforded little improvement. The extra rigidity of the pendant groups in the binapthyl-bridged ligand **48** also failed to provide useful enantioselectivity (12%) and led to a decreased yield (40−56%). This overall decrease in

Chart 16. Calix[4 and 8]arenes Used in Conjunction with Ti(IV) in the Aldol Reaction of Benzaldehyde with Chans' Diene

R$_1$ = H, R$_2$ = R$_3$ = R$_4$ = H   **35**
R$_1$ = t-Bu, R$_2$ = R$_3$ = R$_4$ = n-Pr   **36**
R$_1$ = t-Bu, R$_2$ = R$_4$ = Me, R$_3$ = H   **37**
R$_1$ = t-Bu, R$_2$ = R$_3$ = Me, R$_4$ =H   **38**
R$_1$ = t-Bu, R$_2$ = R$_4$ = OH, R$_3$ = Me   **39**

R = t-Bu, X = CH$_2$CH$_2$CH$_2$CH$_2$ **40**
R = t-Bu, X = CH$_2$CH$_2$OCH$_2$CH$_2$ **41**

Chart 17. Titanium Calix[4]arene Complexes 42 and 43 (R = *tert*-Butyl)

42   **43**
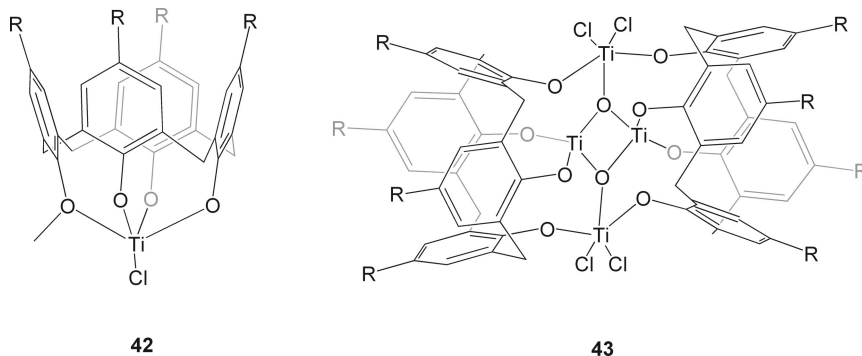
Chart 18. 1,3-Disubstituted Calix[4]arenes 44−48 and Product H (R = *tert*-Butyl)

44: R₁ = H, R₂ =

45: R₁ = R₂ =

48

46: R₁ = H, R₂ =

47: R₁ = R₂ =

H
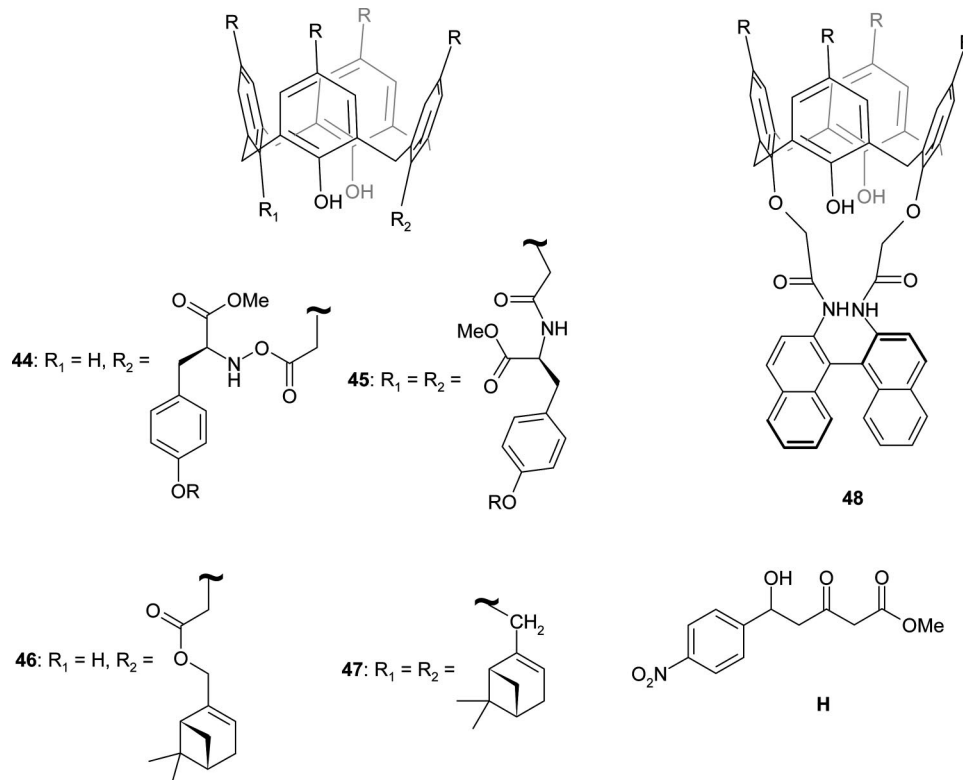
performance was attributed to a number of factors including the lower activity of 1,3-disubstituted calixarenes in general, the large distance between the stereogenic and catalytic centers, and insufficient coordination of the titanium center to the calixarene lower rim phenolic oxygens.

4.2.3. Epoxidation

Calix[4]arenes bearing electron-donating (*t*-Bu) through to electron-withdrawing (NO₂) groups appended to the upper rim have been covalently grafted onto a number of oxide

Chart 19. Silica-Grafted Titanium Calixarene Type Complexes 49−51 (R = *tert*-Butyl)

49   **50**   **51**
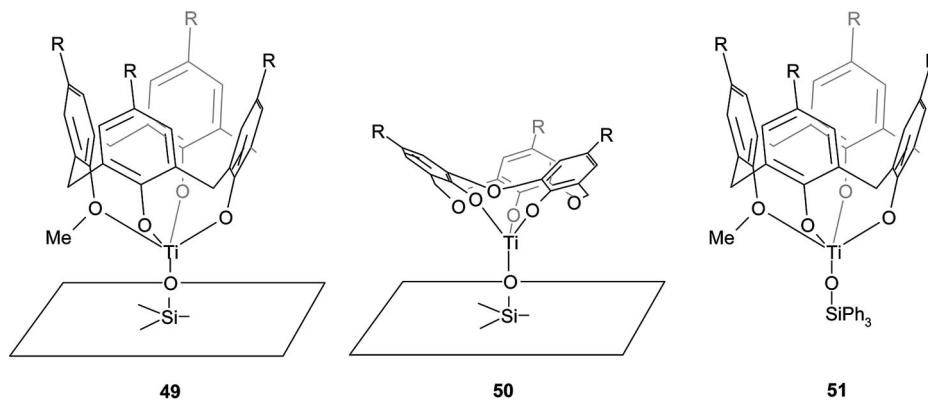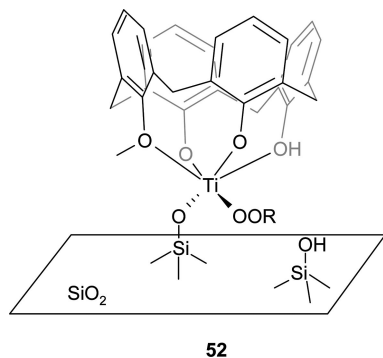
Figure 10. Proposed active species **52**.

Scheme 19. Polyisobutylene Arms from a Calix[8]arene Core (PIB = Polyisobutene)
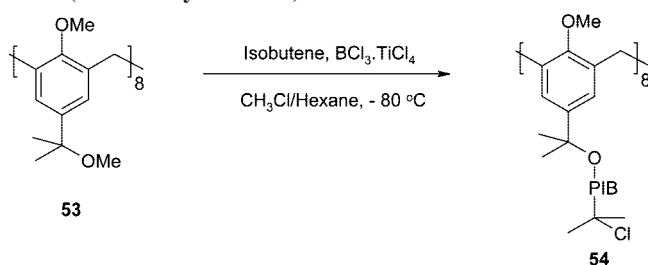
Chart 20. Salen Ligand I and Calixarene-like Salen Ligand 55 (R = H, *tert*-Butyl)
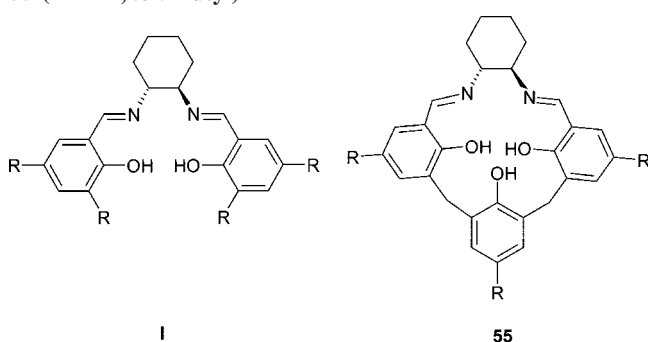
Scheme 20. Asymmetric Friedel−Crafts Reaction of Aromatic Amines with Glyoxylate
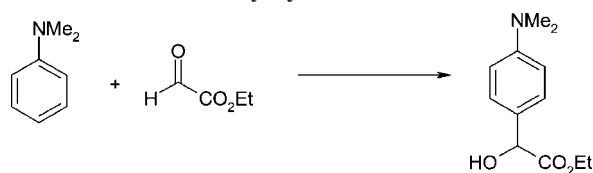
Table 14. Enantioselective Friedel−Crafts Reaction of Anilines with Glycoxylate Catalyzed by Ti-55[a]

amine	glyoxylate	yield (%)	OR/*ee* (%)
N,N-dimethylaniline	ethyl glyoxylate	85	(*S*)-(+) 98
N,N-dimethylaniline	methyl glyoxylate	90	(+) 57
N,N-dimethyl-*o*-toluidene	ethyl glyoxylate	78	(+) 84
N,N-dimethyl-*o*-toluidene	methyl glyoxylate	80	(+) 76
N,N-dimethylaminonapthalene	ethyl glyoxylate	81	(+) 50
N,N-dimethylaminonapthalene	methyl glyoxylate	84	(+) 93

[a] Conditions: aromatic amine (1.0 mmol), glyoxylate (2.0 mmol), catalyst (5 mol %), Et$_2$O (2 mL), 0 °C, 20−24 h.

surfaces by Katz et al., with a view to investigating the relevance of/role played by outer sphere/secondary interactions during the titanium-catalyzed epoxidation of cyclohexene using *tert*-butylhydroperoxide.[73] When grafted on silica,

Scheme 21. Zr(*S*)-BINOL-Catalyzed Allylation of Aldehydes (R = Ph, *n*-C$_7$H$_{15}$; *n* = 4, 6, 8)
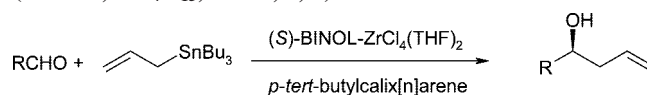
these heterogeneous catalysts have been shown to act in single-site fashion,[74] with the sterics associated with the calixarene ligand leading to discrete titanium centers. This isolation of titanium centers prevented the occurrence of unwanted oligomerization reactions and formation of inactive Ti−O−Ti structures.

During reaction, it was also proposed that the calixarene further imposes enhanced Lewis acidity at titanium by being able to organize the phenoxide ligation in such a way that more conventional monodentate aryloxides/alkoxides are not able to do and that this in turn was beneficial to the observed epoxidation rates. Furthermore, 100% selectivity to epoxide products was achieved. The similarity of the inner sphere coordination environments at titanium was confirmed by the use of UV−visible and solid-date NMR spectra as well as Ti−K edge X-ray absorption measurements. However, once grafted to an oxide surface such as SiO$_2$, TiO$_2$, or Al$_2$O$_3$, the titanium center was exposed to vicinal OH groups with differing acidities, which led to large changes (50-fold) in epoxidation turnover rates; fully hydroxylated TiO$_2$ or Al$_2$O$_3$ possess lower average surface hydroxyl pK_a. No such changes were observed when changes were made to the electronic properties of the upper rim of the calix[4]arene (measured via *ipso*-carbon ^{13}C NMR spectra), an observation that was consistent with the single Ti−O−Si bond and not the three Ti−O(calixarene) bonds, being central to the epoxidation kinetics. Two competing factors were thought to dictate epoxidation rates: (i) equilibrated hydroperoxide binding at the titanium center and (ii) rate-limiting oxygen transfer from the peroxide intermediate to the alkene. Low surface Brønsted acidity favored factor (i), while strongly H-bonded intermediates favored (ii).

Specific epoxidations studied included those of cyclohexene and 2,5-dimethyl-3-hexene using silica grafted titanium calix[4]arene complexes of the type **49** and the titanium hexahomotrioxacalix[3]arene **50** (Chart 19) with *tert*-butyl-hydroperoxide (TBHP) in *n*-octane at 333 K. This proved facile, with, for example, 50% conversion of cyclohexene achieved in ∼2 h, continuing on to >95% conversion.[75] Epoxidation reactions using a mixture of *cis*- and *trans*-2,5-dimethyl-3-hexene were carried out to test for any spatial constraints being placed on the titanium center by the calixarene ligand. Rates of conversion for differing densities of titanium centers were found to be very close, suggesting the presence of similar reactive centers, whereas only a slight increase in rate was observed in the absence of any calixarene framework from **49**, implying that the ligand causes minimal
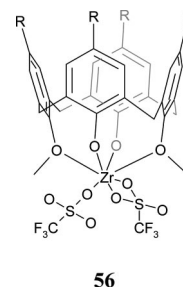

56

Figure 11. Bis(triflate) **56** (R = *tert*-butyl).

spatial constraints upon the metal center during epoxidation. There was a 20-fold increase in activity for the calix[4]arene complex over the hexahomotrioxacalix[3]arene derivative (that containing $-CH_2OCH_2-$ bridging groups), the lower level of activity of **50** was thought to arise from the more persistent coordination of the oxacalix[3]arene during catalytic turnover (i.e., the average titanium coordination number was greater in type **50** systems cf. **49** type systems). As a comparison, the homogeneous system **51** was found to exhibit much smaller epoxidation rates, thought to be due to the different modes of action/decomposition.

The structure **52** (Figure 10) was proposed for the active species, with the bound peroxide possibly H-bonded to nearby phenolic or silanolic groups or perhaps even present as the η^2-complex.[74] The Katz group has also immobilized, in a single step, calix[4]arenes onto silica via the use of SiCl$_4$ to activate the silica surface.[76]

Complexes **15** (section 2.1, Scheme 15) and **36** (section 2.2, Chart 16) were screened as catalysts for the epoxidation of allylic alcohols. For primary and secondary allylic alcohols, yields were good, although runs conducted using **36** required comparatively higher catalyst loadings. The presence of 4 Å molecular sieves proved critical in obtaining the observed yields.[77]

Calix[8]arene initiators of the type **53**, in combination with BCl$_3$/TiCl$_4$, were found to induce the living polymerization of isobutylene (Scheme 19).[78,79] Well-defined star polymers **54**, which consisted of eight polyisobutylene arms, were synthesized with complete conversion of isobutylene and narrow polyisobutylene dispersity. Best results were obtained using the *tert*-methoxy derivative **53**, due to its favorable solubility properties.

Polymerization runs were carried out in two stages. First, **53**/BCl$_3$ was combined with ca. 25% of the required isobutylene at -80 °C in CH$_3$Cl, and then, second, TiCl$_4$/ hexane and the remainder of the isobutylene were added. Polymerizations conducted in the absence of either BCl$_3$ or TiCl$_4$ gave <10% conversion. Termination of this core-first

method was achieved by addition of allyltrimethylsilane, affording *tert*-Cl and allyl end functionalized octa-arm polyisobutylene stars.

A titanium complex, formed via addition of [Ti(O*i*-Pr)$_4$], of the calixarene-like salen ligand **55** (Chart 20), has been utilized (prepared in situ) in the asymmetric Friedel−Crafts reaction of aromatic amines with glyoxylate (Scheme 20 and Table 14). High yields of the corresponding mandelic acid ester derivative were formed, with moderate to excellent enantioselectivity (up to 98% *ee*).[80] Comparative studies using the salen ligands **I** also showed good reactivity but poorer selectivity. It was suggested that a cavity associated with Ti/**55** may well be the source of the observed enantioselectivity.

4.3. Zirconium

For the Zr(*S*)-BINOL-catalyzed allylation of aldehydes, achiral *p-tert*-butylcalix[4]areneH$_4$ has been shown to promote high degrees of enantioselectivity (Scheme 21), using less than 2% of the catalyst.[81] Upon addition of the calix[4]arene, *ee* > 90% (96% for linear aldehydes) were achieved in high yields (85% for salicylaldehyde). Only in the case of cinnamaldehyde were the yield and *ee* poor. The use of the larger calix[6 or 8]arenes also displayed a similar level of promotion, although *ee*s' were lower than those that were achieved by the calix[4]arene system. In practice, the system can be generated in situ by mixing BINOL, ZrCl$_4$(THF)$_2$, and *p-tert*-butylcalix[4]areneH$_4$ with allyltributyltin, the latter helping to solubilize the resulting complex in the reaction medium (Et$_2$O). Without any calixarene present, yields of the desired products were found to be negligible, with starting material being recovered in ca. 80% yield. Interestingly, even the use of other phenols failed to provide the same activating effects. Floriani et al. noted that the bis(triflate) complex **56** (Figure 11) promoted the polymerization of THF.[52]

Chart 21. Vanadium-Based Calixarene (57−60) and Thiacalixarene (61 and 62) Complexes (R = *tert*-Butyl)
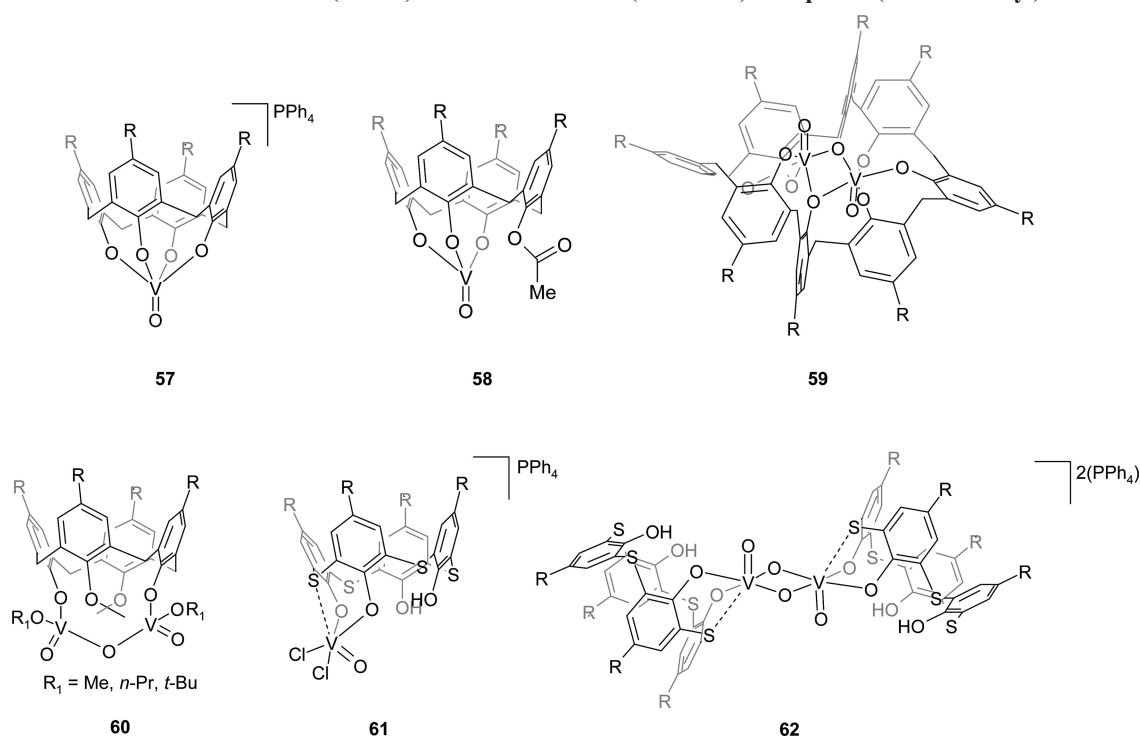
Chart 22. Vanadium-Based Calixarene Complexes 63–68 (R = *tert*-Butyl)

L = MeCN **63**

X = O **64**
X = N*p*-tol **65**

66

67

68

69

Figure 12. {[V(N*p*-tol)]₂calix[8]areneH₂} complex **69** (R = *tert*-butyl).

oxidized more efficiently by **62**, an observation thought to be due to the bimetallic nature of the procatalyst, with the oxidation chemistry occurring at the bridging oxo ligands. For **61**, the active species has been suggested to arise via a double intramolecular HCl elimination on elevating the temperature to afford the thiacalixarene analogue of **57**.

4.4. Vanadium

4.4.1. Oxidative Dehydrogenation

The oxidative dehydrogenation of short chain alkanes and methanol has been evaluated using a variety of vanadium-based calix[4 and 8]arene **57–60** and thiacalix[4]arene complexes **61–62** (Chart 21) by Limberg et al.[82–85] Using nonactivated aliphatic alcohols, no activity was observed for any of these procatalysts. The use of 1-phenyl-1-propargylic alcohol and fluorenol (carbonyl products, i.e., fluorenone, etc., were formed selectively) indicated that although the mononuclear complexes **57** and **58** show only low activities (TOF < 3 h⁻¹), the dinuclear systems demonstrated high activities, with **62** giving activities almost twice as high as the standard to which they were being compared, namely, [VO(acac)₂] (for 9-fluorenol TOF = 43 vs 24 h⁻¹). The versatility of the dinuclear complexes was further highlighted in their ability, albeit with lower activities, to oxidize nonfunctionalized hydrocarbons such as 9,10-dihydroanthracene. The ability of the thiacalixarene-based complexes was also assessed (cf. the methylene bridged counterparts), and an enhancement in activity was observed. Additionally, alcohols such as benzyl alcohol and crotyl alcohol were

4.4.2. Olefin Polymerization

Complex **60** (R₁ = *n*-Pr, Chart 21) as well as the complexes **63–68** (Chart 22) were all shown to catalyze the polymerization of ethylene using dimethylaluminum chloride (DMAC) as the cocatalyst in the presence of the reactivating substance ethyltrichloroacetate (ETA).[86] Trends similar to those seen above for **57–60** were demonstrated, such that the dinuclear *p-tert*-butylcalix[4]arene species were more active than their mononuclear counterparts: 1300–1500 g [PE]/mmol h bar for **64** and **65** vs 8700 g [PE]/mmol h bar for **60** and 10400 g [PE]/mmol hr bar for **66**. Employing hexahomotrioxacalix[3]arene as the ancillary ligand was found to have a dramatic effect upon the catalytic performance. Procatalysts **67** and **68** were found, under analogous conditions to the calix[4]arene procatalysts, to polymerize ethylene with activities as high as 92000 and 130000 g [PE]/mmol h bar, respectively. This phenomenal increase in activity was suggested to occur due to stabilization of the active species by the additional bridging ether groups of the ligand backbone, together with the *endo*-binding of the V = X (X = O, N*p*-tol) groups, which provided a "naked" metal face left easily accessible to incoming monomers.

Complex **69** (Figure 12) was isolated from the reaction of [V(N*p*-tol)(O*t*-Bu)₃] and *p-tert*-butylcalix[8]areneH₈ in ca. 70% yield.[87] At room temperature, **69**/DMAC was able to polymerize ethylene, albeit with a relatively low observed activity of 50 g [PE]/mmol h bar. With **69**/MAO, under comparable conditions, only poor activities were observed (8 g [PE]/mmol h bar); however, it should be noted that in neither screening was the reactivator ETA employed.

4.5. Niobium and Tantalum

The use of *p-tert*-butylcalix[4, 6 and 8]areneH₄,₆,₈ ligands as well as *p-tert*-butylhexahomotrioxacalix[3]areneH₃ ligand has also been extended to the other group V metals (see complexes **70–79**, Chart 23).[88] Structural comparisons showed that the niobium and tantalum analogues were isostructural, while ethylene polymerization screening ex-

Chart 23. Niobium and Tantalum-Based Calixarene Complexes 70−79 (R = *tert*-Butyl)

M = Nb, X = H   **70**
M = Ta, X = H   **71**
M = Nb, X = Me **72**
M = Ta, X = Me **73**

M = Nb **74**
M = Ta **75**

M = Nb **76**
M = Ta **77**

M = Nb **78**
M = Ta **79**
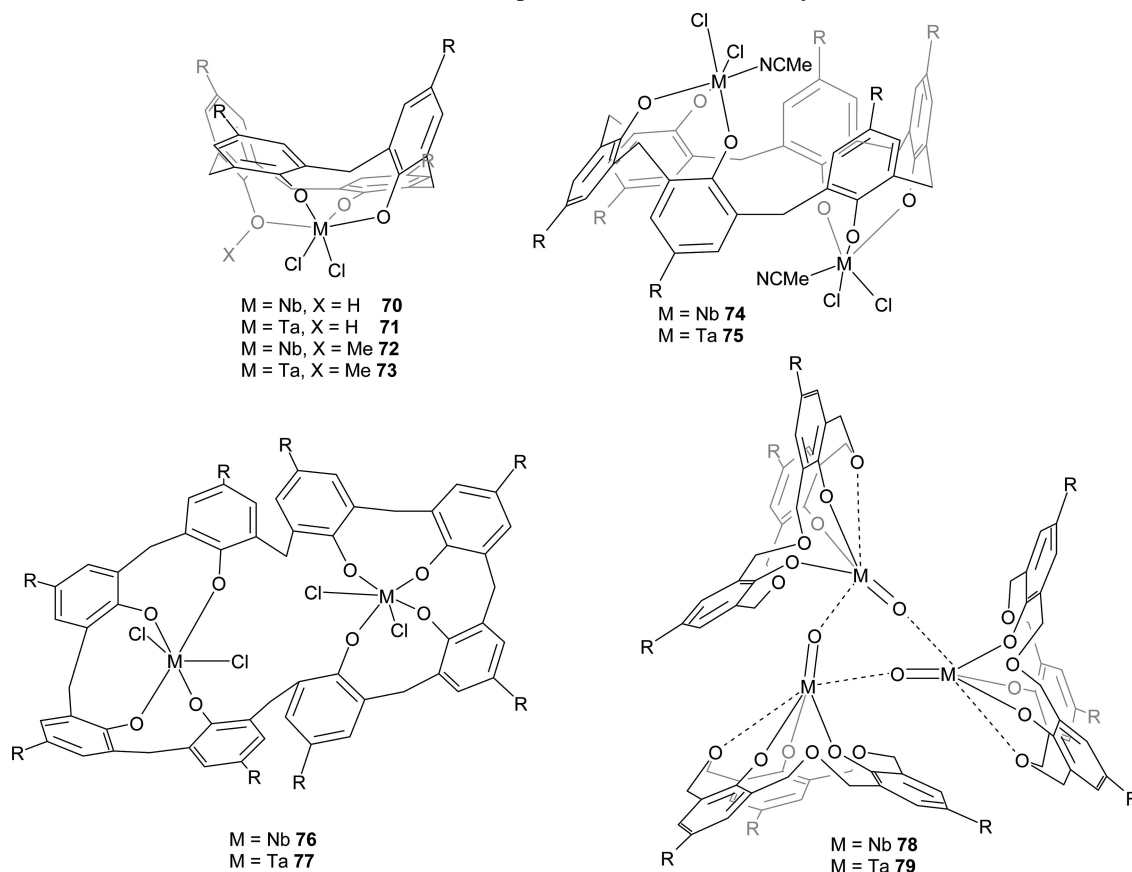
Chart 24. Postulated Structures for the Complex 80a−c (R = *tert*-Butyl)

80a

80b

80c
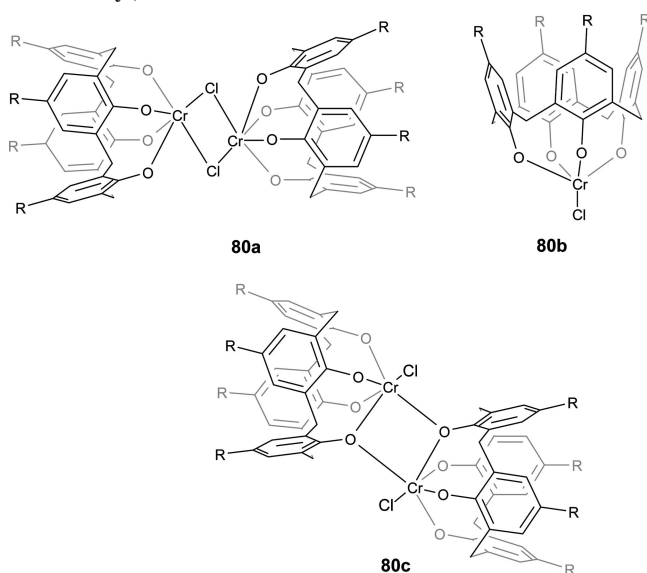
hibited a similar pattern, with both metal systems displaying poor activities (<50 g/mmol h bar) when using DMAC as the cocatalyst. The use of the oxacalix[3]arene ligand system once again was found to promote activities of up to an order of magnitude greater to those seen for the methylene-bridged systems (3−10 g/mmol h bar for **70−77** cf. 30−40 g/mmol h bar for **78** and **79**). However, the observed activities here strongly suggested that the combination of either niobium or tantalum with a calixarene type ligand set was unlikely to lead to a catalytic system to rival the well-established metallocene technology.

4.6. Chromium

As for niobium and tantalum, the combination of a chromium precursor and a calixarene ligand has yet to appear, which is likely to generate industrial interest. Kim et al.[89] found that the system resulting from *p-tert*-butylcalix[4]areneLi$_4$/CrCl$_3$(THF)$_3$/TEA was found to produce strictly linear polyethylene of high crystallinity with an activity of 175 g/mmol h under 3 bar of ethylene. The structure of the procatalyst **80** (Chart 24) was proposed to be either a chloro-bridged dimer (**80a**) or a mononuclear complex with a terminal chloride (**80b**). However, aryloxide bridges derived from the calixarenes (as in **80c**) cannot be ruled out, and such structures have been shown to be common place in calix[4]arene chemistry.[90] The system produced low molecular weight polymers (M_n typically ranging from 910 to 9740) without the additional need of hydrogen gas with a narrow polydispersity $M_w/M_n < 3$, implying single site catalysis. In a number of screening experiments using this system, it was found that the activity was linearly proportional to the chromium concentration. The activity was also linearly proportional to the ethylene pressure at pressures less than 10 bar, whereupon there was a tail-off of catalytic activity. Similarly, activity was observed to increase with increasing temperature up to ca. 60 °C and then quickly levels off, whereas the polymer average molecular weight and melting point both decreased upon increasing the temperature. The catalytic activity was also affected by the choice of cocatalyst (Table 15), with the poorest results obtained when using MAO.

Reaction of *p-tert*-butylcalix[4]areneH$_4$ with 4 equiv of *n*-BuLi and subsequent treatment with CrCl$_3$(THF)$_3$ afforded the aryloxide bridged complex **81**.[91] However, more com-

Table 15. Ethylene Polymerization Behavior of 80[a]

cocatalyst	activity (g/mmol h bar)	M_w ($\times 10^{-3}$)	M_n ($\times 10^{-3}$)	M_w/M_n	mp (°C)	crystallinity (%)
TEA	175	2.95	1.10	2.68	124.1	85.7
TIBA	223	7.16	1.35	5.29	126.4	84.2
MAO	20	23.96	2.47	9.70	131.4	75.0

[a] Conditions: Catalyst concentration = 0.02 mmol in 50 mL of toluene, Al/Cr = 100, 60 °C, 3 bar, 1 h.

Chart 25. Chromium-Based Calixarene Complexes 81−86 [R = *tert*-Butyl, L = MeCN, and L′ = K(THF)₂]

81   **82**   **83**

X = Me 84
X = n-Pr 85

86
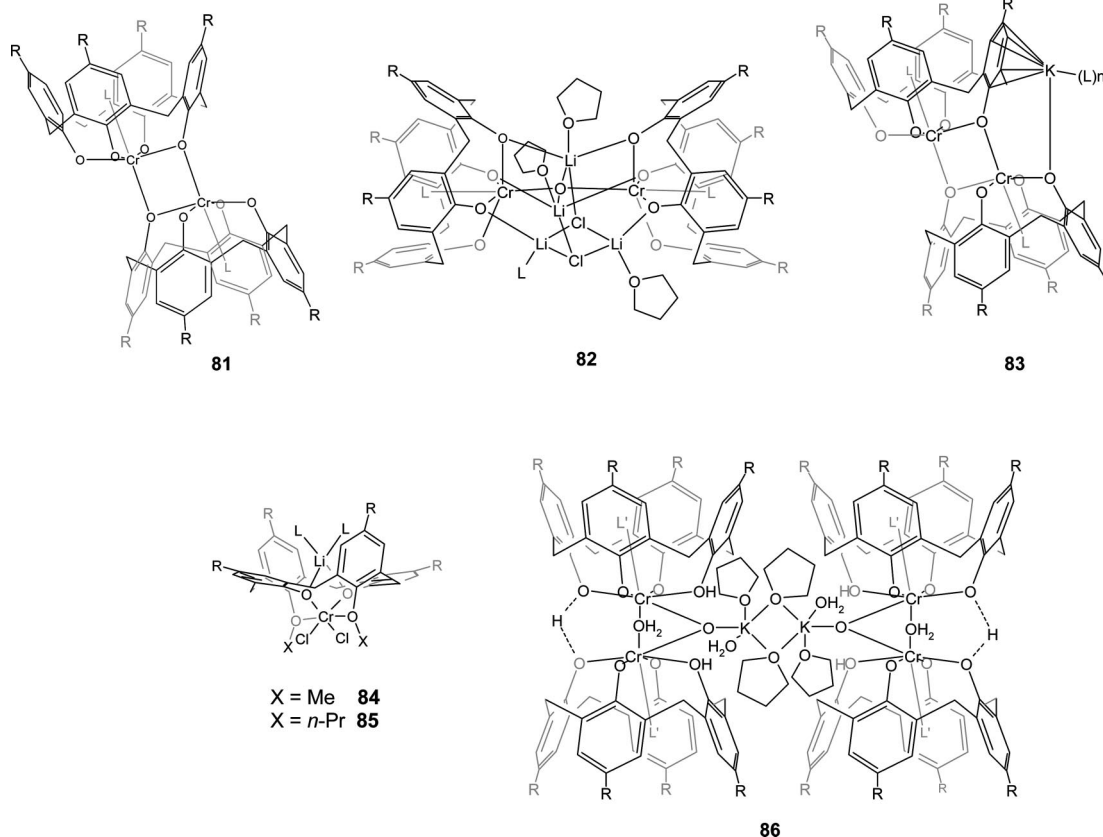
Scheme 22. Metallocyclopentane Formation

R = H **87**
R = Me **88**

R = R' = H **89**
R = Me, R' = H **90**
R = R' = Me **91**
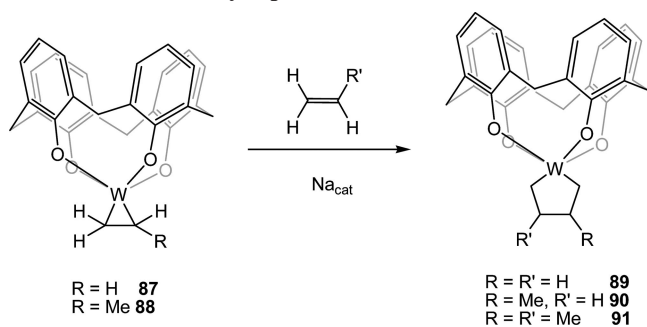
monly, it was found that reactions involving calixarenes/alkali metals and either CrCl₃(THF)₃ or CrCl₂·THF led to products that retained alkali-metal cations (see **82−86**, Chart 25). Under standard conditions and 1 bar of ethylene, these complexes were found to be poor procatalysts for ethylene polymerization with activities of <1 g [PE]/mmol h bar; DMAC was the only cocatalyst to produce any isolable polymer. The resulting polymers had broad polydispersities (>10) implying multiple or ill-defined active sites.

4.7. Tungsten

The group of the late Carlo Floriani published much elegant work concerning olefin rearrangement assisted by a metal-oxo (d² tungsten calix[4]arenes) surface. Of particular note here was the ability of the ethylene and propylene complexes **87** and **88** to undergo an electron-transfer-catalyzed reaction with ethylene and propylene to afford the corresponding metallocyclopentanes **89−91** (Scheme 22). Such metallocyclopentanes were shown to be capable of undergoing photochemical rearrangement to the corresponding alkylidenes.[92]

4.8. Manganese

Manganese salen calix[4]arenes **92−95** (Chart 26), using 4-phenylpyridine *N*-oxide as a coligand and NaClO as an oxygen source, have been tested as enantioselective epoxidation catalysts of (*Z*)-aryl alkenes (Scheme 23).[93] Higher *ee* values were achieved in the presence of the coligand, with steric factors concerning the *β*-carbon atom of the aryl alkene indicating that any group larger than methyl decreased the rate of reaction. The presence of the calixarene moiety, however, could not successfully be shown to increase catalytic selectivity for these epoxidation reactions via molecular recognition mechanisms.

The calix[6]arene-bearing six trioxadecyl groups [(CH₂-CH₂O)₃CH₃] at the lower rim (i.e., **2**, section 2.1), has been utilized in the permanganate oxidation of alkenes, alkynes,

Chart 26. Manganese Salen Calix[4]arene Complexes 92−95 (R = *tert*-Butyl and R$_1$ = *n*-Pr)

92   **93**   **94**   **95**
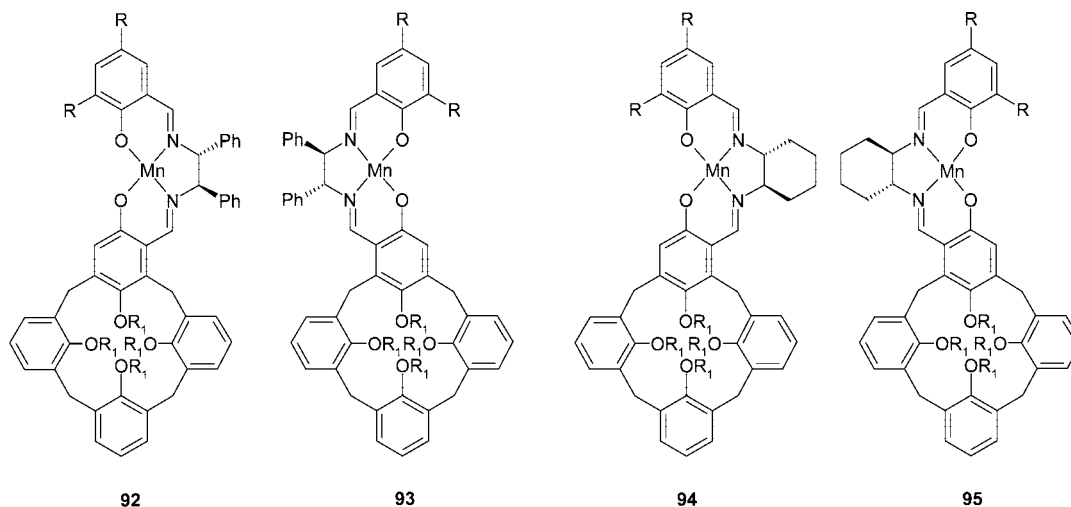
Scheme 23. Epoxidation of (Z)-Aryl Alkenes
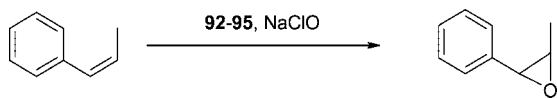
Chart 27. Ligands 96−98 and K (R$_1$ = *n*-Pr)

96: R = *t*-Bu

97a: R = *t*-Bu
97b: R = H

98: R = *t*-Bu

J
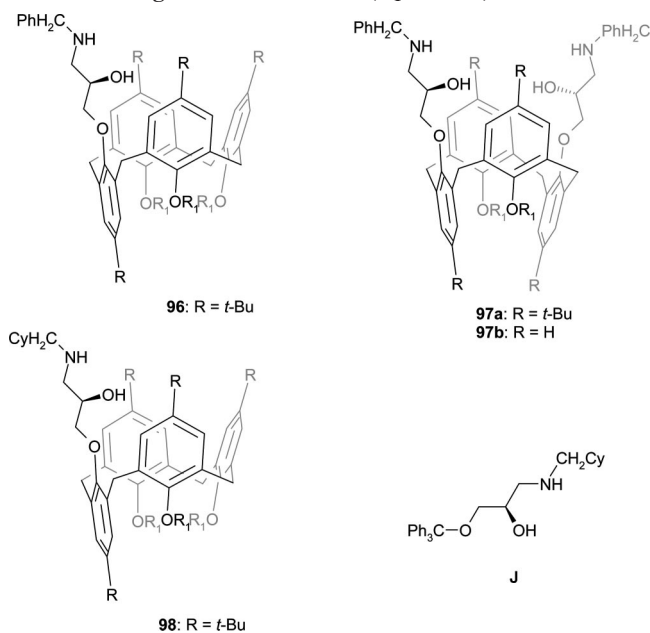
and alcohols. Primary alcohols gave carboxylic acids in near quantitative yields, while secondary alcohols led to ketones in moderate to high yields (for further details, see section 2.2).[32]

Researchers in the Ukraine have presented the catalytic use of calix[4]arenes in a number of permanganate oxidation reactions. The oxidation of primary alcohols and alkenes with excess KMnO$_4$ in the presence of calixarene led to the corresponding carboxylic acid, while secondary alcohols led

Scheme 24. Asymmetric Transfer Hydrogenation of Acetophenone and Reference Compound J

K
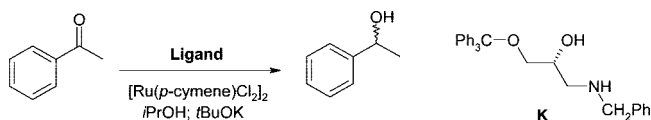
Table 16. Asymmetric Transfer Hydrogenation of Acetophenone^a

ligand	ligand/Ru	S/C	time (h)	conversion^b (%)	*ee* (%) enantiomer (S)^b
96	2	100	1 (3)	75 (97)	87 (86)
96	1	100	1 (3)	47 (67)	87 (87)
97a	1	100	1 (3)	12 (18)	84 (83)
97b	1	100	1 (3)	14 (16)	87 (78)
97b	1	100	22 (6 days)	55 (71)	74 (69)
98	2	100	1 (24)	39 (60)	90 (88)
98	2	100	48	71	88
K	2	100	1 (24)	42 (47)	89 (87)
J	2	100	1 (15)	71 (95)	88 (87)

^{a} Reaction conditions: acetophenone (0.5 mmol), [Ru(*p*-cymene)Cl$_2$]$_2$ (0.005 mmol), and *t*-BuOK (0.6 mmol) in 6 mL of 2-propanol at room temperature. ^{b} Conversion and *ee* were determined by chiral GC analysis.

to ketones, The same group also found that the use of certain

Chart 28. Phosphorus-Bearing Calix[4]arene Ligands 99−107 (R = *tert*-Butyl) and Rhodium Complexes 108 and 109
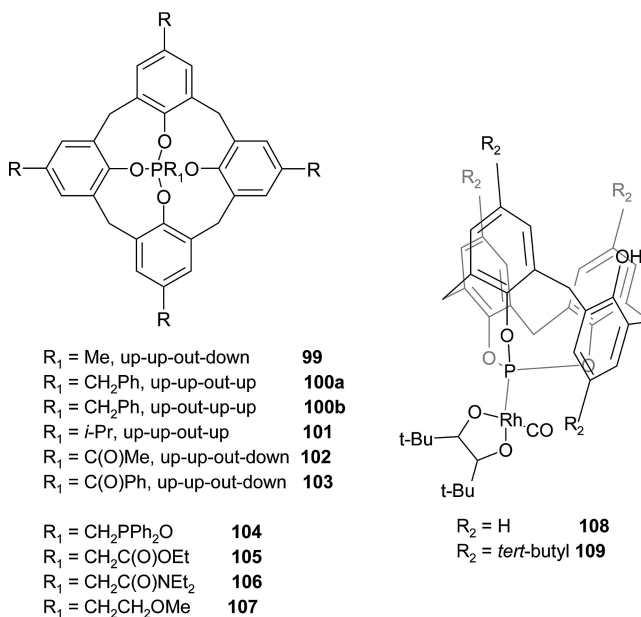
R$_1$ = Me, up-up-out-down **99**
R$_1$ = CH$_2$Ph, up-up-out-up **100a**
R$_1$ = CH$_2$Ph, up-out-up-up **100b**
R$_1$ = *i*-Pr, up-up-out-up **101**
R$_1$ = C(O)Me, up-up-out-down **102**
R$_1$ = C(O)Ph, up-up-out-down **103**

R$_1$ = CH$_2$PPh$_2$O **104**
R$_1$ = CH$_2$C(O)OEt **105**
R$_1$ = CH$_2$C(O)NEt$_2$ **106**
R$_1$ = CH$_2$CH$_2$OMe **107**

R$_2$ = H **108**
R$_2$ = *tert*-butyl **109**

Chart 29. Calix[4]arene Phosphite Conformations Identified by van Leeuwen et al. [R = *tert*-Butyl; X = H, Me, CH₂Ph, *i*-Pr, *n*-Bu, C(O)Me, and C(O)Ph]

L1   **L2**   **L3**
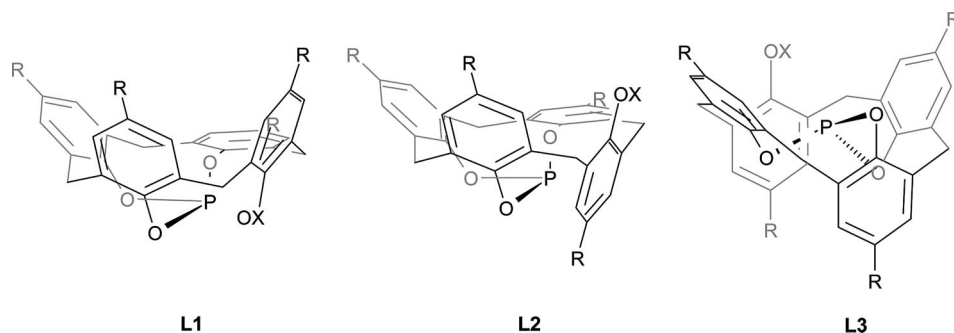
Scheme 25. Hydroformylation of 1-Octene
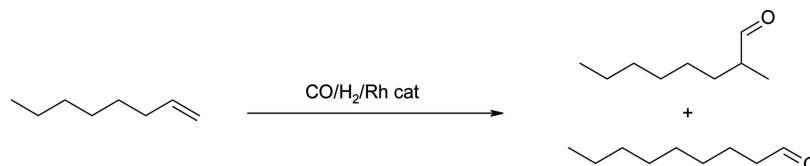
Scheme 26. Hydroformylation of 1-Hexene
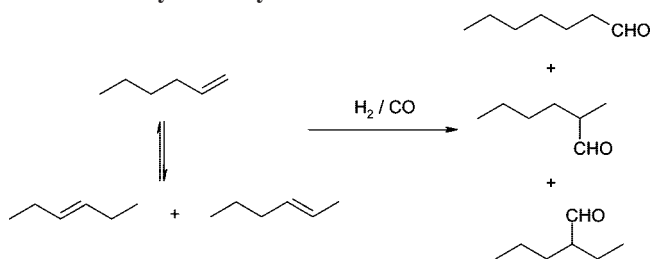
Table 17. Hydroformylation of 1-Hexene Using Complexes 108 and 109[a]

catalyst	$L_{a,b}$:Rh	T (°C)	conversion %	aldehydes (%)	n:i	hexane (%)
108	1	160	99.5	84	1.2	16
108	10	160	99.4	82	1.2	18
109	1	160	99.5	81	1.2	19
109	10	160	99.5	86	1.4	14
109	1	120	99.7	90	1.0	9
109	1	80	99.4	92	0.8	7

[a] Conditions: [Rh] = 0.063 mmol, 1-hexene (18.8 mmol), solvent = CH₂Cl₂, H₂/CO 30 atm 1:1, 160 °C, 60 atm overall pressure, 3 h.

tetra-substituted calixarenes out-performed (in terms of product purity) 18-crown-6 for the alkylation of phenols by esters of bromocarboxylic acid.[94]

5. Late Transition Metals

5.1. Ruthenium

Calix[n]arenes (n = 4, 6, 8) functionalized at the lower rim with dichloroacetate units have been shown to initiate the living radical polymerization of methyl methacrylate (MMA). The process was catalyzed by RuCl₂(PPh₃)₃ in the presence of Al(O*i*-Pr)₃ and led to tetra-, hexa-, and octa-armed polymers, respectively. Hydrolysis of the ester linkage allowed for the isolation of linear polymers, the number average molecular weight of which were ca. 1/4, 1/6, and 1/8 of those observed for the respective [n]-armed star polymer. AB-block star copolymers of MMA and *n*-butyl methacrylate were synthesized by sequential living polymerization initiated by the calix[8]arene-based initiator.[95]

Chiral calix[4]arenes bearing β-amino alcohols at the lower rim (Chart 27) have been synthesized via the use of glycidyl groups and subsequent ring opening with amine. In the presence of [Ru(*p*-cymene)Cl₂]₂, the monofunctionalized ligands **96** and **98** proved to be useful catalysts (the exact nature of the catalyst is not known) in the asymmetric transfer hydrogenation of acetophenone (Scheme 24 and Table 16), while the bifunctionalized ligands **97a** and **97b** proved less promising.[96] Results were compared with the reference compounds **J** (a trityl ether) and **K** (a β-amino alcohol).

5.2. Rhodium

5.2.1. Hydroformylation

Rhodium-catalyzed hydroformylation of olefins is a major area of homogeneous catalysis[97] and as such has attracted a large amount of calixarene-based research, particularly phosphate- and phosphine-derived calixarenes or so-called "phosphacalixarenes".[98]

Calix[4]arene phosphites such as those depicted in Chart 28 can exist in six possible conformations. Under the conditions employed by van Leeuwen et al., only three conformations (**L1**−**L3**, Chart 29) were identified (two by X-ray crystallography). Variable temperature ¹H NMR experiments showed that even for X = H or Me, there was no inversion of the phosphorus configuration. To assess the conformational effect of the calixarene ligand upon catalytic activity, the **99**−**103**/[Rh(acac)(CO)₂]-catalyzed hydroformylation of 1-octene (Scheme 25) at 80 °C using 20 bar CO/H₂ was undertaken.[99]

All systems exhibited fast catalytic performances with TOF's ranging from 1600 to 8100 h⁻¹ for 0.1 mM [Rh]. A noticeable difference was observed upon changing of the calix[4]arene conformation; **99** and **100b**, where the phosphorus lone pairs are embedded into the calix[4]arene cavity, showed the slowest catalytic behavior, whereas **100a** and **101** afforded the highest activities due to decreased steric hindrance of the phosphorus lone pair as indicated by X-ray crystallography.

Proligands **104**−**107**, found exclusively in the cone conformation, afforded under analogous conditions to those of **99**−**103**, TOF's of up to 4500 h⁻¹ (**97**).[100] In the case of

Chart 30. Phosphorus-Bearing Calix[4]arenes 110–118

R = *t*-Bu, R₁ = *t*-Bu, R₂ = OMe **110**
R₁ = *i*-Pr, R₂ = H **111**
R₁ = Me, R₂ = H **112**
R₁ = R₂ = H **113**

114, 115, 116 and 117

118

114: R = *t*-Bu
115: R = H   R' =
118: R = *t*-Bu

116: R = *t*-Bu   R' =
117: R = H
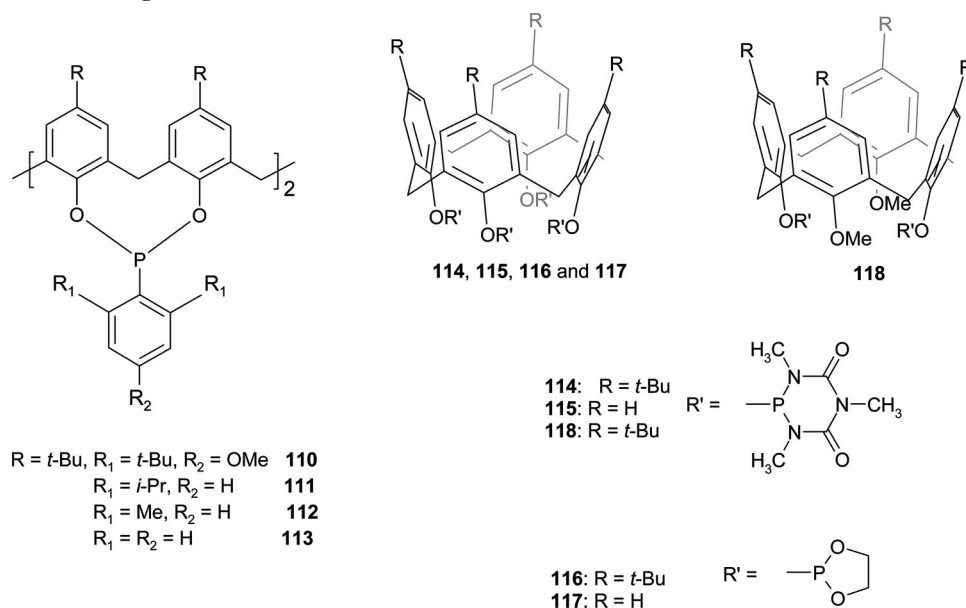
Table 18. Hydroformylation of 1-Octene Catalyzed by 110–113[a]

ligand	conversion of 1-octene (%)	selectivity (%)			nonanal regioselectivity (%)
		nonanals	*n*-octenes	octane	
110	63 (8 h)	61	12	27	99.5
111	65 (4 h)	75	13	12	96.4
112	53 (4 h)	16	16	13	92.4
113	90 (4 h)	12	82	6	70.0

[a] Conditions: Rh as [Rh(CO)₂(acac)], olefin/Rh = 4000, L/Rh = 5; ligand **110**: 20 bar, 100 °C; ligands **111–113**: 5 bar, 80 °C.

Table 19. Hydroformylation of 1-Octene Catalyzed by 119–121[a]

ligand	Rh:ligand	yield (%)	*n*-nonane (%)	*i*-octane (%)	*i*-heptane (%)	*i*-hexane (%)	n:i
119	1:1	58.7	61.8	32.5	4.3	1.4	1.62
119	1:2	70.5	60.7	32.4	5.0	1.9	1.54
119	1:10	89.2	58.4	35.0	5.2	1.4	1.40
121	1:0.5	80.9	41.7	36.6	12.3	9.4	0.72
121	1:1	99.9	49.6	34.9	9.5	6.0	0.98
121	1:2	90.8	51.6	34.8	8.5	5.1	1.07
121	1:10	54.2	63.4	36.6			1.73
120	1:1	83.3	53.4	35.1	7.3	4.2	1.15
120	1:2	85.4	58.9	34.0	5.0	2.1	1.43
120	1:10	46.0	59.2	39.0	1.5	0.3	1.45

[a] Conditions: [Rh(acac)(COD)] 0.604 mM, 5 mL of toluene, 15 mL of 1-octene, 40 bar, 100 °C.

102, however, the activities are ca. 1.6 times lower. For **104–107**, activities were found to decrease with increasing donor strength in the sidearm oxo group, i.e., **107** > **104** > **105** > **106**. For good donors, there was also evidence for an increased linear:branched aldehyde product ratio.

In the hydroformylation of 1-hexene (Scheme 26 and Table 17), high levels of monomer conversion (>99%) were achieved with both monophosphites **108** and **109**, for which the calix[4]arene ligands adopt "up–up–out–down" orientations (see **L2**, Chart 29); regioselectivity was, however, very low (n:i ∼ 1:1).[101]

Using **110** (Chart 30 and Table 18) in the hydroformylation reaction of 1-octene with [Rh(CO)₂(acac)] at 20 bar CO/H₂ gave aldehyde selectivity of 61% and a high regioselectivity in favor of *n*-nonanal (99.5%).[102] Upon reduction of the bulk

of the phosphite moiety, **111** and **112** gave increased activity with only a slight decrease in regioselectivity (>90%). As predicted by molecular modeling, the use of **113** led to a dramatic decrease in regioselectivity due to loss of steric protection around the metal center; yet, this system managed to demonstrate the highest level of activity with 90% conversion of starting material in just 4 h.

At 40–50 bar H₂/CO, [(acac)Rh(COD)]/**114** catalyzed the hydroformylation of 1-octene,[103] and for this process, it was found that changing the solvent from toluene to THF increased the regioselectivity. The use of two methoxy groups

Chart 31. Phosphorus-Bearing Calix[4]arenes 119–121 (R = *tert*-Butyl)

119

120

121
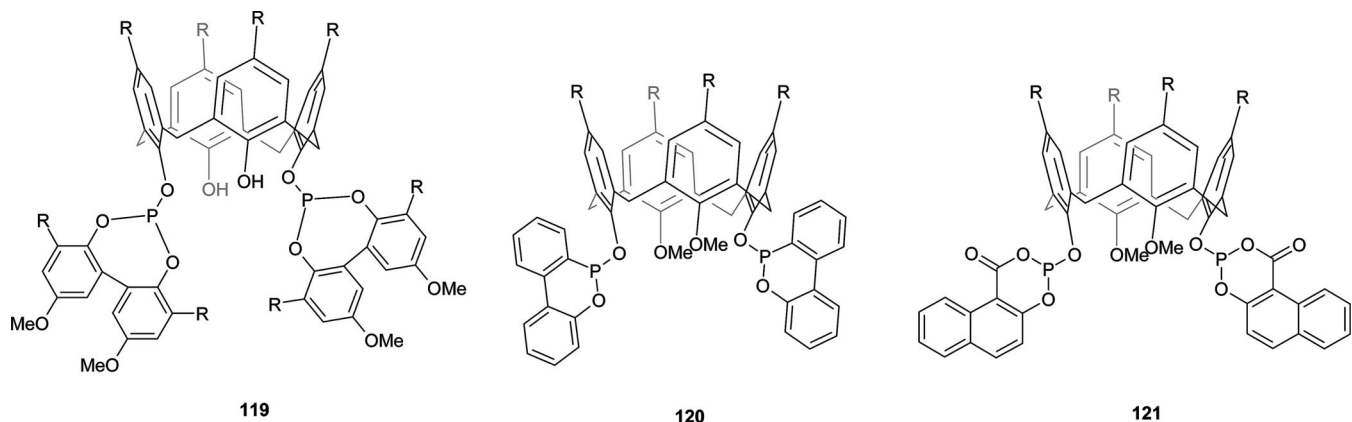
Chart 32. Phosphorus-Bearing Rhodium Calix[4]arene Complexes 122−128

Y = *n*-Pr, R = Me, X = H **123**
Y = *n*-Pr, R = *i*-Pr, X = H **124**
Y = *n*-Pr, R = Ph, X = Br **125**

Y = *n*-Pr, R = Me **126**
Y = *n*-Pr, R = *i*-Pr **127**
Y = *n*-Pr, R = Ph **128**

122
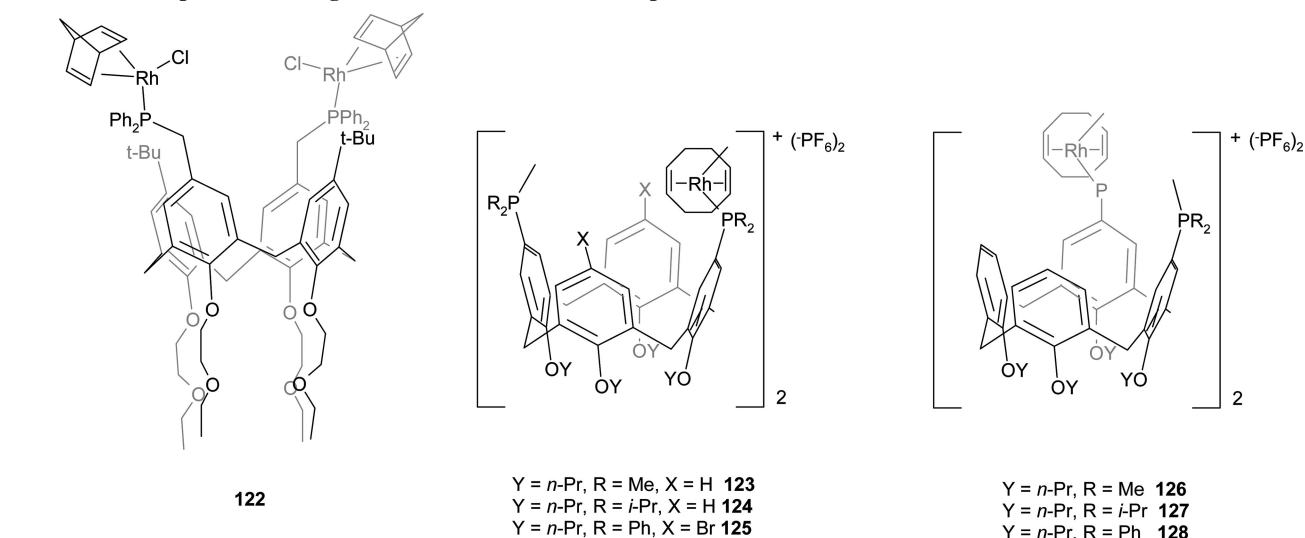
Chart 33. Upper-Rim Functionalized Calix[4]arenes 129 and 130 and TPPTS

Ar = *m*-MOSO$_2$C$_6$H$_4$
M = (n = 1) 9 x Na$^+$, 1 x H **129**
    (n = 2) 10 x Na$^+$ **130**
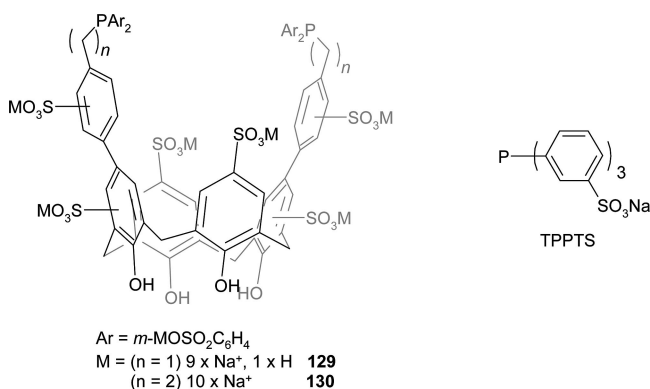
in **118** gave no increase in activity as compared to that of **114**, with all catalytic systems giving good/excellent activities with yields of ca. 90% in most cases. Procatalysts **116** and **117** displayed a higher degree of sensitivity with respect to the reaction conditions than did **114**, **115**, and **118**; an increase in the Rh:ligand ratio from 1:1 to 1:5 led to the death of the catalytic reaction.

Catalytically active species for the hydroformylation of 1-octene were formed in situ by the mixing of **119**, **120**, or **121** (Chart 31 and Table 19) with [(COD)Rh(acac)] prior to catalysis.[104] Proligands **119**−**121**/Rh favored the formation of aldehydes with yields of 50−65%. With **119**, an increase in ligand:Rh ratio was found to increase activity, while regioselectivity remained almost constant. For **120** and **121**, the reverse trend was observed, whereby a maximum ratio of 1:1(**120**) and 2:1(**121**) of ligand:Rh produced the highest yield of aldehyde; any increase beyond this led to a drop in activity and an increase in *n*-selectivity (*n*/*i*: 0.72 to 1.73 for **120** and 1.15 to 1.45 for **121**).

Other phosphorus-containing calixarenes have been found to be active in olefin hydroformylation.[105] The dinuclear rhodium complex **122** (Chart 32) catalyzed the hydroformylation of styrene (CO/H$_2$ = 1 bar; 70 °C with a styrene/Rh ratio of ∼585) in the presence of NEt$_3$. Products obtained indicated a high level of regioselectivity for the branched aldehyde (*n*/*i* = 9:91) with a turnover frequency of 31 mol of alkene/mol of Rh/h. The addition of 1 equiv of the free diphosphine ligand was found to maintain selectivity, while

improving activity by over 60% was due to increased electron density on the two rhodium centers from the additional phosphorus donors. There was no catalyst decomposition during the hydroformylation runs. The upper rim functionalized rhodium complexes **123**−**128** have shown activity for the hydroformylation of 1-hexene, styrene, vinyl acetate, vinyl benzoate, and vinyl *p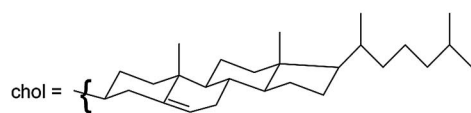-tert*-butylbenzoate; 1-hexene gave the highest turnover frequencies (up to 250 h^{-1}) with increasing bulk of the phosphine groups leading to increased activities.[106] Regioselectivites vary substantially depending upon the substrate in question. Best results were observed with vinylbenzoate and *p-tert*-butylbenzoate giving an *i*-selectivity of over 99% (pressure = 70 atm, 50 °C). Under less harsh conditions (7 atm, 35 °C), **124** and **127** were still able to catalyze the hydroformylation of 1-hexene with TOF and regioselectivities comparable to those of industrial catalysts. Preliminary results using styrene and vinyl acetate as the substrates gave comparable regioselectivity with increased activity in the case of vinyl acetate.

Use of the upper rim functionalized calix[4]arenes **129** or **130** (Chart 33)/[Rh(acac)(CO)$_2$] with a 1:1 mixture of carbon monoxide and hydrogen in water at 100 °C and 4 MPa for 12 h converted 1-octene to nonanals with high yields (up to 73%), as compared to 21% conversion for the standard TPPTS/[Rh(acac)(CO)$_2$] (TPPTS = triphenylphosphine trisulfonate) complex.[107] Decreasing the length of the alkane chain was found to have a detrimental effect upon catalytic activity. Furthermore, **130** showed retention of catalytic ability and selectivity when recycled two or three times. The addition of TPPTS to the **130**-catalyzed system resulted in a significant enhancement in selectivity but somewhat lower yield. The system using **130** was also effective for the hydroformylation of dec-1-ene. In the presence of 2,6-di-*O*-methyl-*β*-cyclodextrin, high activity was also observed for internal alkenes.[108] Reusability experiments with **129** indicated that activity was maintained after five reaction cycles.

A lower rim proximally functionalized diphosphinocalix[4]-arene when complexed with [Rh(CO)$_2$(THF)$_2$]BF$_4$ gave complexes **131** and **132** (Chart 34), both of which were found to be active for the hydroformylation of styrene.[109] Activities in these instances were lower (TOF = 0.5 h^{-1}) under harsher conditions (1:1 CO/H$_2$ = 40 bar, 40 °C for 144 h), with the usual low selectivity for branched aldehydes (*n*/*i* = 5:95). Hydrogenation of cyclohexene (H$_2$ 50 bar, 60 °C) in

Chart 34. Diphosphinocalix[4]arenes 131−138 (R = *tert*-Butyl)

R₁ = R₂ = Et **131**
R₁ = H, R₂ = (*R*)-CHMePh **132**

R₃ = *n*-Pr **133**
R₃ = CH₂CO₂Et **134**
R₃ = CO₂chol **135**

R₄ = H **136**
R₄ = SiMe₃ **137**
R₄ = CH₂(O)NHCH(Me)Ph **138**

chol =
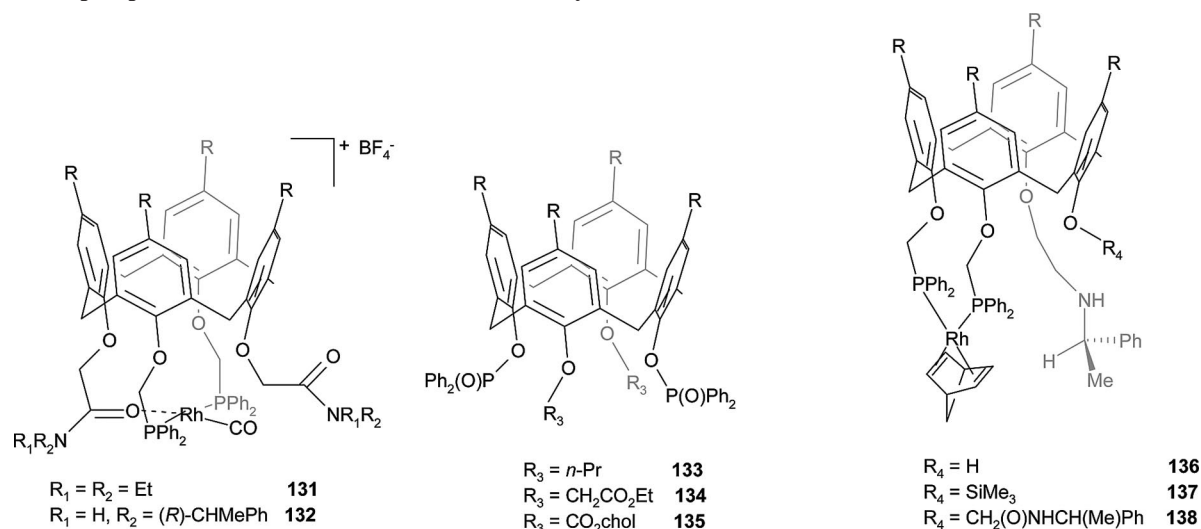
methanol using **132** also gave low activities (TOF 145 h⁻¹) attributed to unfavorable sterics surrounding the metal center. [Rh(acac)(CO)₂] when mixed with the lower rim functionalized calix[4]arene phosphites **133−135**, effectively catalyzed the hydroformylation of 1-octene,[110] with the highest TOF (1204 mol/mol Rh) found for **133** in a ligand to metal ratio of 1:1. Large selectivity for linear aldehydes, especially using **134** and **135** (*n/i* ca. 10), arose from a bite angle significantly larger than 90°, which resulted in the equatorial−equatorial binding of the phosphite groups to the rhodium center. "Pockets" formed by the ligand (and possible hemilabile coordination of the C=O groups in the case of **134** and **135**) favored the formation of "Rh(*n*-alkyl)" and ultimately linear aldehydes. This trend for increased selectivity for linear aldehydes was also observed for the hydroformylation of styrene, which due to its increased bulk was influenced by the presence of these pockets to an even greater degree (*n/i* ratio for **134** = 34/66). For olefin hydrogenation, it was found that procatalyst **138**, having the two phosphorus atoms bound distally (these ligands, and the 1,3-regioisomers, have also been employed in the palladium-catalyzed alkylation of 1,3-diphenylprop-2-enyl acetate—see section 5.4.4), readily reduced the monomer dimethyl itaconate with a TOF of 267 h⁻¹.[111] Decreasing the size of the R group led to a

Chart 35. Ligands 140−144

140a R₁ = *t*Bu, R₂ = CH₂CH₂CH₃ (*S,S*)
140b R1 = *t*Bu, R₂ = CH₂CH₂CH₃ (*R,R*)
141a R1 = *t*Bu, R₂ = CH₂Ph (*S,S*)
141b R1 = *t*Bu, R₂ = CH₂Ph (*R,R*)
142 R₁ = *t*Bu, R₂ = CH₂— (*S,S*)

143 R₁ = *t*Bu, R₂ = (*R,R*)

144 R₁ = H, R₂ = CH₂CH₂CH₃ (*S,S*)
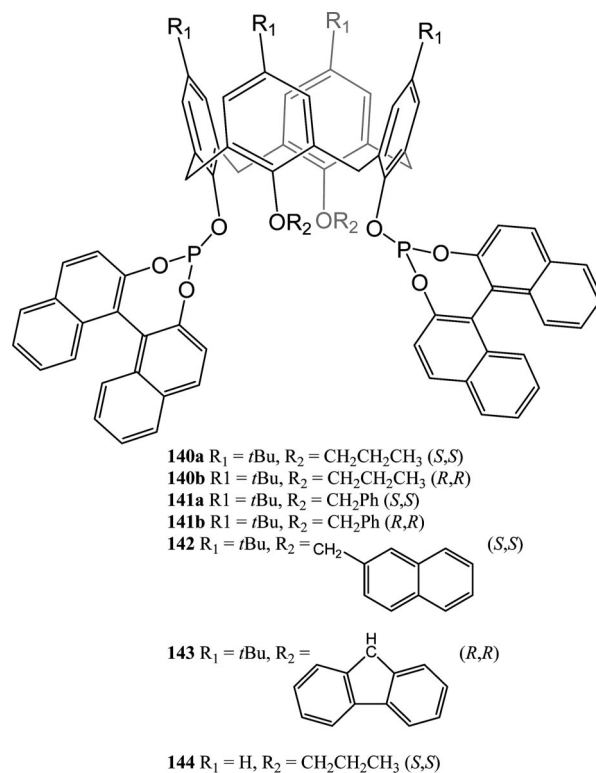
further increase in the TOF such that **137** and **136** displayed a TOF of 1176 and 2000 h⁻¹, respectively, as well as an improvement in the enantioselectivity of the products (*ee* for **136** being 48%).

The diagonal regioisomer of distal **138**, namely, **139** (Figure 13), has been utilized in the hydroformylation of styrene.[112] At 40 °C and 40 bar (CO/H₂ 1:1) in dichloromethane/benzene using a styrene to metal ratio of 350:1, 100% conversion was achieved in 48 h (ca. 7.5 turnovers per Rh per h). This slow reaction rate was thought to be due to partial encapsulation of the metal center, thereby hindering substrate approach. Product analysis revealed high regiose-
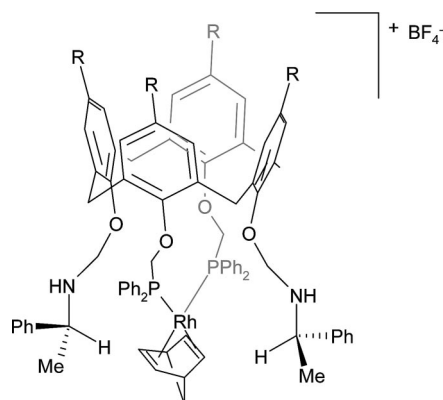
Figure 13. Complex **139**.

Table 20. Rhodium-Catalyzed Hydroformylation of Styrene Using Diphosphites 140 and 141[a]

ligand	$p(CO/H_2)$ (bar)	time (h)	conversion (%)	TOF	branched x (%)	linear (%)
140	20	5	18.3	180	41.2	58.8
140	10	5	21.7	220	34.8	65.2
		24	58.7	120	3.6	67.4
141	20	4.5	19.1	210	26.4	73.6
141	10	5.5	21.4	200	23.9	76.1
		24	64.4	134	23.4	76.6

[a] Conditions: styrene (10 mmol), styrene/Rh = 5000, ligand/Rh = 10, CO/H_2 = 1:1, 80 °C, toluene/n-decane (15 mL/0.5 mL).

Scheme 27. Rhodium-Catalyzed Hydroformylation of α-Olefins (R^1 = C_6H_{13}, Ph)
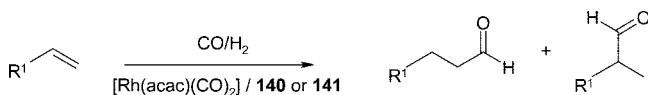
lectivity with 2-phenylpropanal and 3-phenylpropanal formed in the ratio 95:5.

For the hydroformylation of 1-octene, TOF's up to 1440 h^{-1} were achieved by Rh complexes of **140** and **141** (Chart 35, and Scheme 27, Table 20), giving linear:branched ratios for the products as high as 58:1.[113] Switching from 1-octene to *trans*-2-octene led to a drop in activity; however, selectivity of the resulting products remained high (ca. 4.5 as compared to 0.9 for PPh$_3$). When assessed for styrene hydroformylation (Table 20), both catalysts favored linear aldehyde formation with an increase in steric bulk of the catalyst leading to increased linear selectivity (up to 73.6%). A reduction in the H$_2$/CO pressure led to a further increase in selectivity (76.1%).

This work has been followed up by a more recent study in which the family of di-*O*-alkylated diphosphite ligands was extended to include CH$_2$-napthyl (**142**) and *o*-fluorenyl (**143**) derivatives. The bite angle associated with this ligand family is ca. 110°. Reaction with [Rh(acac)(CO)$_2$] afforded **145** in high yield (75%). In complex **145** (Figure 14), the rhodium center sits in a pocket defined by the two napthyl planes (which are related by a C_2-axis) and by the two apical R groups. Preliminary reactivity studies with CO/H$_2$ (5 bar) suggested the formation of a [RhH(CO)$_2$L] type complex, in which the phosphorus centers are equatorial. Calculations gave insights into the nature of the cleft in which the rhodium center resides and highlighted the directional constraints imposed upon incoming olefinic substrates.

For octene hydroformylation, conducted at 80 °C under 20 bar CO/H$_2$ and in situ-generated catalyst, the observed
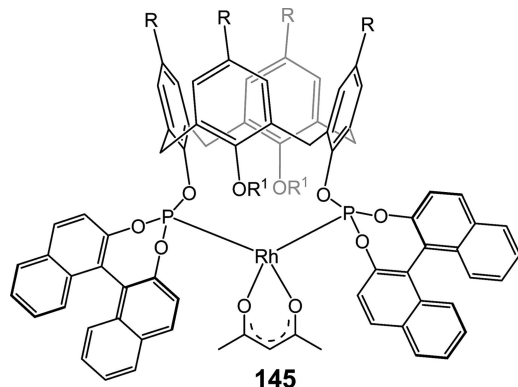
linear-to-branched (aldehyde) product ratio increased from the 58:1 observed using **140a** to 100:1 using **142**, provided that an excess of diphosphite was used. Limiting the amount of diphosphite resulted in systems possessing "naked" rhodium, which tends to behave as an unselective catalyst. The preference for linear products using **141a** and **142** was maintained over the duration (typically 24 h) of the reaction. Interestingly, the introduction of the fluorenyl groups (i.e., **143**) led to poor selectivity (linear:branched ratio = 3.3:1), and it was thought that the larger bulk of these groups leads to increased steric interactions between the calixarene backbone and the napthyl groups, which ultimately disturbs the shape of the cleft in which the catalytic center resides. The presence of the *tert*-butyl groups on the upper rim also proved to be beneficial for catalytic activity and regioselectivity (see Table 21).

Catalytic results for *trans*-2-octene screening revealed that isomerization was more effective than hydroformylation—a linear:branched ratio of 25:1 was observed. Only for runs involving **144** did the linear to branched product ratio decrease during catalysis.

Hydroformylation of styrene also gave predominantly linear aldehyde. Changes in regioselectivity were observed on changing the CO/H$_2$ pressure and also on increasing the size of the R group, for example, for **140a** (linear to branched product ratio = 1.9:1), **141a** (linear to branched product ratio = 3.2:1), and **142** (linear to branched product ratio = 3.4:1). It was postulated that the shape of the pocket available was unsuitable for η^3-complex formation with styrene, preferring instead to form a σ-aryl complex.

Linear products also dominated when such catalysts were used in the tandem hydroformylation/amination of styrene (linear to branched product ratio ≈ 3:1). Analysis of the products revealed enamines, aldehydes, and amines (see Scheme 28). Enamines were present in between 51 and 98%, although an increase in temperature from 80 to 130 °C favored hydrogenation.

Hydroformylation of allylbenzylether led to linear: branched product ratios of up to 20:1. In the case of the asymmetric hydroformylation of norbornene, these rhodium catalysts (*S* conformation only) gave mostly low *ee*'s (see Table 22). The exception here is the fluorenyl derivative **143**, which gave an *ee* of 61% at 55 °C (run 5).

Calixarenes **146−152** (Chart 36) bearing phosphorus-derived ligands were shown to catalyze the hydroformylation of C$_7$−C$_{12}$ linear alkenes using [Rh(acac)(CO)$_2$] in toluene at 50 °C; **149**/Rh, a calix[6]arene-based complex, displayed selectivity for 1-undecene, demonstrating the ability of the calix[6]arene to accommodate a larger guest molecule into the central cavity prior to catalysis.[114] The use of the calix[6]arene diphosphite ligand **150** with [Rh(acac)(CO)$_2$] has also been shown to catalyze the hydroformylation of monomers such as styrene with selectivity for branched aldehydes.[115,116] Variations in pressure and temperature and their effect on yield and regioselectivity were studied, and the complex Rh(**150**)$_2$ was characterized. Complexes **151** and **152** when mixed with [Rh(nbd)Cl$_2$] gave aldehyde selectivity for the hydroformylation of styrene comparable to that of best rhodium catalysts at 55 °C, with near identical regioselectivites.[117] With increasing temperature, selectivity toward branched aldehydes decreased rapidly; however, it was found that the addition of PPh$_3$ again favored branched aldehydes even at elevated temperatures (86−87% at 105 °C).

Figure 14. Complex **145** (R = *tert*-butyl and R^1 = CH$_2$Ph).

Scheme 28. Rhodium-Catalyzed Hydroaminovinylation of Styrene
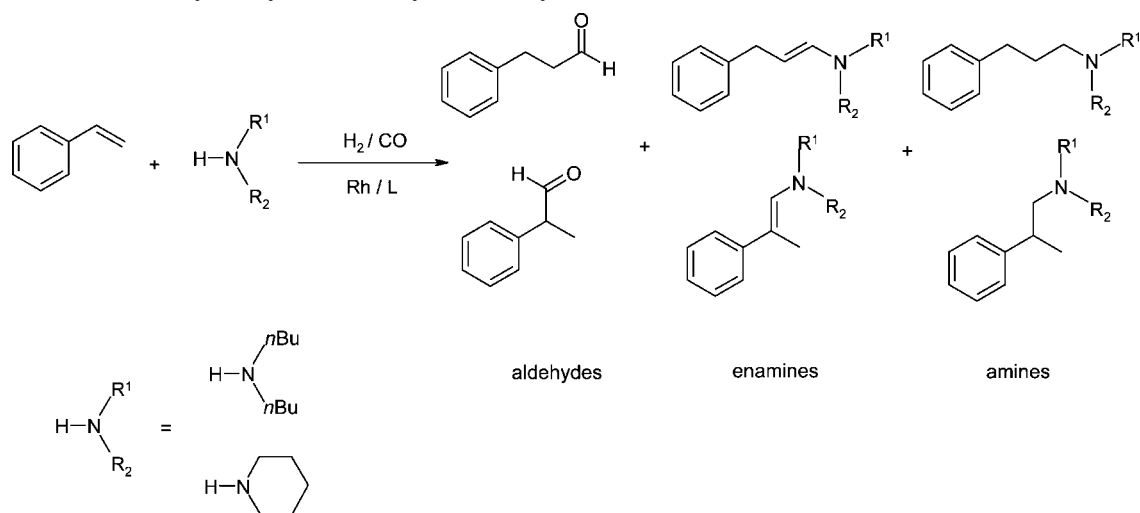
Table 21. Rhodium-Catalyzed Hydroformylation of 1-Octene Using Diphosphites 140a and 141−144[a]

| | | | | | product distribution | | | |
| | | | conversion[b] | | olefins[d] | aldehydes[e] | | |
run	L	L/Rh	t (h)	(%)	TOF[c]	(%)	(%)	l:b[f]
1	**140a**	10	1.2	34.5	1440	17.0	17.5	58.0
			8	98.5	620	46.7	51.8	56.3
2	**140a**	1	1	13.2	660	3.8	9.4	3.9
			8	76.2	480	22.4	53.8	2.5
3	**141a**	10	1	23.9	1190	3.0	20.9	>100[g]
			4	53.3	670	3.5	49.8	78.3
			24	87.3	180	12.1	75.2	80.1
4	**141a**	1	1	23.1	1150	2.6	20.5	7.2
			24	95.5	200	22.6	72.9	1.9
5	**141b**	10	1	24.2	1200	1.8	22.4	>100[g]
			24	94.5	200	13.6	80.9	71.0
6	**142**	10	1	14.4	720	6.3	8.1	>100[g]
			4	48.5	600	29.5	19.0	101.6
7	**143**	10	4	28.8	360	2.0	26.8	3.3
8	**144**	10	1	19.7	980	7.9	11.8	91.6
			4	51.0	640	22.2	28.8	86.9
			24	98.5	205	44.4	54.1	34.0

[a] 1-Octene (10 mmol), 1-octene/Rh = 5000, $P(CO/H_2)$ = 20 bar, T = 80 °C, toluene/n-decane (15 mL/0.5 mL), incubation overnight at 80 °C under $P(CO/H_2)$ = 15 bar. [b] Conversion: determined by GC using decane as the standard. [c] mol(converted 1-octene) mol(Rh)$^{-1}$ h^{-1}. [d] Isomerized 1-octene/initial 1-octene. [e] Aldehydes/initial 1-octene. [f] The l:b aldehyde ratio takes into account branched aldehydes (which consist mainly of 2-methyloctanal). [g] Exact value not determined because of a very low amount of branched aldehydes.

Table 22. Rhodium-Catalyzed Asymmetric Hydroformylation of Norbornene Using Diphosphites 140a, 141a, and 142−144[a]

run	L	T (°C)	$P(CO/H_2)$ (bar)	conversion[b] (%)	exo[b] (%)	endo[b] (%)	ee(exo)[c] (%)
1	**140a**	80	20	100	99.0	1.0	6 (S)
2	**141a**	80	20	100	82.7	17.3	16 (S)
3	**142**	80	20	100	91.3	8.7	18 (S)
4	**143**	80	20	100	100	traces	52 (R)
5	**143**	55	20	100	100		61 (R)
6	**143**	30	20	71.1	100		51 (R)
7	**143**	80	10	100	100	traces	22 (R)
8	**143**	55	10	57.9	100		41 (R)
9	**143**	30	10	35.7	100		5 (R)
10	**144**	80	20	100	97.5	2.5	6 (S)

[a] Norbornene (0.8 mmol), L/Rh = 10, norbornene/Rh = 200, 12 mL of toluene, 24 h, incubation overnight at 80 °C under $P(CO/H_2)$ = 15 bar. [b] Conversion: determined by ^{1}H NMR spectroscopy. [c] Determined by GC using a chiral column (Chirasil-DEX CB, 25 m × 0.25 mm) after reduction into the alcohols.

A larger cavity was available by using the C_3-symmetric hexahomotrioxacalix[3]arene triphosphine, which on reaction with [Rh(acac)(CO)$_2$] under 20 bar H$_2$/CO at 70 °C afforded the trigonal bipyramidal complex **153**, possessing a linear H−Rh−CO fragment (Figure 15). The complex was characterized by a strong carbonyl stretch (1977 cm^{-1}), a quartet (−9.70 ppm, J_{PH} 14 Hz) in the ^{1}H NMR spectrum for the hydrido ligand, and a doublet (36.4 ppm, J_{RhP} 153 Hz) in the ^{31}P NMR spectrum. 2D ROESY experiments revealed that the hydride was positioned close to the ArCH$_2$O groups as well as the PCH$_2$ protons and, therefore, must be directed toward the oxacalix[3]arene cavity. Such an orientation was probably favored by weak interactions with the phenolic oxygen atoms. When used in the hydroformylation of styrene, **153** afforded products with a linear to branched ratio of 12−88%, which given the resemblance of this ratio to that obtained using

classical catalysts, suggested that the oxacalixarene cavity was not playing a major role as a substrate receptor here.[118]

5.2.2. Hydrogenation

The use of the enantiopure calix[4]-BINOL- and calix[4]-TADDOL-containing diphosphites combined with the capping of the three remaining hydroxyl groups by a μ_3-bridging phosphorus atom produced a ligand system with a high level of intrinsic steric bulk and also a stereocenter located on the pendent phosphorus atom (**154**).[119] The resulting mild hydrogenation (25 °C, 5 bar H$_2$) of dimethylitaconate **M** (Scheme 29) and α-(acyl-amino)acrylate **N** (Scheme 30), using [Rh(nbd)$_2$BF$_4$]/**154a,b**/**155a,b** (Chart 37) produced highly active systems. For dimethylitaconate, complete conversion was achieved in 4 h with ee of up to 94% (R-configuration). Interestingly, it was found that changing the solvent system from dichloromethane to dichloromethane/toluene (1:3) led to a decrease in efficiency of the catalyst and also the opposite stereoinduction (Table 23). Overall, the TADDOL-containing ligand **155a** gave the best catalytic performance. Hydrogenation of methyl α-acetamidoacrylate gave the alanine derivative with high enantiomeric selectivity (ee = 94%), with **155a** again demonstrating best catalytic performance.

Chart 36. Phosphinite, Diphosphite, and Phosphine Calix[*n*]arenes 146−152 (R = *tert*-Butyl)

X = Y = OPPh$_2$, n = 2 **146**
X = OPPh$_2$, Y = OH, n = 2 **147**
X = OPPh$_2$, Y = OMe, n = 2 **148**
X = Y = OPPh$_2$, n = 3 **149**

150

X = OPPh$_2$ **151**
X = PPh$_2$ **152**

153
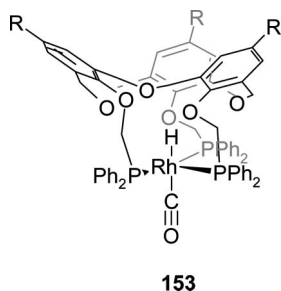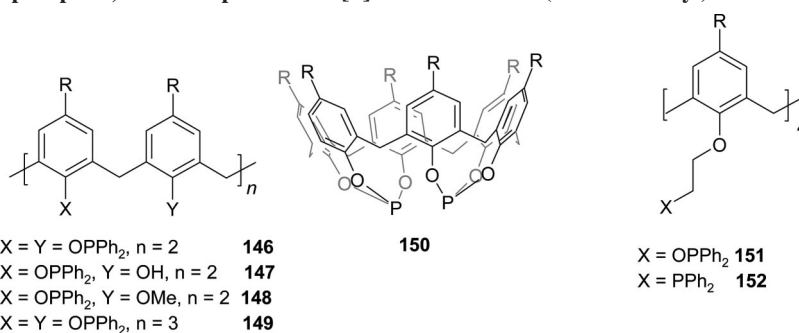
Figure 15. Rhodium hydride complex **153** containing a C_3-symmetric hexahomotrioxacalix[3]arene triphosphine.

Scheme 29. Hydrogenation of Dimethylitaconate M
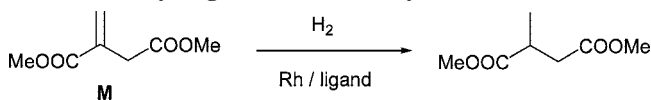
Scheme 30. Hydrogenation of α-(Acyl-amino)acrylate N
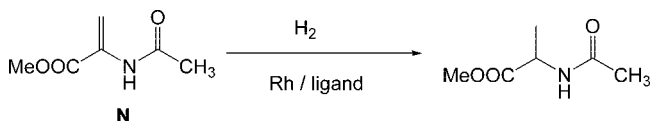
5.2.3. Cyclopropanation

The biscalix[4]arene-dirhodium complex **156** (Figure 16) was formed upon the reaction of the parent calix[4]areneH$_4$ and [Rh$_2$(OAc)$_4$].[120] Cyclopropanation (Scheme 31) using 1 mol % of **156** at 20 °C in CH$_2$Cl$_2$ was successful for styrene (98%; *E/Z* 72:28), cyclohexene (63%; *endo/exo* 72:28), and 2-methyl-2-butene (52%; *anti/syn* 45:55). These values varied considerably from the same reactions using [Rh$_2$(OAc)$_4$] with MDA (MDA = methyl diazoacetate), indicative of a steric influence of **156**.

Complex **156** also catalyzed intramolecular C−H insertions of α-diazo-β-ketoesters (Scheme 32) with high preference for carbene insertion into the aromatic C−H bond comparable to that of the [Rh$_2$(OOCCPh$_3$)$_4$] catalyst.

For the calix[4]arene-derived tetracarboxylate dirhodium(II) inclusion complexes **157** and **158** (Chart 38), two of the carboxylate arms were found to bridge the dirhodium core in a *trans* orientation (polycarboxylates are usually *cis* in such structures), while one of the acetate ligands was found to reside in the calixarene bowl.[121] The second acetate ligand, which was not encapsulated, was readily displaced by different carboxylic acids. Screening for the oxidative amination of C−H bonds within a series of sulfamate esters (**O1**−**O3**, Scheme 33), revealed that these calixarene-based systems out-performed most other dinuclear rhodium catalysts, with only Rh$_2$(esp)$_2$ (esp = α,α,α′,α′-tetramethyl-1,3-benzenedipropionate) proving to be more effective (Table

24). For the calixarene-based systems, catalyst turnover revealed a dependence on the steric and electronic nature of the exposed acetate ligand, with highly labile acetates favoring catalyst decomposition.

5.3. Nickel

Phosphorus-containing calix[4]arenes bearing nickel atoms have shown high levels of activity for ethylene dimerization/oligomerization/polymerization.[122] Matt et al., using NiX$_2$ (X = halogen) with upper rim distally diphosphinated calix[4]arene, synthesized complexes **159** and **160** (Chart 39) in high yields (70−73%). Activation of the corresponding NiBr$_2$·diphosphine complexes with 400 equiv of MAO at 20−30 bar of ethylene gave superior systems to that of [NiBr$_2$(dppe)] (dppe = Ph$_2$PCH$_2$CH$_2$Ph$_2$) with a high selectivity for butenes (>95%). It was found that activities for **159** were almost twice as high as those for that using **160** under analogous conditions, the explanation being one of decreased steric hindrance around the nickel center. TOF's of 0.83×10^6 h^{-1} recorded for **160** were, at the time, the highest known for an NiX$_2$(diphosphine) type system. Under dilute conditions, **159** demonstrated TOF's of 1.2×10^6 h^{-1}, suggesting a beneficial interaction of the bromine atom and the intermediate Ni-alkyl complex.

Procatalysts **159** and **160** have also been screened for propene dimerization.[123] In the presence of 400 equiv of MAO and using chlorobenzene as solvent, both **159** and **160** proved to be highly efficient catalysts. Indeed, activities were 2−3 times greater than those observed using other arylphosphine procatalysts under similar conditions. Systems using **159** and **160** also exhibited impressive C$_6$ selectivity (>80%), whereas use of [NiCl$_2$(PCy$_3$)$_2$], the fastest dimerization catalyst known, afforded only a 29.5% C$_6$ selectivity under the same conditions. The activity of **160** was found to be 10−20% higher than that of **159** over a range of procatalyst concentrations—see Tables 25 and 26.

Tables 25 and 26 also illustrate the product distribution, revealing that these systems gave high methylpentene selectivities. Higher temperatures and pressures favored isomerization of the pentenes. Complex **159**/MAO also produced a catalytically active system for the polymerization of norbornene, giving high activities [TOF of 7.5×10^5 mol(NBE)/mol(Ni) h see Table 27].[124]

IR spectroscopy carried out upon the resulting polymer displayed a lack of absorption bands in the region 1620−1680 cm^{-1}, which ruled out the possibility of polymer formation through a ROMP process, and from ^{1}H/^{13}C NMR spectroscopy, a conventional vinyl polymerization mechanism was inferred. While the interaction of **159** with MAO resulted in a system that could be used instantly, complex **161** required

Chart 37. Chiral Diphosphite Calixarene 154a,b/155a,b (R = *tert*-Butyl)

(R) **154a** (S) **154b**

(R,R) **155a** (S,S) **155b**
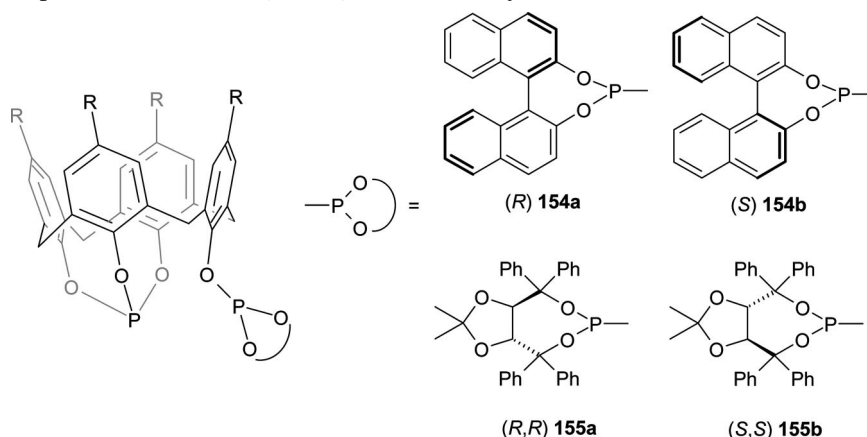
Table 23. Hydrogenation of Dimethylitaconate M and α-(Acyl-amino)acrylate N Catalyzed by 154a,b/155a,b[a]

ligand	substrate	% conversion [t (h)]	% ee (configuration)
154a	L	100 (20)	74 (R)
154a	L	100 (4)	74 (R)
154a[b]	L	100 (4)	76 (R)
154a[c]	L	60 (20)	20 (S)
154a	M	100 (20)	32 (R)
155a	L	100 (20)	92 (R)
155a	L	100 (4)	92 (R)
155a[b]	L	100 (4)	94 (R)
155a[d]	L	100 (20)	92 (R)
154b	M	100 (20)	94 (R)
154b	L	100 (20)	75 (S)
155b	L	100 (20)	92 (S)

[a] Conditions: [R] = 1mM, ligand/Rh = 1.5, substrate/Rh = 100, solvent = CH_2Cl_2 (2.0 mL), 5 bar, 25 °C, catalyst precursors prepared in situ. [b] Substrate/Rh = 1000. [c] Solvent = CH_2Cl_2/toluene 1:3. [d] Ligand/Rh = 5.
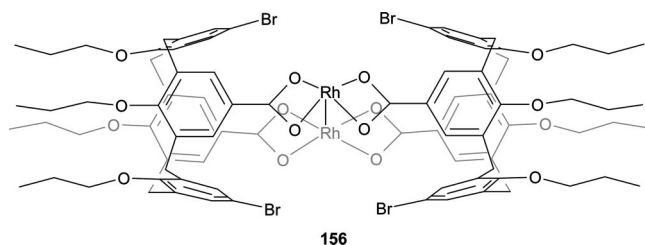
Figure 16. Biscalix[4]arene-dirhodium complex **156**.

Scheme 31. Cyclopropanation of Olefins Using 156 (Alkenes = Styrene, Cyclohexene, or 2-Methyl-2-butene)
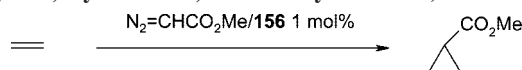
an induction period of 30 min, reflecting the ability to displace the Cp group (vs Br). Activities for **161**, although high, were less than those observed for **159**.

Orthogonal tandem (one-pot, two steps) catalysis, using **159** in conjunction with [Cp$_2$ZrCl$_2$] and MAO, afforded LLDPE with narrow polydispersity. It was possible in this system to control branching (ethyl groups only were present) by simply varying the Ni/Zr ratio or by changing the time of addition of the second catalyst.[125]

Use of a proximally functionalized diphosphine ligand, on treatment in dichloromethane with NiCl$_2$ pretreated with ethanol for solubility purposes, led to the paramagnetic blue complex **162** (Figure 17). The coordination geometry at nickel is neither tetrahedral nor square-planar, rather some-

Scheme 32. Intramolecular C—H Insertions of α-Diazo-β-ketoesters (R = Me, Ph)
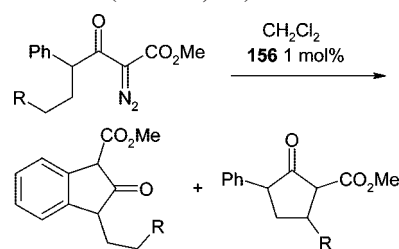
Chart 38. Tetracarboxylate Dirhodium(II) Inclusion Complexes 157 and 158
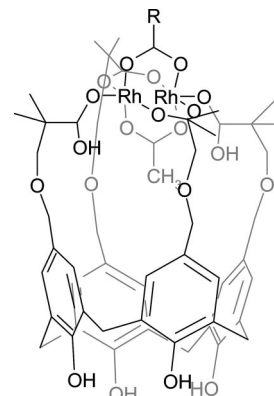
157: R = CH$_3$
158: R = CF$_3$

Scheme 33. Oxidative Amination of C—H Bonds

O1: R$_1$ = R$_2$ = Me
O2: R$_1$ = Ph, R$_2$ = H
O3: R$_1$ = Me, R$_2$ = H
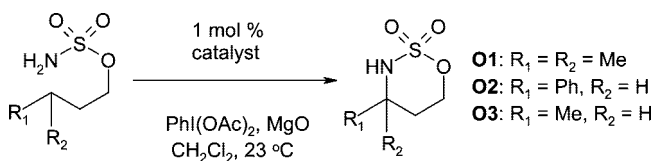
where in between the two forms. Use of NiBr$_2$ as starting material led to a tetrahedral complex together with a structure adopting a similar geometry to that found in **162**. The two forms of the dibromide in the solid-state could be separated manually and presumably exist in equilibrium in solution. Complex **162** was screened, in the presence of MAO, as an oligomerization catalyst (see Table 28). At 10 bar of ethylene pressure, C$_4$ to C$_{12}$ oligomers were obtained with an observed catalyst activity of 8.7 g/mmol h bar. Increasing the pressure

Table 24. Comparative Data for C—H Amination Mediated by Rh₂ Complexes[a]

catalyst	substrate	conversion (%)	yield (%)
Rh(CLX-H₂)(OAc)₂	**O1**	100	93
Rh(CLX-H₂)(OAc)(O₂CCF₃)	**O1**	<10	
Rh(CLX-H₂)(OAc)₂	**O2**	90	81
Rh(CLX-H₂)(OAc)(O₂CCF₃)	**O2**	<10	
Rh(CLX-H₂)(OAc)(O₂CCPh₃)	**O2**	95	88
Rh(CLX-H₂)(OAc)₂	**O3**	65	58
Rh(CLX-H₂)(OAc)(O₂CCPh₃)	**O3**	0	69
Rh(CLX-H₂)(OAc)(O₂CAd)[b]	**O3**	65	
Rh₂(O₂CC₇H₁₅)₄	**O3**	20	
Rh₂(O₂CCPh₃)₄	**O3**	10	
Rh₂(esp)₂[c]	**O3**	100	90

[a] Reaction performed with 1.1 equiv of PhI(OAc)₂ and 2.3 equiv of MgO at 0.15 M [substrate] in CH₂Cl₂. Conversion percentages are estimated based on integration of the ¹H NMR of the unpurified reaction mixture. [b] Ad = 1-adamantyl. [c] Rh₂(esp)₂ = Rh₂(α,α,α′,α′-tetramethyl-1,3-benzenedipropionate)₂.

Chart 39. Nickel Complexes 159−161

R = n-Pr, X = Br **159**
R = n-Pr, X = H **160**

R = n-Pr **161**
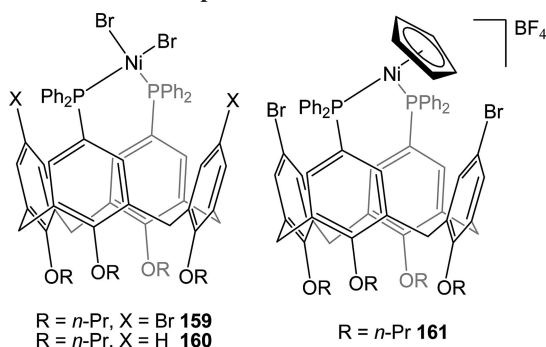
of ethylene had little effect on either the activity or the product distribution. The preference for short oligomers here suggested that the nickel center favored reductive elimination over chain propagation.[126]

Functionalization of the upper rim of calix[4]arene allowed for the formation of mono- and bis-ylide-containing ligands **163−166** (Chart 40). Ethylene oligomerization/polymerization was carried out with [Ni(COD)₂], the ylide [Ph₃P = CHC(O)Ph] being employed as the standard. In direct contrast to previous observations using Ni-based systems for the SHOP process, the bis-ylide complexes **163** and **166** unexpectedly showed a decreased activity as compared to the standard, while **164** and **165** showed increased activity.[127] At 80 °C, **166** was found to be almost double the activity of the standard giving TOF of 63400 h⁻¹, suggesting that the calixarene unit exhibits sufficient intrinsic bulk to prevent deactivation pathways. Polymers formed by the phenolic-containing ligands **165** and **166** exhibited higher molecular weights (Mw = 6000−7000 g/mol) due to the better donor properties of the phenolic groups, resulting in increased electron density pushed into the metallocycles, which in turn favored chain growth over β-H elimination. Use of a 1:1 Ni:PPh₃ ratio with **163−166** produced highly linear oligomers, for which the α-olefin content was 98−99% over the C₄−C₁₆ range. Again, the monoylide-containing ligands showed a marked improvement over the standard (up to 30% increase in activity), thought to be due to the presence of PPh₃ in the system; the direct effect the calixarene had on the activity of the oligomerization was unclear.

5.4. Palladium

5.4.1. Wacker Oxidation

A range of water-soluble calix[4 and 6]arenes modified at the lower rim (**167−173**, Chart 41) were investigated in the Wacker oxidation of linear alkenes (Scheme 34) using [Pd²⁺] as the catalytic center and a copper(II) salt as a reoxidizing agent.[128−130] In general, for the oligoglycerol and oxyethylated calixarenes **167−170**, it was found that the size of the cavity had an effect on substrate selectivity, with the calix[6]arene cavity preferring the longer linear alkenes due to increased cavity size as compared to that of the calix[4]arene analogues. Increasing the length of the pendant chains on the calixarene also increased specific product yields with a bias toward the longer linear alkenes such as 1-octene and 1-nonene. In all cases, the major products were the corresponding methylketones (95−98%). Substrate selectivity due to differing host−guest interactions was also witnessed with **171** and **172**. With **171**, 1-octene was most efficiently oxidized, whereas **172** displayed a preference for 1-hexene, **171** being the least active throughout.

Calixarenes bearing sulfonic acid groups on their upper rim are also highly water-soluble (see also Figures 3 and 5), a required property for effective Wacker oxidation.[131] The alkylated calixarenes **174−176** (Chart 42), as well as the propionitrile-bearing calixarene **177**, were evaluated under analogous conditions to those of **167−173** using C₆−C₁₀ substrates. Again, the major products of the oxidation reactions were ketones (85−97%). For the calix[4]arene-based systems, oxidation rates were found to peak for 1-hexene producing quantitative yields in 3 h. Increasing the length of the alkyl groups on the calix[4]arene reduced the overall catalytic activity. For 1-hexene oxidation, no such trends were observed when employing calix[6]arene-based catalysts. The propionitrile-modified calix[4]arene **177** showed increased activity over the previous catalysts, with quantitative yields achieved in only 2 h. However, any increase in the ratio of nitrile to calixarene from 1:1 led to dramatic decreases in activity, due to the low lability of the nitrile group coordinated to the palladium center.

The relationship between substrate (linear alkene) and complex was further witnessed in the ligands **178** and **179** (Chart 43), where the orientation of the benzonitrile group (ortho or para) altered the size of pocket for substrate binding such that for **178**/Pd, 1-hexene was most efficiently oxidized (70%), whereas for **179**/Pd the reaction favored 1-heptene (75%).[132] This was explained by the distance of the palladium center relative to the calixarene cavity. With **179**, the increased distance between the palladium and the calixarene cavity was such that for 1-hexene, cooperative substrate binding was less likely. Upon increasing the length of the alkyl chain, the probability of such interactions increased. In **178**/Pd, the palladium was located closer to the calixarene cavity and so the probability of cooperative interactions for the short chain alkenes was again increased. For differing sizes of calix[n]arene, different temperatures were found to be optimal for activity, for example, 50 °C for calix[4]arene and 60 °C for calix[6]arene.[133]

Simple sulfonic acid derivatives of calix[4, 6, and 8]arenes **3** (Figure 3)/Pd were also shown to be able to carry out successful Wacker oxidation, although in general it was found that corresponding activities were much lower than those systems reported previously.[134,135] As expected, the increased cavity size of calix[6]arene vs calix[4]arene led

Table 25. Propene Dimerization Using 159[a]

run	P(C₃H₆) (bar)	V (solv.) (mL)	time (h)	T_{init} (°C)	Ni (μmol)	TOF[b] (10⁻⁵)	C₆(wt %)	product distribution (mol %)[c]					
								4M1P	4M2P	2M1P	2M2P	hex	TMEN
1[d]	5	30	0.25	25	4.5	0.57	89.2	18.1	29.7	30.9	12.5	8.3	0.5
2	5	30	0.25	25	4.5	2.19	79.9	2.7	31.0	21.7	33.9	8.1	2.4
3	5	30	0.5	25	4.5	1.61	86.6	1.7	31.3	23.9	34.5	6.6	2.2
4	5	30	1	25	4.5	1.08	81.2	5.3	28.1	19.2	36.2	8.1	3.2
5	5	30	0.25	5	4.5	1.56	87.7	2.8	31.0	24.7	31.9	8.3	1.3
6	3	30	0.25	25	4.5	1.13	87.3	3.1	32.6	26.2	28.9	7.7	1.5
7	1	30	0.25	25	4.5	0.46	93.9	10.8	36.1	19.8	18.7	14.0	0.6
8	5	50	0.25	25	0.848	0.20	97.1	30.5	28.0	21.1	11.0	9.0	0.5
9[e,f]	5	50	0.25	25	0.848	7.62	90.6	6.0	35.0	15.2	36.6	6.2	0.9
10[f,g]	5	50	0.25	25	0.225	12.11	93.8	8.8	36.7	9.3	40.0	4.8	0.5
11[f,h]	5	50	0.25	25	0.090	19.28	95.1	9.9	38.1	9.2	35.5	7.0	0.4
12[h]	5	50	0.50	25	0.090	14.98	93.7	6.1	38.2	9.7	42.5	3.1	0.4
13[f,h]	5	50	1	25	0.090	14.01	94.3	6.6	39.4	8.3	41.0	4.3	0.5

[a] PhCl, MAO 400 equiv/Ni (MAO amount, 89 mg), yield determined by GC calibrated on heptane. [b] mol (C₃H₆) mol⁻¹ (Ni) h⁻¹. [c] 4M1P, 4-methyl-1-pentene; 4M2P, 4-methyl-2-pentene; 2M1P, 2-methyl-1-pentene; M2P, 2-methyl-2-pentene; hex, hexenes; and TMEN, 2,3-dimethyl-2-butene. [d] Toluene. [e] MAO 2100 equiv/Ni(MAO amount, 89 mg). [f] For the experiments, the results were averaged. [g] MAO 7900 equiv/Ni (MAO amount, 89 mg). [h] MAO 19800 equiv/Ni (MAO amount, 89 mg).

Table 26. Propene Dimerization Using 160[a]

run	P(C₃H₆) (bar)	V (solv.) (mL)	time (h)	T_{init} (°C)	Ni (μmol])	TOF[b] (10⁻⁵)	C₆ (wt %)	product distribution (mol %)[c]					
								4M1P	4M2P	2M1P	2M2P	hex	TMEN
1[d]	5	30	0.25	25	4.5	2.37	86.5	1.8	31.7	19.3	31.6	13.9	1.8
2	5	30	0.25	15	4.5	2.63	84.8	2.6	30.1	21.9	35.9	7.4	2.1
3	5	30	0.25	5	4.5	2.59	90.7	1.4	32.6	20.1	27.7	17.2	1.1
4	5	30	0.25	−5	4.5	0.98	94.8	10.8	32.4	23.6	24.2	8.6	0.5
5	5	30	0.25	−15	4.5	0.36	96.8	24.2	29.0	20.2	16.5	9.7	0.3
6	3	30	0.25	5	4.5	1.20	91.5	5.6	33.1	22.7	30.4	7.3	0.8
7	1	30	0.25	5	4.5	0.80	92.2	2.7	30.1	30.5	30.0	5.7	1.0
8[d]	5	50	0.25	25	0.09	25.99	94.9	6.8	36.8	12.3	39.2	4.6	0.4
9[d]	5	50	0.50	25	0.09	17.82	95.0	8.1	39.7	7.4	40.1	4.2	0.4
10[d]	5	50	1	25	0.09	13.49	94.3	9.2	37.0	9.5	39.9	3.8	0.5

[a] PhCl, MAO 400 equiv/Ni (MAO amount, 89 mg), yield determined by GC calibrated on heptane. [b] mol (C₃H₆) mol⁻¹ (Ni) h⁻¹. [c] 4M1P, 4-methyl-1-pentene; 4M2P, 4-methyl-2-pentene; 2M1P, 2-methyl-1-pentene; M2P, 2-methyl-2-pentene; hex, hexenes; and TMEN, 2,3-dimethyl-2-butene. [d] MAO 19800 equiv/Ni (MAO amount, 89 mg); for these experiments, the results were averaged.

Table 27. Data for the Polymerization of Norbornene Using Catalyst 159[a]

time	isolated yield		TOF (×10⁵)
	g	wt %	
5	0.530	80	7.50
20	0.580	88	2.00
60	0.630	96	7.40
5	0.080	12	1.10

[a] Conditions: **155** (0.09 mmol), chlorobenzene, [Al]/[Ni] = 19800, [NBE]/[cat] = 77300, concentrated [NBE] = 0.14 M, 35 °C, total volume = 35 mL.

to a preference for larger substrate binding (from 1-hexene to 1-octene). Interestingly, the logical prediction that a further shift in preference to higher alkenes such as 1-nonene or even 1-decene would be observed with $n = 8$ did not hold, rather it was found that 1-hexene was most readily oxidized in preference to the larger alkenes, due to a suggested twisting of the calix[8]arene molecule forming two discrete "calix[4]arene" units.

5.4.2. Mannich Type Reactions

It is also noteworthy here that water-soluble calixarenes bearing upper rim sulfonic acid groups were found to act as palladium-free catalysts in Mannich type reactions in water. Yields were greatly improved by employing a calix[4]resorcinarene sulfonic acid.[136]
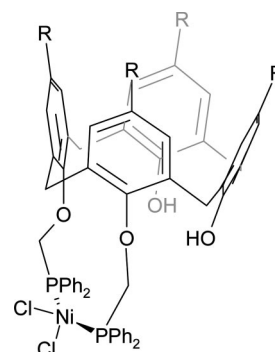
Figure 17. Complex **162** (R = *tert*-butyl).

5.4.3. CO/Ethylene Copolymerization

The cationic complex reported by Parlevliet et al. **180** (Chart 44), featuring a calix[6]arene containing two phosphite groups, was found to be active for the copolymerization of carbon monoxide and ethylene with TOF's in the region of 850−5300 mol[polymer]/mmol[Pd] h at 25 °C under 20 bar of carbon monoxide/ethylene.[137] Molecular weights of the resulting copolymers were all in the region of $M_n = 34000$ with narrow PDI (∼2.3). Successful copolymerization was rationalized by characteristic peaks in the ¹³C NMR spectrum at δ 35.1 and 212.0 ppm relating to methylene and carbonyl groups, respectively. End group analysis via ¹³C NMR spectroscopy indicated that hydrolysis of the polymer chains was facile with a large presence of carboxylic acid groups

Table 28. Ethylene Oligomerization Using 162[a]

P(C_2H_4) (bar)	α (°)	TOF (mol C_2H_4)/ (mol [Ni] h)	activity (g C_2H_4/ (mmol [Ni] h bar)	olefin distribution (wt %)					
				4-C	6-C	8-C	10-C	12-C	14-C
10	0.18	3100	8.7	73.9	19.9	4.8	1.1	0.3	
30	0.22	9800	9.1	68.4	22.6	6.6	1.8	0.5	0.1

[a] Conditions: Complex **162** (6 μmol), MAO (0.500 g), toluene (20 mL), initial temperature (25 °C).

Chart 40. Ylide Ligands 163−166
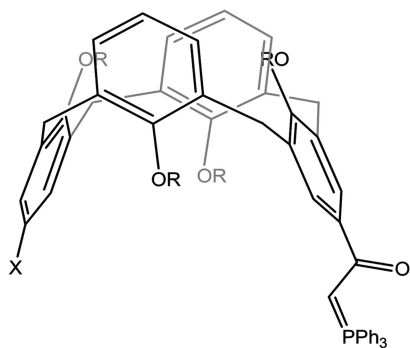
R = n-Pr, X = C(O)CH=PPh₃ **163**
R = n-Pr, X = H **164**

R = n-Pr, X = H **165**
R = n-Pr, X = C(O)CH=PPh₃ **166**

Chart 41. Water-Soluble Calix[4 and 6]arenes 167−173

R = t-Bu, n = 4, X = H **167**
R = t-Bu, n = 6, X = H **168**
R = t-Bu, n = 4, X = CH₂OH **169**
R = t-Bu, n = 6, X = CH₂OH **170**

X = p-CH₂PhCN, Y = CH₂CH₂CH₂SO₃Na **171**
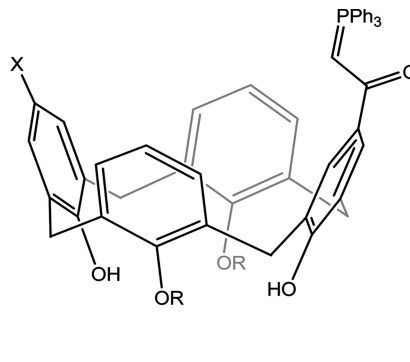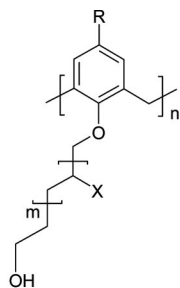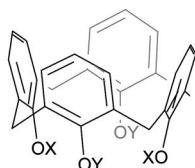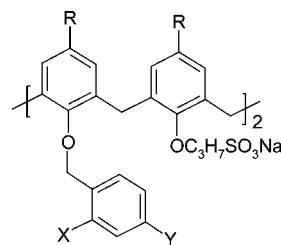X = o-CH₂PhCN, Y = CH₂CH₂CH₂SO₃Na **172**
X = Y = CH₂CH₂CH₂SO₃Na **173**

Chart 43. Benzonitrile-Bearing Calix[4]arenes 178 and 179 (R = tert-Butyl)

X = CN, Y = H **178**
X = H, Y = CN **179**

5.4.4. Alkylation

The Pd(Me-allyl) complexes **183−185** (Chart 45), prepared from [Pd(Me-allyl)(THF)₂]BF₄ and the parent calixarene ligand, were found to alkylate 1,3-diphenylprop-2-enyl acetate with dimethyl malonate (Scheme 35 and Table 29) in the presence of BSA (BSA = Me₃SiOC(NSiMe₃)CH₃) giving TOFs of ca. 30 h⁻¹ (complete conversion in ca. 4 h), comparable to those of known Pd-based alkylation catalysts.[111] Reduction in steric bulk of the R-substituent was found to increase *ee* to as high as 67% for R = H, while with R = CH₂C(O)NHCH(Me)Ph, where two identical substituents are distally bound, no steric induction was observed in the products. Such complexes also gave quantitative yields of linear products for the alkylation of 3-phenylallyl acetate with dimethyl malonate (>98%, see Scheme 36).[113] The high selectivity was attributed to the formation of pockets around the metal center, which help to control the approach of incoming monomers.

The related 1,3-disposed palladium phosphines (**186−189**) and phosphinites (**190** and **191**), see Chart 46 for complexes and Chart 47 for ligands, were also screened in the alkylation of 1,3-diphenylprop-2-enyl acetate (Table 30). Full conversion of substrate was realized after 4 h, although this was accompanied by disappointingly low *ee*.[111b]

Scheme 34. Wacker Oxidation of Linear Alkenes
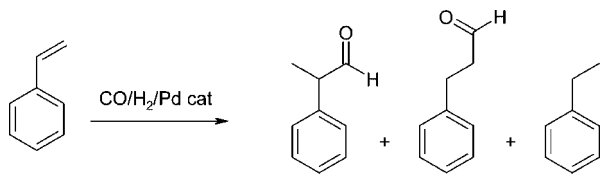
Chart 42. Alkylated Calixarenes 174−176 and the Propionitrile Calixarene 177
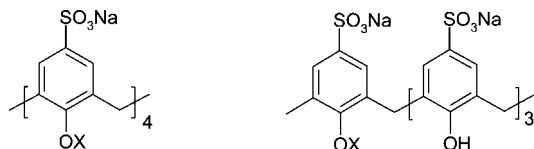
X = CH₃ **174**
X = (CH₂)₄CH₃ **175**
X = (CH₂)₅CH₃ **176**

X = CH₂CH₂CN **177**

as well as a minor percentage (15%) of vinyl end groups, the small number of vinyl groups being due to the suppressing nature of phosphite ligands with bite angles over 90° for β-hydrogen elimination.

Chart 44. Palladium Calixarene Complexes 180−182 (R = *tert*-Butyl)

180

R$_1$ = CH$_2$CH$_2$CH$_3$ **181**
R$_1$ = CH$_2$Ph **182**

Chart 45. Palladium Complexes 183−185 (R = *tert*-Butyl)

R$_1$ = H **183**
R$_1$ = SiMe$_3$ **184**
R$_1$ = CH$_2$C(O)NHCH(Me)Ph **185**

Scheme 35. Alkylation of 1,3-Diphenylprop-2-enyl Acetate with Dimethyl Malonate
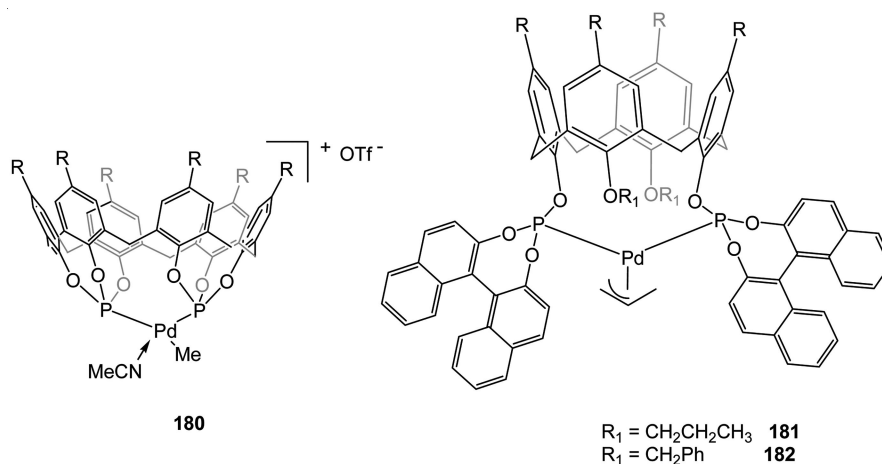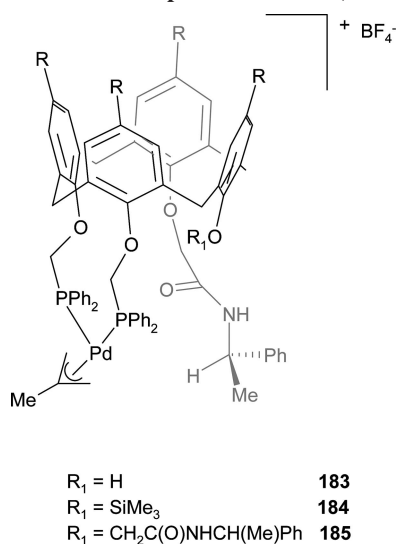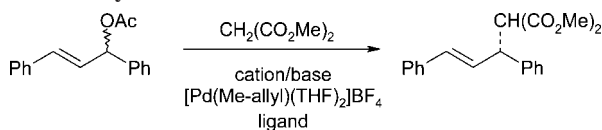

Table 29. Data for the Palladium-Catalyzed Alkylation of 1,3-Diphenylprop-2-enyl Acetate Using Catalysts 183−185[a]

complex	time (h)	*ee* (%)	TOF (h^{-1})
183	3.3	67	30
184	3.3	45	30
185	3.8	0	26

[a] Conditions: **183−185** (0.012 mmol), allylacetate (1.2 mmol), BSA (2.4 mmol), dimethyl malonate (2.4 mmol), KOAc (0.06 mmol), T = 0 °C, CH$_2$Cl$_2$.

5.4.5. Hydroformylation

The complex resulting from the in situ addition of PdCl$_2$(PhCN)$_2$ and the ligand **152** (see Chart 36 and section 5.2.1) gave quantitative yields for the hydroformylation of styrene, as well as reasonable yields (39−70%) in the hydroalkoxycarbonylation reaction of styrene (Scheme 37) with alcohol affording a 1:1 ratio of branched to linear products.[113] The same reaction using **151**/[PdCl$_2$]$_2$ gave

Scheme 36. Alkylation of 3-Phenylallyl Acetate with Dimethyl Malonate
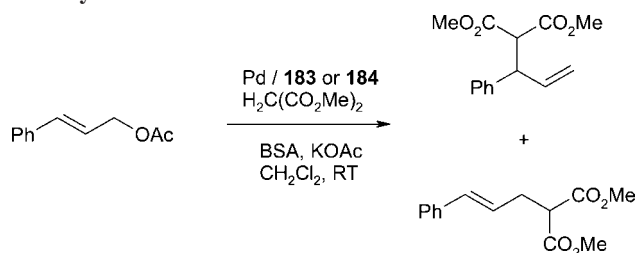
negligible yields due to cleavage of the C−O−P bond of the ligand by the alcohol.

5.4.6. Suzuki Cross-Coupling

The water-soluble calixarenes **3** (Figure 3) and **192−194** (Chart 48) were screened in the Suzuki coupling of iodobenzene with phenyl boronic acid (biphenyl product). The calixarene-based catalysts all outperformed β-cyclodextrin.[138]

Imidazolium-substituted calix[4]arenes are readily available from chloromethyl precursors, locked in the cone conformation by *n*-propyl groups at the lower rim. Further treatment with Pd(OAc)$_2$ in DMSO at high temperature led to chelates of the form *cis*-**195** (Chart 49); the *cis* configuration was confirmed by single crystal X-ray diffraction. Such systems were screened in situ as catalysts in the Suzuki cross-coupling of 4-chlorotoluene and phenylboronic acid (Scheme 38).[139] Results revealed that 4-methylbiphenyl was obtainable in 95% yield over 24 h using CsCO$_3$. Increasing the steric bulk of the imidazolium salt, for example, from methyl to mesityl, led to increased catalytic efficiency, although on increasing the bulk of the *ortho* substituents, for example, on going from mesityl to 2,6-diisopropylphenyl, led to a slight decrease in product yield.

Subsequently, a more comprehensive screening program[140] compared results against the noncyclic analogues **Q** (Chart 49). Bulky substituents on both the calixarene and the heterocyclic motif were found to enhance catalytic efficiency, which was thought to be the result of increased strain in the palladium chelate complex, favoring dissociation of an NHC ligand. The use of the potentially hemilabile ether group CH$_2$OMe on the upper rim of the calixarene frame (bound to the other two "heterocyclic-free" aryl rings) did not improve the catalytic activity. In the case of the substrate, best yields were obtained using aryliodides and bromides, while trifluoromethyl- and methoxy-substituted chloroben-

Chart 46.　1,3-Phosphines and Phosphinites of Palladium

187 $R_1 = R_2 = CH_2C(O)NHCHMePh$
188 $R_1 = CH_2CH_2OCH_3$ $R_2 = CH_2C(O)NHCHMePh$
189 $R_1 = R_2 = CH_2C(O)OMent$

186

190 $R = CH_2CH_2OMe$
191 $R = CH_2C(O)OMent$
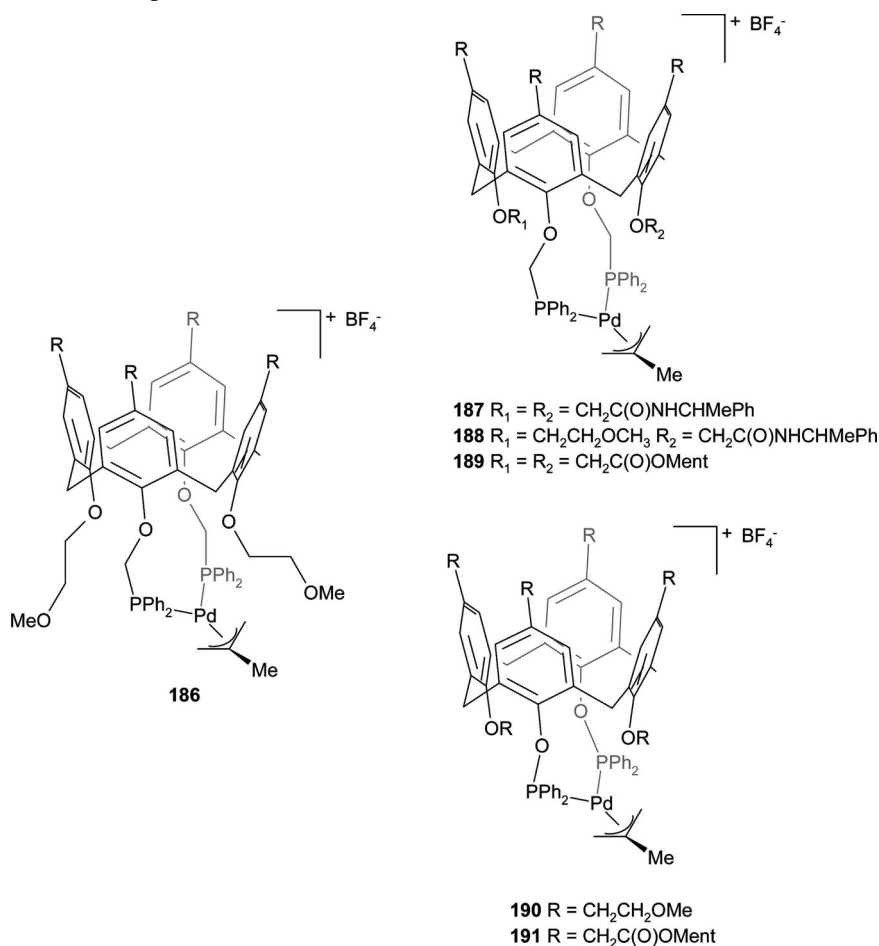
Chart 47.　Ligands P1−P6 Associated with Table 30

P1

P2 $R_1 = R_2 = (R)\text{-}CH_2C(O)NHCHMePh$
P3 $R_1 = CH_2CH_2OMe;$
　　$R_2 = (R)\text{-}CH_2C(O)NHCHMePh$
P4 $R_1 = R_2 = CH_2C(O)OMent$

P5 $R_1 = R_2 = CH_2CH_2OMe$
P6 $R_1 = R_2 = CH_2C(O)OMent$

OMent =
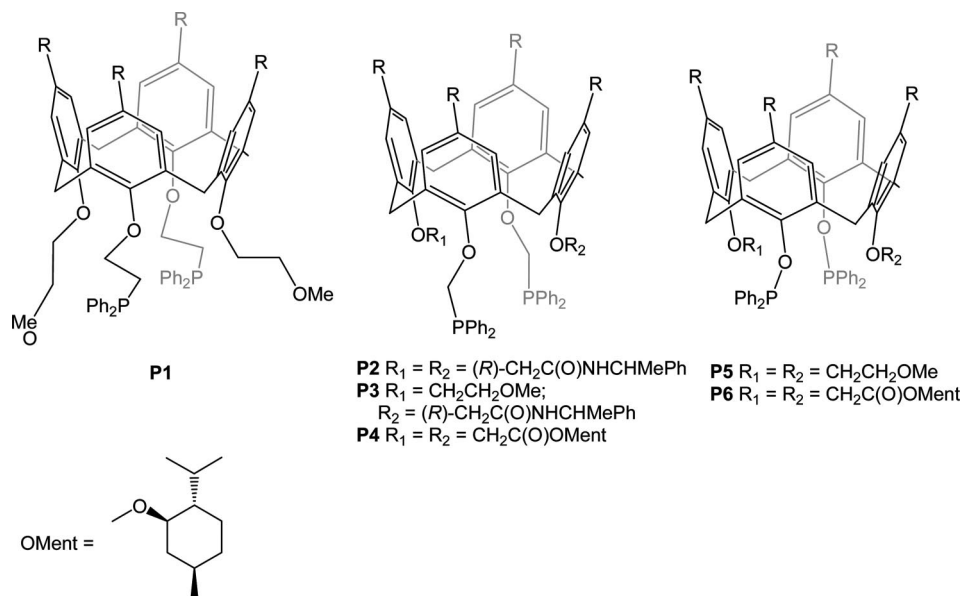
zenes gave results similar to 4-chlorotoluene. An interesting difference in reactivity was highlighted on comparing 2-, 3-, and 4-chlorobenzenes. Both the *ortho*- and the *meta*-isomers gave <10% of biaryl as compared to 60% for the *para*-isomer, and this difference was thought to arise through the ability of the calixarene cavity to more favorably encapsulate/trap the *para*-isomer. The reaction medium was also varied, and good results were obtained in 1:1 dioxane/water mixtures. The use of the pure solvents had dramatic effects upon

the amount of homocoupled product (4,4′-dimethylbiphenyl) formed, with <1% formed for all reactions in pure dioxane, yet between 3 and 12% for reactions conducted in pure water.

The *trans*-bromides **196** and **197** were also screened in the cross-coupling of aryl halides and arylboronic acids. Best results were obtained when an activated bromoarene (e.g., 4-bromoacetophenone) was used, and when in situ-generated catalysts, formed via addition of [Pd(OAc)$_2$] to

Table 30. Palladium-Catalyzed Alklation of 1,3-Diphenylprop-2-enyl Acetate[a]
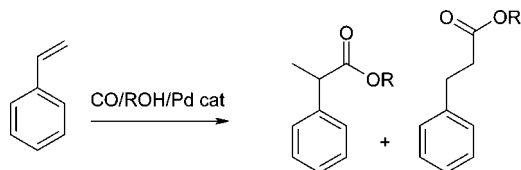
complex	ligand	reaction time (h)	turnover[b]
186	P1	5	20
187	P2	3	33
188	P3	5	20
189	P4	3	33
190	P5	4	25
191	P6	4	25

[a] Reaction conditions: 1.2 mmol of allyl acetate, 0.012 mmol of catalyst, 2.4 mmol of dimethyl malonate, 2.4 mmol of NaH; Pd:allyl acetate:malonate ratio = 1:100:200; T = 67 °C; solvent THF. [b] In mol per mol per h.

Scheme 37. Hydroalkoxycarbonylation Reaction of Styrene (R = Me, *tert*-Butyl)

the salts **198** and **199** (Chart 50) in dioxane, were employed.[141]

A separate study screened a series of cyclodextrins and calixarenes in the Suzuki cross-coupling of 1-iodo-4-phenylbenzene and phenylboronic acid in aqueous medium.[142] The presence of either set of macrocycles was found to be beneficial to cross-coupling, and rates of up to 92 times those recorded in the absence of the macrocycles were observed.

5.5. Platinum

Platinum complexes of thioether- and thiacrown-derivatized calix[4]arenes **200**–**202** (Chart 51) reported by Chen et al.[143] were found to effectively catalyze the hydrosilylation of α-olefins. In the case of **200**, it was found that successful complexation of [K₂PtCl₄] can be achieved in acetone to give the corresponding Pt^{2+} complex of the form [Pt(**200**)Cl₂]. Preliminary results using equimolar amounts of alkene and triethoxysilane with low catalyst loading indicated that in all cases 59–90% yields of hydrosilylated products were achievable in 75 min. In the case of styrene hydrosilylation with triethoxysilane, it was found that the branched isomers were the major product. Over a range of temperatures (40–60 °C), **201** was found to perform hydrosilylation on 1-decene with triethoxysilane[144] in 90% yield within 30 min. At 70 °C, these yields were found to decrease to around 82%. Under the same conditions, **202** favored the higher catalytic temperature, demonstrating 90% yield of decyltriethoxysilane. Selectivity based on size of substrate was observed upon hydrosilylation of 1-dodecene and allylbenzene, with yields of dodecyltriethoxysilane and phenylpropyl triethoxysilane being typically 30% lower than those observed for 1-decene under analogous reaction conditions. The addition of mercury into the polymerization system did not hinder the catalytic reaction of 1-decene, suggesting that the active component was homogeneous in nature.

For the hydroformylation of styrene using {[PtCl₂]₂(**151**) (Chart 36)}/SnCl₂ or the complex formed on addition of **152** (Chart 36) to PtCl₂(PhCN)₂/SnCl₂ at 80 bar H₂/CO over the temperature range 50–105 °C, two aldehyde regioisomers were formed, PhCH(CH₃)CHO and Ph(CH₂)₂CHO. With the **151**-derived system, an increase in temperature was found

to decrease regioselectivity toward branched aldehydes, whereas that containing **152** demonstrated a constant regioselectivity irrespective of the temperatures employed; selectivity at 50 °C for branched aldehydes being close to 50% for both systems.[117]

5.6. Copper

5.6.1. Cyclopropanation

At a 1:1 molar ratio of Cu⁺/**203** (Figure 18), cyclopropanation of styrene by ethyl diazoacetate was found to have *cis* selectivity.[145] This selectivity could be rationalized by taking into account the intermediate carbene complex formed, whereby the calixarene macrocycle blocks one hemisphere of the catalyst, which in turn favored relative orientations of the two substituents closer to the *syn*-periplanar than to *anti*-periplanar. Use of these concave ligands, when complexed with copper(I) triflate, for the cyclopropanation of alkenes with the diazoacetates **R** (Scheme 39 and Table 31) led to mostly the *syn*-product, particularly when a cyclic olefin was employed.

Interestingly, the concave 1,10-phenanthroline ligands **204** (Chart 52), under similar conditions, led to an excess of *anti*-product (*anti*:*syn* = 99:1).[146] The size of the ester **R** had an influence on the diastereoselectivity, whereby with **204**, larger esters increased the *anti*-selectivity, while with **203** a decrease in the *syn*-selectivity was observed. The side reaction to produce maleic or fumaric esters (*cis* and *trans* in Scheme 39) can be suppressed by keeping the concentration of diazo compound low.

5.6.2. Phosphate Diester Cleavage

High catalytic activity was found for **205** (Chart 53) in catalytic phosphate diester cleavage (Scheme 40) and was thought to be the result of a synergetic action of the two preorganized dynamic Cu(II) centers.[147] The catalytically active species was generated in situ by the mixing of **205** and Cu(ClO₄)₂·6H₂O in stoichiometric quantities. The *trans*-esterification of RNA was modeled using 2-(hydroxypropyl)-*p*-nitrophenyl phosphate (HPNP), while the catalytic hydrolysis of DNA was modeled using ethyl-*p*-nitrophenyl phosphate (EPNP). As a standard, a mononuclear species was also tested. In both cases, **205** was found to be considerably more active for the catalytic reactions than the mononuclear counterpart, indicating a positive interaction between the two copper atoms on **205**. Changing the pH was found to have a dramatic effect on the rate of **207** for HPNP with a maximum found at 6.2 over the range 5.4–7.2. A pH > 7.2 further produced a linear rate increase, while for EPNP the optimum pH was found to be 6.4. Both **206** and **207** were also found to be active catalysts toward HPNP, **206** being comparable to **205** at pH 6.2 with **207** requiring a pH of 7.4 to achieve higher activity.[148]

The Reinaud group has utilized the calix[6]arene ligand as a supramolecular platform in an attempt to mimic the coordination environment found in metalloenzymes. Suitably functionalized calix[*n*]arenes have the potential to provide not only the requisite first coordination sphere but also secondary interactions that could well prove pivotol in achieving the catalytic activity observed in the natural systems. Studies by the French group have focused primarily on mimicking monocopper enzymes. Functionalization of the lower rim in alternate fashion provided a series of N₃-donor

Chart 48. Water-Soluble Calixarenes 192−194 Used in Suzuki Coupling

192   193   194
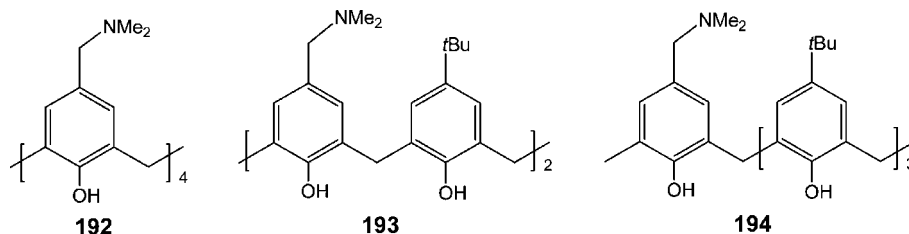
Chart 49. Complexes 195−197 (R = nPr; R′ = nPr, nBu) and Q
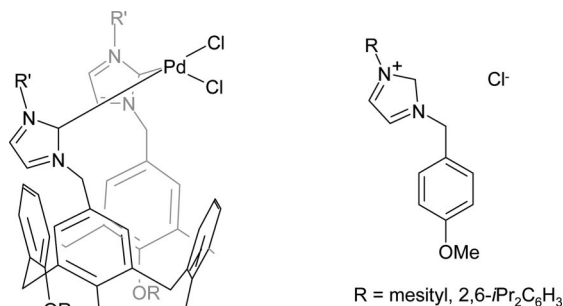
X = Cl, R′ = nPr   cis-**195**
X = Br, R′ = nPr   trans-**196**
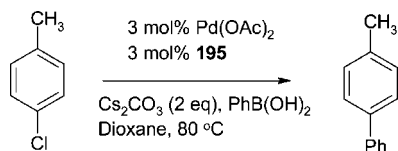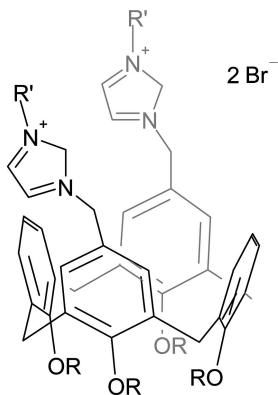X = Br, R′ = nBu   trans-**197**

R = mesityl, 2,6-iPr$_2$C$_6$H$_3$

Q

Scheme 38. Suzuki Cross-Coupling of 4-Chlorotoluene Using 195

Chart 50. Bis(imidazolium) Salts 198 and 199

R′ = nBu **198**
R′ = iPr   **199**

sets (pyridyls, picolyls, etc.), which were mimics of a polyimidazole environment. Typically, these first generation models provided three amino arms, which when bound to the copper center, resulted in the adoption of a cone conformation for the calix[6]arene. A guest molecule (GM) resided in the inner cavity coordination site and played a dictating role in determining the overall shape of the calixarene structure. In the second generation model, a fourth donor group was appended to one of the arms of the N$_3$-donor set and prevented any exogeneous binding other than that originating from the cavity. In certain cases, particularly

Chart 51. Thioether (200) and Thiacrown (201 and 202) Derivatized Calix[4]arenes (R = tert-Butyl)

200

R$_1$ = H **201**
R$_1$ = Me **202**
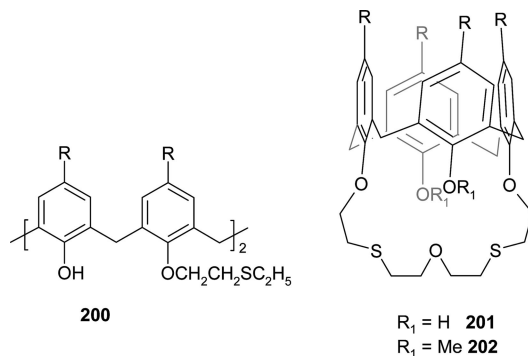
in the presence of potentially coordinating anions, multimetallic complexes were formed, and these were plausible models for multicopper enzymes. However, the binding restrictions could be further reinforced by the deployment of a cap, which was readily formed by covalently linking the three arms together, a so-called third generation model. This also led to an enhanced chelate effect and prevented bimetallic interactions. This is best illustrated by the tren ligand, the use of which resulted in calix[6]tren **208** (Scheme 41), a member of the calix[6]azacryptand series. For such systems, an on/off guest binding process in the calixarene pocket could be electrochemically controlled.[149] As this review is strictly concerned with calixarene-based catalysis, we have restricted our discussion below to only those complexes that have indeed been catalytically screened.

The structure of the tetranuclear copper complex **209** (Figure 19) was revealed to be a rare "stepped-cubane" core, which was shown to be stable in coordinating solvents such as acetonitrile. One of the three imidazole arms of the calix[6]arene ligand resides in the calixarene cavity. Given the resemblance of this complex to the type 3 copper protein Catechol oxidase, it was screened for its ability to dehydrogenate 3,5-di-tert-butylcatechol. Immediate reduction of the copper(II) centers was observed, with **209** acting as a four electron sink, but subsequent regeneration of **209** was slow.[150]
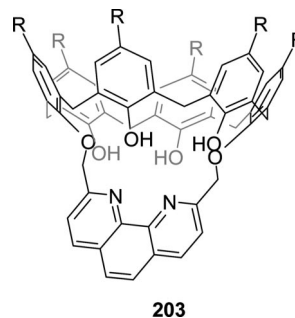
203

Figure 18. Calix[6]arene ligand **203** containing a 1,10-phenanthroline bridge.

Scheme 39. Cyclopropanation of Alkenes with Diazoacetates R

Table 31. Alkenes, Diazoacetates (R), and Products Associated with Scheme 39

R^1	R^2	R^3	R^4
C_6H_5	H	H	Et
C_6H_5	H	CH_3	t-Bu
-(CH$_2$)$_3$-		H	Me
-(CH$_2$)$_4$-		H	
-(CH$_2$)$_4$-		CH_3	
-(CH$_2$)$_3$-O-		H	
			H

Chart 52. Concave 1,10-Phenanthroline Ligands 204 (Where X Is Typically $-CH_2(CH_2OCH_2)_nCH_2-$; $n = 2$ or 3)

204

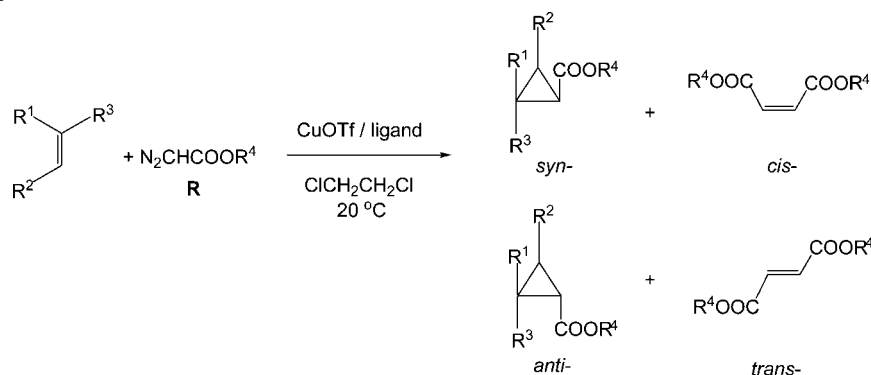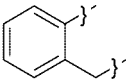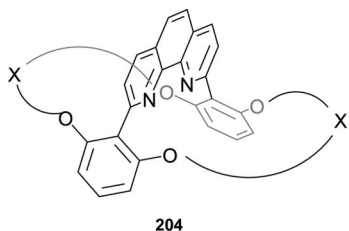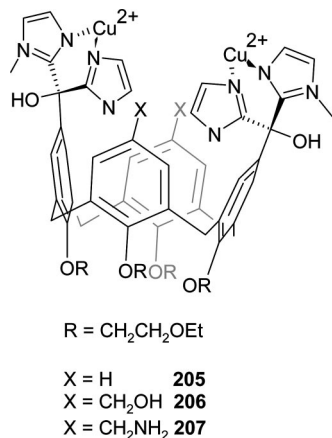**Chart 53. Copper Calix[4]arene Complexes 205–207**

R = CH$_2$CH$_2$OEt

X = H   **205**
X = CH$_2$OH   **206**
X = CH$_2$NH$_2$ **207**

Related calix[6]arene ligands (Scheme 42), which bear a combination of imidazole, amine-phenolate, and methoxy groups at the lower rim, were treated with Cu(H$_2$O)$_6$(ClO)$_2$ affording paramagnetic, mononuclear Cu(II) complexes of the type **210**. The square-based pyramidal geometry imposed at the metal center was such that the labile ligand (S) must be encapsulated within the calix[6]arene cavity. Cyclic voltametry revealed a fully reversible oxidation, as well as a sluggish reduction process. Low temperature studies (−45 °C) allowed for the observation of an oxidized redox form

of the complex, namely, [L^{2+}Cu(MeCN)]$^{2+}$, which in the UV−vis spectrum possessed an intense phenoxyl π to π^* transition (405 nm). This and other data were consistent with the formation of the Cu(II) phenoxy radical species [L^{2}Cu(MeCN)]$^{2+}$, reminiscent of the situation found in the copper enzyme galactose oxidase. Indeed, complex **210** was similarly found to be capable of the oxidation of alcohols to aldehydes (at −45 °C under argon).[151]

In terms of copper-based catalysis, it is also worthy of note that calix[4, 6, and 8]arenes bearing halide-containing substituents on the upper rim have been used to initiate the atom transfer radical polymerization (ATRP) of styrene and methyl methacrylate, in the presence of CuX (X = Cl, Br)/2,2′-bipyridyl,[152−154] affording well-defined polystyrene and poly(meth)acrylate stars. It was found necessary to restrict the polymerizations to low conversions (<20%) to prevent star−star coupling.

5.7. Zinc

5.7.1. ROP of L-Lactide

The ring-opening polymerization of L-lactide (Scheme 43 and Table 32) by **211** (Chart 54) at 60 °C in toluene produced poly(lactic acid) in over 90% yield with low PDI (<1.5).[155] Shortening of the alkane chain on the zinc from ethyl to methyl as in **212** led to increased reactivity due to the inherent increase in nucleophilicity. The molecular weight of the polymer was found to be four times higher than the theoretical values. Polymerization reactions using **213** and **214**, having inequivalent zinc centers, were carried out to assess the conformational effect if any, imparted by the calixarene ligand. In all cases, end group analysis gave identical ^{1}H NMR spectra, indicating that only the external zinc atom was directly involved in the polymerization process. The mononuclear pathway for the ring-opening polymerization of L-lactide was further supported by the synthesis and testing of **215**, producing identical polymeric material to that of **211/212**.

5.7.2. Cyclization of HPNP/Ester Cleavage

Rate enhancement arising from two zinc centers in close proximity had previously been found in the upper rim-modified zinc/calix[4]arene system **216** (Chart 55).[156] When compared with **217** and a standard pyridine bis-amine complex **S**, it was found that for the catalytic cyclization of 2-(hydroxypropyl)-p-nitrophenylphosphate (HPNP), **216** displayed reaction rate enhancement of up to 23000 times at pH 7 and 25 °C. Complex **218** was found to be 50 times less active than **216** but six times more active than the

Scheme 40. Models for Catalytic Phosphate Diester Cleavage
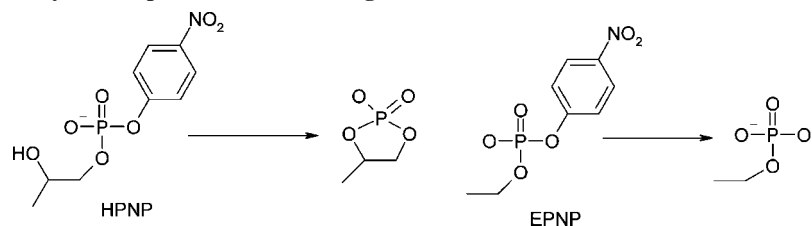
Scheme 41. Copper(II) Complexation by Calix[6]tren 208
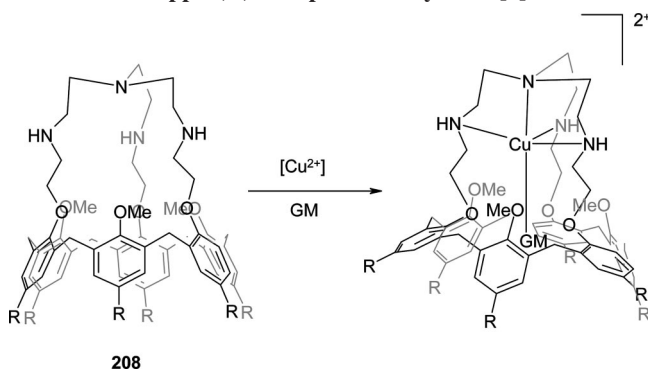
pyridine standard. Further experiments using **216** showed negative results for the hydrolysis of diethyl *p*-nitrophenol phosphate, ethyl *p*-nitrophenol phosphate, or *p*-nitrophenol phosphate, illustrating the importance of the β-hydroxyl group found in HPNP.

Appending two dimethylamino groups to the upper rim afforded a further example of a complex (**217**) capable of phosphate diester bond cleavage in HPNP, with one of the dimethylamino groups present acting as a base during deprotonation of the hydroxyl group of HPNP.[157] A bifunctional mechanism (Figure 20) was proposed to account for all of the above observations, one zinc center acting as a Lewis acid activator, while the other activated the nucleophilic β-hydroxyl giving rise to a relatively fast intramolecular reaction.

Complex **216** and its 1,2-isomer **219**, together with the trinuclear 1,2,3-Zn(II) complex **220** (Chart 56), have been

screened as catalysts for ester cleavage of **T1** and **T2**. In the case of **T1**, the 1,2-catalyst out-performed the 1,3-catalyst, whereas for **T2** the opposite result was observed. However, for both **T1** and **T2**, the trinuclear 1,2,3-complex out-performed the dinuclear complexes.[158] Further investigations revealed the importance of a good match between ester size and intermetal distance.[159]

Saturated kinetics and pH variation studies on **216** indicated that high catalytic activity originated from high substrate binding affinity. The importance of flexibility of the ligand frame in **216** was highlighted by screening the more rigid framework **221**, containing a crown ether bridge, under similar conditions. Complex **221** was shown to exhibit both lower substrate binding and lower catalytic activity. Use of the trinuclear complex **220** induced a rate acceleration of 32000 and resulted in decreased substrate affinity and increased catalytic rate as compared to dinuclear **216**. The overall order of catalytic activity for these systems was therefore **220** > **216** > **221** > **218** > **S**, in line with the inferred cooperativity between zinc centers.[160]

The trinuclear complex **220** also efficiently catalyzed the cleavage of RNA dinucleotides, where for different nucleobases, large differences in rate were observed. Use of a heterotrinuclear Zn$_2$Cu analogue proved to be beneficial to activity, whereas changing to a Cu$_3$ type system was not.[161] As for copper (section 5.6), a number of biomimetic zinc complexes have been reported; however, such systems are yet to demonstrate catalysis.[162]

6. Rare Earth Metals

6.1. Styrene Polymerization

Of all the calix[*n*]arene-metal complexes applied to olefin polymerization, the vast majority of research has centered on the rare earth metal-containing species, in particular neodymium. Zheng et al. have shown complex **222** (Chart 57) to be a highly active catalyst for the homopolymerization of styrene in the presence of di-*n*-butylmagnesium and hexamethyl phosphoramide (HMPA), exhibiting activities in the range of $0.5-1.0 \times 10^3$ kg[PSt]/mmol[Nd] h in solution polymerization and 1.3×10^3 kg[PSt]/mmol[Nd] h in bulk polymerization,[163,164] the corresponding molecular weights of the polymers being ca. 10×10^4 and 22×10^4 gmol^{-1}, respectively. At elevated temperatures, conversion of the styrene monomer was quantitative, with a further increase in temperature from 70 to 90 °C leading to decreased polymerization time. To investigate the influence of the R groups upon the 1,3-disubstituted calix[4]arene, complexes **223** and **224** were synthesized and tested under analogous conditions to that of **222**.[165] Both **223** and **224** were found to be active styrene polymerization catalysts, producing polymers comparable to those of **222**. However, it was found that upon increasing the steric bulk of the R groups, the yield
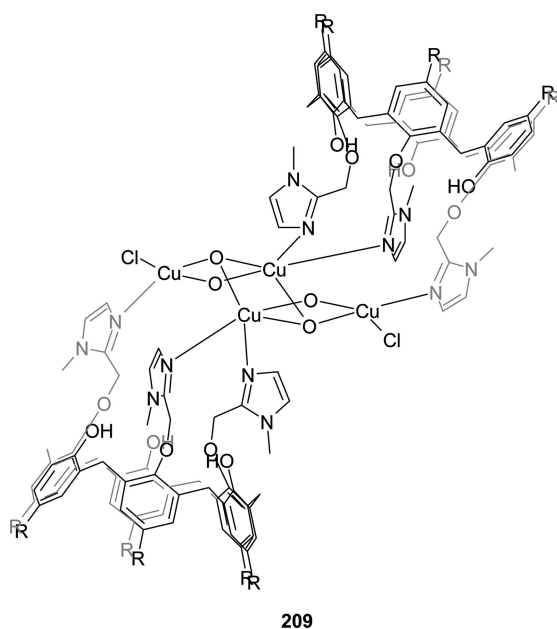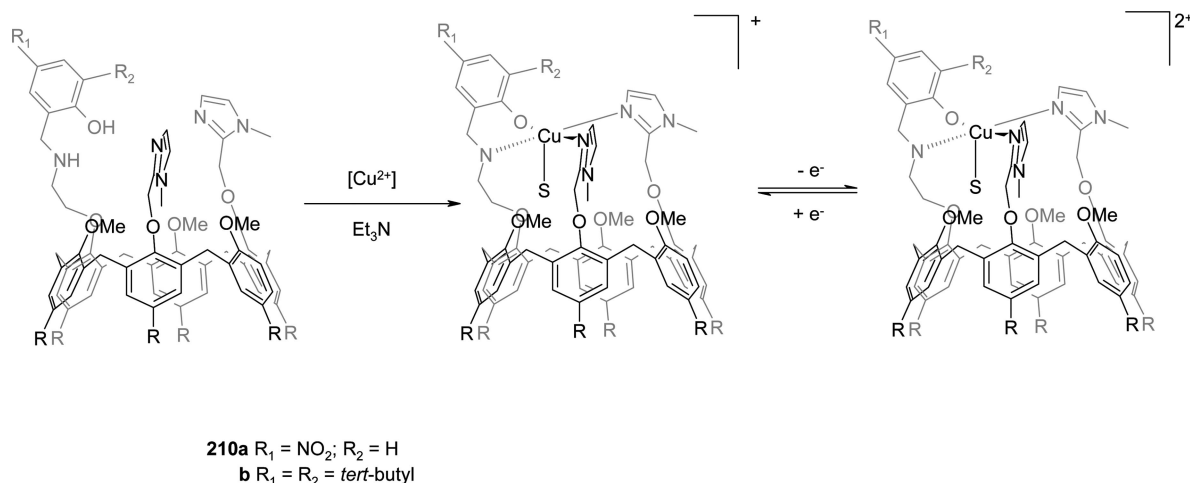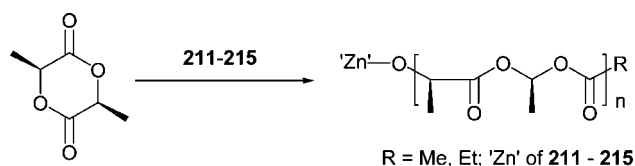

209

Figure 19. Tetra-copper complex **209** (R = *tert*-butyl).

**Scheme 42. Formation and Redox Behavior of the Complex 210 (R = *tert*-Butyl)**

210a R₁ = NO₂; R₂ = H
   b R₁ = R₂ = *tert*-butyl

Scheme 43. ROMP of L-Lactide

R = Me, Et; 'Zn' of **211 - 215**

Table 32. Ring-Opening Polymerization of Lactide Using 211 and 212[a]

catalyst	LA/**211** or **212**	conversion (%)	M_n (kDa)	PDI
211	200	98	72	1.45
212	50	98	60	1.16
212	100	97	103	1.11
212	200	98	143	1.06

[a] Conditions: toluene (2 mL), catalyst concentration (1 μmol/mL), 15 h.

Chart 54. Zinc Calix[4]arene Complexes 211−215

X = Y = Et   **211**
X = Y = Me   **212**
X = Me, Y = Et   **213**
X = Et, Y = Me   **214**

215
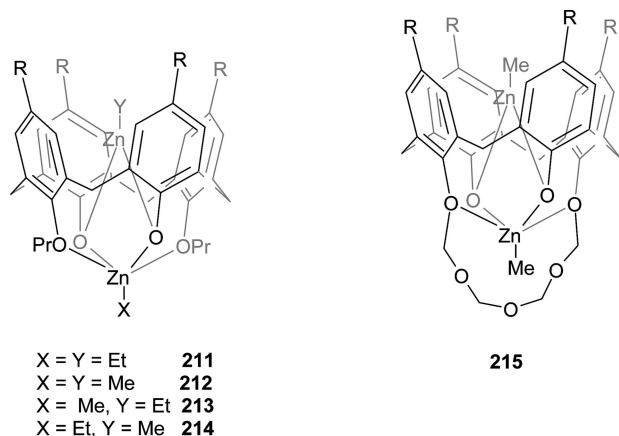
of polystyrene decreased dramatically from 55.4 (**222**) to 42.8 (**223**) and 26.4% (**224**), respectively.

The isostructural yttrium complex **225**, when compared to **222** [in the presence of HMPA and Mg(*n*-Bu)₂·AlEt₃], displayed substantial improvement in activity for the polymerization of styrene: **225**/97% as compared with **224**/53%. The resulting polymer was found to be of ultrahigh molecular weight ($M_n = 56.9 \times 10^4$).[166] We also note that an yttrium tris(triphenolate) catalyst has been employed in the formation of calixarene-based star-shaped poly(ϵ-caprolactone)s.[167]

The homopolymerization of 4-vinyl pyridine (4-VP) in the presence of **222**/di-*n*-butylmagnesium/hexamethyl phosphoramide produced polymers of increased molecular weight when compared to the polymerization of 4-VP in the absence of **222** (4.65×10^6 vs 5.62×10^5 g mol⁻¹, respectively).[168] Furthermore, it was reported that for 4-VP/styrene copolymerization, the incorporation ratio of the 4-VP unit into the polymer chain was dependent upon the sequence of monomer addition. If 4-VP was added after an initial period of homostyrene polymerization, incorporation levels of 4-VP were of the order 4.9−23.3 mol %; if, however, both monomers were added simultaneously, this ratio rose to between 44.0 and 66.3 mol %.

Catalytic activities of the lanthanide complexes, whose structures are analogous to the neodymium complexes screened for ethylene polymerization in Table 33 (see section 6.3), were found to vary greatly, although all were inferior to the neodymium/Al(*i*-Bu)₃ system (activities <40 g/mmol h). Ultrahigh molecular weight polystyrene was produced most favorably by the C₆Nd/di-*n*-butylmagnesium/HMPA system with 99% conversion of monomer. Indeed, the activity of this system mirrored that seen for the butadiene polymerization (see section 6.4), that is, C₆ > C₄ > C₈. Both catalyst aging and choice of solvent (toluene being preferred) were influencing factors. The rate of the polymerization was found to be first-order with respect to styrene and C₆Nd concentrations, with a polymerization activation energy of 41.7 kJ/mol. The resulting polystyrene was of ultrahigh molecular weight with a syndiotactic triad content of 81%.[169] Neodymium calix[6]arene complexes also actively catalyzed the ring-opening polymerization of styrene oxide with up to 70% conversion found at 58 °C. Neodynium, lanthanum, and yttrium calix[4, 6, and 8]arenes were also found to be capable of ring-opening polymerization of cyclic carbonates with conversion up to 84% forming monomodal polymers with narrow PDI (<2).[170−172] In the case of styreneoxide, the resultant poly(styreneoxide) possessed a head-to-tail atactic chain structure.[173]

6.2. Propyleneoxide Polymerization

The combination of cationic Nd/calix[4]arene complex **226** (Figure 21)/Al(*i*-Bu)₃/H₂O was found to be effective for the polymerization of propylene oxide, displaying high yields (66−73%) and a high isotactic content (58.0−70.6%) for the resulting polymer.[174] Increasing the Al/Nd ratio was

Chart 55. Zinc Complexes 216−218 and S

X = H **216**
X = CH$_2$N(CH$_3$)$_2$ **217**

R = CH$_2$CH$_2$OEt

218

S
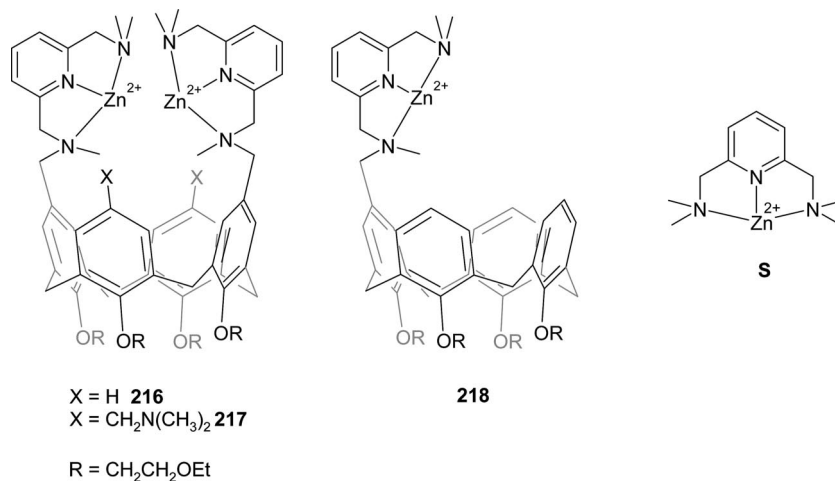
found to increase the activity of the system, while lowering the isotactic content of the polymer (ca. 58%). The catalyst displayed good thermal stability with activities increasing up to 70 °C. Above this temperature, however, both activities and the percentage of isotactic polymer were found to decline.

6.3. Ethylene Polymerization

Reaction of *p-tert*-butylcalix[8]areneH$_8$ and Na in 2-propanol/benzene, followed by the addition of NdCl$_3$, gave the bimetallic complex **227** (Figure 22) as a green solid. For ethylene polymerization, **227**/Al(*i*-Bu)$_3$ gave poor activities, typically 24 g[PE]/mmol[Nd] h at 80 °C, producing polymers with an M_w of 97.7 × 10^4.[175]

At a 1:1 molar ratio of Ln(O*i*-Pr)$_3$ (Ln = La, Sm, Nd, Dy, Y) to calix[*n*]arene (*n* = 4, 6, 8), a series of lanthanide complexes were generated and their ethylene polymerization behavior was assessed. For the neodymium procatalyst, activities were at best described as low, producing linear polyethylene as evidenced by the melting points of the polymers produced (Table 33).[176]

Work carried out by Shen et al., focusing on rare earth metal calix[4, 6, and 8]arenes found that in each instance, the complexes were effective catalysts for the homopolym-

erization of butadiene, isoprene, ethylene, styrene, propylene oxide, styrene oxide, trimethylene carbonate, and 2,2-dimethyl-trimethylene carbonate.[177] In the case of 2,2-dimethyl-trimethylene carbonate, NMR analysis of the polymerization mixture indicated that the polymerization proceeded via a coordination−insertion mechanism. The polymerization activity differed in various solvents, with increased solvent polarity leading to decreased activity (Table 34).[178]

For the ring-opening polymerization of trimethylene carbonate using **227**, it was found that a ratio of monomer/Nd of 2000 was optimal at 80 °C for 16 h, producing monomodal high molecular weight polymer (M_w = 60000).[179] High temperatures were found to be preferable, with an increase from 50 to 100 °C increasing the conversion yield from trace amounts to 99%. NMR spectroscopy indicated the presence of trimethylene ether groups, consistent with a cationic polymerization mechanism.

6.4. Butadiene Polymerization

For 1,3-butadiene polymerization, the reverse trend (to that observed for styrene) was observed with **222** (see Chart 57) being totally inactive for the formation of *cis* polybutadiene, while **223** and **224** produced quantitative levels of *cis* polymer (93.7−95.7%) in increasing yields (14.9 and 56.3%, respectively). The dramatic increase in yield seen for **224** was ascribed to the presence of the additional oxygen donors on the R substituent, capable of coordinating to the neodymium center. This was not surprising, as the addition of alcohol to neodymium-based procatalysts for 1,3-butadiene polymerization had previously led to accelerated activities.[180]

Systems of the type C$_n$Nd/Al(*i*-Bu)$_3$/Al(*i*-Bu)$_2$Cl (C$_n$ = calix[n]arene where *n* = 4, 6, and 8) were also found to be effective catalysts for the 1,4-butadiene polymerization. The systems were found to be active in the absence of the halogen source but did show improved catalytic activity on addition of the Al(*i*-Bu)$_2$Cl. The polymer obtained had M_w ca. 2 × 10^5 and a *cis*-1,4 content of 90%.[181] Such systems also showed activity for butadiene polymerization, with an activity order of C$_6$ > C$_4$ > C$_8$.[182] For isoprene polymerization, the system C$_6$Nd/Al(*i*-Bu)$_3$ [containing 10% Al(*i*-Bu$_2$H)]/Al$_2$Et$_3$Cl$_3$ afforded a high *cis*-1,4 content (95%) polymer of high molecular weight and viscosity (M_w = 40 × 10^4). Elevating the temperature of the polymerization reaction led
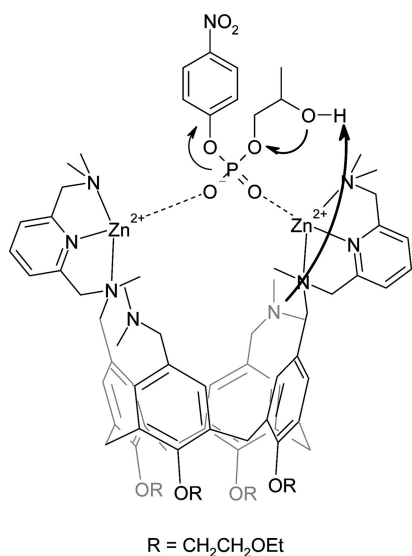
R = CH$_2$CH$_2$OEt

Figure 20. Representation of a possible mechanism for HPNP transesterification catalyzed by **217**.

Chart 56. Zinc Complexes 219−221, with Esters T1 and T2 (R = CH₂CH₂OEt; R₁ = n-Pr)

219

220

221

T1

T2
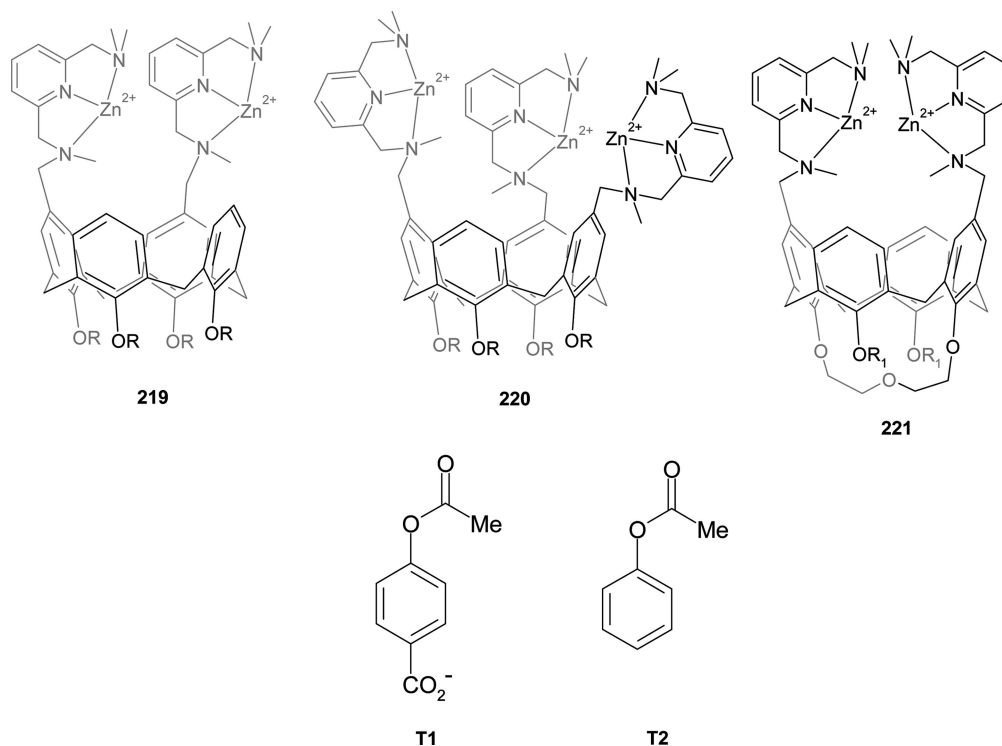
Chart 57. Rare Earth Calix[4]arene Complexes 222−225

R = CH₃, M = Nd   **222**
R = CH₂Ph, M = Nd   **223**
R = CH₂-p-t-BuOPh, M = Nd   **224**
R = CH₃, M = Y   **225**
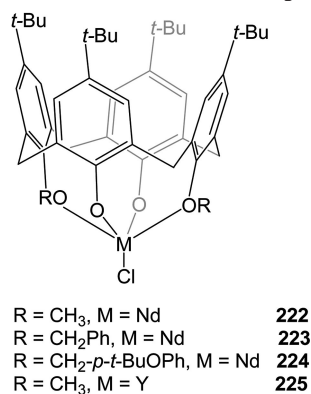
Table 33. Ethylene Polymerization Using Neodymium Calix[4, 6, and 8]arenes[a]

complexes	PE yield (g)	activity (g PE/mmol Nd h)	M_v (×10⁻⁴)	mp (°C)
calix[4]Nd	0.715	28.6	14.7	128.3
calix[6]Nd	0.987	39.5	93.1	135.5
calix[8]Nd₂	0.221	8.8	97.3	132.8
Nd(Oi-Pr)₃[b]	inactive	inactive	inactive	inactive

[a] Conditions: [Nd] (1.0×10^{-3} M), Al/Nd = 15, 80 °C, 0.5 h, ethylene pressure (1.2 Mpa), toluene (50 mL). [b] [Nd] = 2.0×10^{-3} M, 2 h.

to a decrease in the molecular weight of the polymers formed; however, the *cis*-1,4% remained unchanged.

6.5. Phenol Hydroxylation

The homobimetallic cerium(IV) calix[8]arene **228** (Figure 23) was found, in the presence of H_2O_2 in acetonitrile, to catalyze the hydroxylation of phenolic substrates (Scheme 44) with a high degree of regioselectivity.[183] It was shown that for substituted phenols, including salicylaldehydes, that single products were achievable in moderate yields (30−45%,

Table 35). To achieve oxidation of 1 mol of a phenolic substrate, it was found necessary to use 0.5 mmol of **228**. When **228** was present in excess, any alkyl groups present were oxidized. The same reaction with toluene or anisole yielded no hydroxylated products, indicating the need for a hydroxyl group on the substrate.

7. Main Group

7.1. Aluminum

Kuran et al. reported that the reaction of dimethoxy-calix[4]areneH₂ at a 1:1 molar ratio with AlEt₂Cl in toluene gave a monometallic aluminum structure **229** (Figure 24).[184] For the polymerization of propylene oxide (PPO) (Scheme 45 and Table 36) using fresh **229**, yields ranging between 20 and 40% were achieved giving polymers of low molecular weights (M_n = 780−4160). For polymerization of cyclo-hexene oxide (CHO), higher yields of 65−78% were achieved, again producing polymers with low molecular weights (M_n = 1150−1260). In the PPO case, the product

226
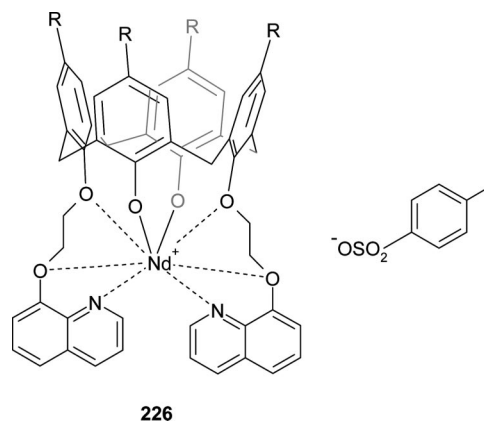
Figure 21. Cationic Nd/calix[4]arene complex **226** (R = *tert*-butyl).
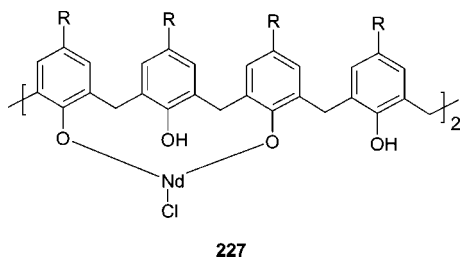
Figure 22. Neodymium calix[8]arene complex **227** (R = *tert*-butyl).

Table 34. Effect of Solvent on the Trimethylene Carbonate Polymerization Catalyzed by Calix[6]arene-neodymium[a]

solvent	dielectric constant	conversion (%)	M_v ($\times 10^{-4}$)
toluene	2.4	86.2	2.34
dichloromethane	8.9	69.7	0.90
tetrahydrofuran	7.6	47.7	0.70
acetonitrile	37.5	2.85	

[a] Conditions: [TMC]/[Nd] = 200, 80 °C, 4 h.
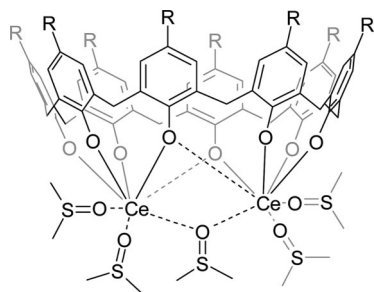
Figure 23. Cerium calix[8]arene complex **228** (R = *tert*-butyl).

Scheme 44. Hydroxylation of Phenolic Substrates with H_2O_2 (for Phenols Screened, See Table 35)
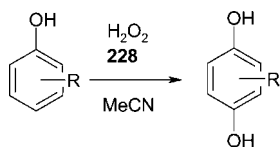
Table 35. Hydroxylation of Phenols Using 228[a]

Reactant	Product	Yield (%)
Phenol	1,4-Benzenediol	40
2,5-Dimethylphenol	2,5-Dimethyl-1,4-enzoquinone	38
2,6-Dimethylphenol	2,6-Dimethyl-1,4-benzenediol	44
Resorcinol	1,2,4-Benzenetriol	42
Hydroquinone	1,2,4-Benzenetriol	39
Toluene	No product	-
Anisole	No product	-
Salicylaldehyde	1,4-Benzenediol	28
	1,2-Benzenediol	26
	2-Hydroxy benzoic acid	20

[a] Conditions: Complex **228** (0.5 mmol), H_2O_2 (5 mL), MeCN (100 μ:), 25 °C, 4–5 h.

contained predominantly isotactic diads, whereas in the CHO screenings, neither isotactic nor syndiotactic diads were dominant.

In both cases, a narrow distribution of molecular weights for the resulting polymers was observed (PDI = 1.36–1.51), with the chlorine-containing moiety as the chain end group. Successful copolymerizations with carbon dioxide gave copolymers in low yields (26–38%) with 13–18% inclusion of carbon dioxide into the polymer chain and displaying low

Figure 24. Aluminum calix[4]arene complex **229** (R = *tert*-butyl).

Scheme 45. Polymerization of Propylene Oxide (PPO) Using 229
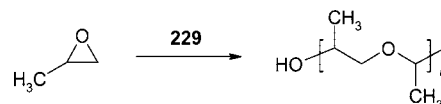
Table 36. Polymerization of Propylene Oxide (PPO) and Cyclohexene Oxide (CHO) Using 229[a]

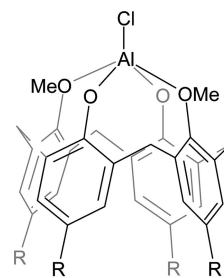| reaction conditions			oligoethers	
monomer	temperature (°C)	time (h)	yield (mol %)	M_n
PO	35	500	40	780
				690
PO	35	168	20	1960
PO	70	168	20	4160
CHO	35	264	78	1260
CHO	70	264	65	1150

[a] Conditions: PO = 100 mmol (5.8 g), CHO = 50 mmol (4.9 g), solvent = toluene; for run 1, 16 mL; for runs 2–5, 10 mL; amount of **229** = 2 mmol.

molecular weights (M_n < 6000). Further analysis of the CHO/CO_2 copolymer by alkaline hydrolysis indicated that *trans*-1,2-cyclohexanediol was in a 7-fold excess to that of *cis*-cyclohexanediol and that, for this to be the case, an inversion of configuration at the carbon atom of the cleft epoxide C–O bond must have occurred during the course of the polymerization.

8. Concluding Remarks

This review highlights the wide range of catalytic reactions to which calixarenes have been successfully employed in the past decade or so. They mainly involve carbon–carbon bond-forming reactions, including a number of well-known organic transformations, aldol type reactions, Suzuki cross-coupling, etc., as well as being utilized in the catalytic polymerization of the likes of ethylene and of styrene. In a number of these processes, it has become clear that the ability of the calixarene frame to "hold" the metal center and the substrate at a certain distance from one another is critical to the success of the catalytic process, as is the ability of the calixarene to undergo conformational change (e.g., cone, partial cone, and 1,3-alternate conformers for the calix[4]arene). Furthermore, the ability of calixarenes to simultaneously bind a number of potentially catalytic centers is leading to useful cooperatives effects, and there is potential for developing mixed-metal systems for catalysis. Indeed, the field of calixarene-based catalysis is an immensely fertile area, particularly in view of the ability to tune either their sterics or electronics (or both) of either the lower or the upper rim, combined with the availability of "pockets", which have the potential to provide subtle substrate specificities. Such

pockets/cavities are also attracting attention from those involved in metalloenzyme mimic synthesis, due to the potential to provide multiple secondary interactions. The ability to make calixarenes water-soluble has allowed for their use as catalysts in aqueous media, and the use or not of other solubilizing groups means that calixarene-based systems can be employed as either homo- or heterogeneous catalysts. The availability of inherently chiral calixarenes offers a further dimension to calixarene-based catalysis. All of this, together with their affordability and multigram accessibility, makes the use of calixarenes an extremely attractive, potentially environmentally friendly proposition for those who work in both academia and industry.

9. Abbreviations

Ac	acetate
Acac	acetylacetate
Binol	1,1′-bi-2-napthol
BSA	*N*,*O*-bis(trimethylsilyl)acetamide
C4	*p-tert*-butylcalix[4]arene
C6	*p-tert*-butylcalix[6]arene
C8	*p-tert*-butylcalix[8]arene
Cat	catalyst
β-CD	*β*-cyclodextrin
CHO	cyclohexene oxide
Cod	cyclooctadiene
Conc	concentration
DMAC	dimethylaluminum chloride
DMSC	dimethylsulfurcalix[4]arene
DMSO	dimethylsulfoxide
DNA	deoxyribonucleic acid
ee	enantiomeric excess
EPNP	ethyl-*p*-nitrophenyl phosphate
Eq	equivalent
ETA	ethyltrichloroacetate
h	hour
HMPA	hexamethylphosphoramide
HPNP	2-(hydroxypropyl)-*p*-nitrophenyl phosphate
HTPB	hexadecyltributylphosphonium bromide
i-Bu	iso-butyl
i-Pr	iso-propyl
LLDPE	linear low density polyethylene
MAO	methylaluminoxane
MDA	methyldiazoacetate
MeCN	acetonitrile
MMA	methylmethacrylate
M_n	number average molecular weight
mp	melting point
M_w	weight average molecular weight
MPa	Megapascal
n-Bu	*n*-butyl
NBD	norbornadiene
NBE	norbornene
NMR	nuclear magnetic resonance
PE	polyethylene
PDI	polydispersity index
PPM	parts per million
PPO	propylene oxide
PSt	polystyrene
RNA	ribonucleic acid
ROMP	ring opening metathesis
rpm	revolutions per minute
RT	room temperature
SHOP	shell higher olefin process
Solv	solvent
Taddol	(−)-*trans*-α,α′-(dimethyl-1,3-dioxolane-4,5-diyl)-bis(diphenylmethanol)
TBAB	tetrabutylammonium bromide
TBHP	*tert*-butylhydroperoxide
t-Bu	*tert*-butyl
TEA	triethylaluminum
Tf	triflate
THF	tetrahydrofuran
TMA	trimethylaluminum
TMC	trimethylene carbonate
TOF	turnover frequency
Tol	tolyl
TPPTS	triphenylphosphine trisulfonate
V	volume
VP	vinylpyridine

10. Acknowledgments

11. References

(1) Baeyer, A. *Ber.* **1872**, *5*, 280–282.
(2) Zinke, A; Ziegler, E. *Ber.* **1941**, *B74*, 1729–1736.
(3) Arduini, A.; Casnati, A. In *Macrocycle Synthesis*; Parker, D., Ed.; Oxford University Press: New York, 1996; Chapter 7.
(4) Gutsche, C. D. *Calixarenes*; The Royal Society of Chemistry: Cambridge, England, 1989.
(5) Lenthall, J. T.; Steed, J. W. *Coord. Chem. Rev.* **2007**, *251*, 1747–1760.
(6) (a) For−OCH₂O−, see Araki, K.; Hashimoto, N.; Shinkai, S. *J. Org. Chem.* **1993**, *58*, 5958−5963. (b) Matsumoto, H.; Nishio, S.; Takeshita, M.; Shinkai, S. *Tetrahedron* **1995**, *51*, 4647–4654. For− S−, see (c) Sone, H. T.; Ohba, Y.; Moriya, K.; Kumada, H.; Ito, K. *Tetrahedron* **1997**, *53*, 10689–10698. (d) Kumagai, H.; Hasegawa, M.; Miyanari, S.; Sugawa, Y.; Sato, Y.; Hori, T.; Ueda, S.; Kamiyama, S.; Miyano, S. *Tetrahedron Lett.* **1997**, *38*, 3971–3972. For−CH₂NRCH₂−, see (e) Shinmyozu, N.; Shibakawa, N.; Sugimoto, K.; Sakane, H.; Takemura, H.; Sako, K.; Inazu, T. *Synthesis* **1993**, 1257–1260. (f) Takemura, H.; Shinmyozu, N.; Miura, H.; Khan, I. U.; Inazu, T. *J. Inclusion Phenom.* **1994**, *19*, 193–206. (g) Hampton, P. D.; Tong, W. D.; Wu, S.; Duesler, E. N. *J. Chem. Soc., Perkin Trans 2* **1996**, 1127–1130. (h) Chirakul, P.; Hampton, P. D.; Duesler, E. N. *Tetrahedron Lett.* **1998**, *39*, 5473–5476. (i) Grannas, M. J.; Hoskins, B. F.; Robson, R. *Inorg. Chem.* **1994**, *33*, 1071–1079.
(7) Bohmer, V. *Angew. Chem. Int. Ed. Engl.* **1995**, *34*, 713–745.
(8) Ikeda, A.; Shinkai, S. *Chem. Rev.* **1997**, *97*, 1713–1734.
(9) (a) Ungaro, R.; Casnati, A.; Sansone, F.; Segura, M. *Chem. Comput. Simul. Butlerov Commun.* **2000**, *3*, 45–49. (b) Casnati, A.; Sansone, F.; Ungaro, R. *Acc. Chem. Res.* **2003**, *36*, 246–254.
(10) (a) Diamond, D.; Mc Kervey, M. A. *Chem. Soc. Rev.* **1996**, 15–24. (b) Cadogen, F.; Nolan, K.; Diamond, D. In *Calixarenes 2001*; Asfari, Z., Böhmer, V., Harrowfield, J., Vicens, J., Eds.; Kluwer Academic Publishers: Dordrecht, 2001. (c) Kim, J. S.; Quang, D. T. *Chem. Rev.* **2007**, *107*, 3780–3799. (d) Lumetta, G. J., Rogers, R. D., Gopalan, A. S., Eds. *Calixarenes for Separation*; American Chemical Society: Washington, DC, 2000. (e) Vicens, J., Harrowfield, J., Eds. *Calixarenes in the Nanoworld*; J. Springer Publishers: Dordrecht, The Netherlands, 2007. (f) Wei, A. *Chem. Commun.* **2006**, 1581–1591. (g) McMahon, G.; O'Malley, S.; Nolan, K. *Arkivoc* **2003**, *VII*, 23. (h) Ludwig, R.; Dzung, N. T. K. *Sensors* **2002**, *2*, 397–416. (i) Ishida, M.; Fujita, J.; Narihiro, M.; Ichihashi, T.; Nihey, F.; Ochiai, Y. *NEC Technol. J.* **2007**, *1*, 57. (j) Atwood, J. L.; Bridges, R. J.; Juneka, R. K.; Singh, A. K. U.S. Patent 94-178610, 5,489,612, 1996. (k) Ludwig, R. *Microchim. Acta* **2005**, *152*, 1–19. (l) Sebti, S. M.; Hamilton, A. D. *Oncogene* **2000**, *19*, 6566–6573.
(11) Matthews, S. E.; Beer, P. D. In *Calixarenes 2001*; Asfari, Z., Böhmer, V., Harrowfield, J., Vicens, J., Eds. Kluwer Academic Publishers: Dordrecht, 2001; Chapter 23.
(12) (a) Dalgarno, S. J.; Atwood, J. L.; Raston, C. L. *Chem. Commun.* **2006**, 4567–4574. (b) Coleman, A. W.; Jebors, S.; Shahgaldian, P.; Ananchenko, G. S.; Ripmeester, J. A. *Chem. Commun.* **2008**, 2291–2303.
(13) Roundhill, D. M. *Prog. Inorg. Chem.* **1995**, *43*, 533–592.
(14) Wieser, C.; Dieleman, C. B.; Matt, D. *Coord. Chem. Rev.* **1997**, *165*, 93–161.
(15) Sliwa, W. *Croat. Chem. Acta* **2002**, *75*, 131–153.
(16) Harvey, P. D. *Coord. Chem. Rev.* **2002**, *233*, 289–309.
(17) Redshaw, C. *Coord. Chem. Rev.* **2003**, *244*, 45–70.
(18) Cotton, F. A.; Daniels, L. M.; Lin, C.; Murillo, C. A. *Inorg. Chim. Acta* **2003**, *347*, 1–8.

(19) Petrella, A. J.; Raston, C. L. *J. Organomet. Chem.* **2004**, *689*, 4125–4136.

(20) (a) Steyer, S.; Jeunesse, C.; Armspach, D.; Matt, D.; Harrowfield, J. In *Calixarenes 2001*; Asfari, Z., Böhmer, V., Harrowfield, J., Vicens, J., Eds.; Kluwer Academic Publishers: Dordrecht, 2001; Chapter 28. (b) Floriani, C.; Floriani-Moro, R. *Adv. Organomet. Chem.* **2001**, *47*, 167–233.

(21) Kotzen, N.; Vigalok, A. *Supramol. Chem.* **2008**, *20*, 129–139.

(22) See, for example, (a) Arnott, G.; Heaney, H.; Hunter, R.; Page, P. C. B. *Eur. J. Org. Chem.* **2004**, 5126–5134. (b) Richeter, S.; Rebek, J., Jr *J. Am. Chem. Soc.* **2004**, *126*, 16280–16281. (c) Arnott, G.; Hunter, R.; Su, H. *Tetrahedron* **2006**, *62*, 977–991. (d) Guo, P.-F.; Zhu, W.-P.; Shen, Z.-Q. *J. Polym. Sci. A, Polym. Chem.* **2008**, *46*, 2108–2118. (e) Shenoy, S. R.; Pinacho Crisóstomo, F. R.; Iwasawa, T.; Rebek, J., Jr *J. Am. Chem. Soc.* **2008**, *130*, 5658–5659.

(23) See, for example, (a) Yu, H. H.; Xu, B.; Swager, T. M. *J. Am. Chem. Soc.* **2003**, *125*, 1142–1143. (b) Yang, Y.; Swager, T. M. *Macromolecules* **2006**, *39*, 2013–2015.

(24) (a) Floriani, C. *Chem. Eur. J.* **1999**, *5*, 19–23. (b) Floriani, C.; Floriani-Moro, R. In *Calixarenes 2001*; Asfari, Z., Böhmer, V., Harrowfield, J., Vicens, J., Eds.; Kluwer Academic Publishers: Dordrecht, 2001; Chapter 29.

(25) Shimizu, S.; Kito, K.; Sasaki, Y.; Hirai, C. *J. Chem. Soc., Chem. Commun.* **1997**, 1629–1630.

(26) Shimizu, S.; Suzuki, T.; Shirakawa, S.; Sasaki, Y.; Hirai, C. *Adv. Synth. Catal.* **2002**, *344*, 370–378.

(27) Nomura, E.; Taniguchi, H.; Kawaguchi, K.; Otsuji, Y. *Chem. Lett.* **1991**, 2167–2170.

(28) Nomura, E.; Taniguchi, H.; Kawaguchi, K.; Otsuji, Y. *J. Org. Chem.* **1993**, *58*, 4709–4715.

(29) Taniguchi, H.; Nomura, E. *Chem. Lett.* **1988**, 1773–1776.

(30) Komiyama, M.; Isaka, K.; Shinkai, S. *Chem. Lett.* **1991**, 937–940.

(31) Chawla, H. M.; Pathak, M. *Bull. Soc. Chim. Fr.* **1991**, *128*, 232–243.

(32) Nomura, E.; Taniguchi, H.; Otsuji, Y. *Bull. Chem. Soc. Jpn.* **1994**, *67*, 792–799.

(33) Nomura, E.; Taniguchi, H.; Otsuji, Y. *Bull. Chem. Soc. Jpn.* **1994**, *67*, 309–311.

(34) Gutsche, C. D.; Alam, I. *Tetrahedron* **1988**, *44*, 4689–4694.

(35) Shinkai, S.; Mori, S.; Koreishi, H.; Tsubaki, T.; Manabe, O. *J. Am. Chem. Soc.* **1986**, *108*, 2409–2416.

(36) Taniguchi, H.; Otsuji, Y.; Nomura, E. *Bull. Chem. Soc. Jpn.* **1995**, *68*, 3563–3567.

(37) Harris, S. J.; Kinahan, A. M.; Meegan, M. J.; Prendergast, R. C. *J. Chem. Res.* **1994**, 342–343.

(38) Taton, D.; Saule, M.; Logan, J.; Duran, R.; Hou, S.; Chaikof, E. L.; Gnanou, Y. *J. Polym. Sci. A, Polym. Chem.* **2003**, *41*, 1669–1676.

(39) Okada, Y.; Sugitani, Y.; Kasai, Y.; Nishimura, J. *Bull. Chem. Soc. Jpn.* **1994**, *67*, 586–588.

(40) Okada, Y.; Kasai, Y.; Ishii, F.; Nishimura, J. *J. Chem. Soc., Chem. Commun.* **1993**, 976–978.

(41) Araki, K.; Yanagi, A.; Shinkai, S. *Tetrahedron* **1993**, *49*, 6763–6772.

(42) Cacciapaglia, R.; Casnati, A.; Mandolini, L.; Ungaro, R. *J. Am. Chem. Soc.* **1992**, *114*, 10956–10958.

(43) Cacciapaglia, R.; Casnati, A.; Mandolini, L.; Ungaro, R. *J. Chem. Soc. Chem. Commun.* **1992**, 1291–1293.

(44) Cacciapaglia, R.; Mandolini, L.; Arnecke, R.; Bohmer, V.; Vogt, W. *J. Chem. Soc., Perkin Trans 2* **1998**, 419–423.

(45) Baldini, L.; Bracchini, C.; Cacciapaglia, R.; Casnati, A.; Mandolini, L.; Ungaro, R. *Chem. Eur. J.* **2000**, *6*, 1322–1330.

(46) Cacciapaglia, R.; Casnati, A.; Di Stefano, S.; Mandolini, L.; Paolemili, D.; Reinhoudt, D. N.; Sartori, A.; Ungaro, R. *Chem. Eur. J.* **2004**, *10*, 4436–4442.

(47) PengFei, G.; WeiPu, Z.; ZhiQuan, S. *Sci. China, Ser. B: Chem.* **2007**, *50*, 648–653.

(48) Bochmann, M. *J. Chem. Soc., Dalton Trans.* **1996**, 255–270.

(49) Zurek, E.; Ziegler, T. *Organometallics* **2002**, *21*, 83–92.

(50) Zanotti-Gerosa, A.; Solari, E.; Giannini, L.; Floriani, C.; Re, N.; Chiesi-Villa, A.; Rizzoli, C. *Inorg. Chim. Acta* **1998**, *270*, 298–311.

(51) Capacchione, C.; Neri, P.; Proto, A. *Inorg. Chem. Commun.* **2003**, *6*, 339–342.

(52) Giannini, L.; Caselli, A.; Solari, E.; Floriani, C.; Chiesi-Villa, A.; Rizzoli, C.; Re, N.; Sgamellotti, A. *J. Am. Chem. Soc.* **1997**, *119*, 9198–9210.

(53) Frediani, M.; Semeril, D.; Comucci, A.; Bettucci, L.; Frediani, P.; Rosi, L.; Matt, D.; Toupet, L.; Kaminsky, W. *Macromol. Chem. Phys.* **2007**, *208*, 938–945.

(54) Ozerov, O. V.; Rath, N. P.; Ladipo, F. T. *J. Organomet. Chem.* **1999**, *586*, 223–233.

(55) Li, Y.; Zheng, Y. S.; Xie, G. H. *Acta Polym. Sin.* **1998**, 101–103.

(56) Kemp, R. A.; Brown, D. S.; Lattman, M.; Li, J. *J. Mol. Catal. A: Chem.* **1999**, *149*, 125–133.

(57) Chen, Y.; Zhang, Y.; Shen, Z.; Sun, W. *Acta Polym. Sin.* **2000**, *2*, 239–241.

(58) (a) Diaz-Barrios, A.; Liscano, J.; Trujillo, M.; Agrifoglio, G.; Matos, J. O. Assignee: Intevep S.A. U.S. Patent 5,767,034, 1998. (b) Matos, J. O.; Diaz-Barrios, A.; Liscano, J.; Trujillo, M.; Agrifoglio, G. Assignee: Intevep. S.A. European Patent EP1125951, 2001.

(59) Nagy, S. Assignee: Equistar Chemicals LP. U.S. Patent 6,984,599, 2006.

(60) Grynszpan, F.; Goren, Z.; Biali, S. E. *J. Org. Chem.* **1991**, *56*, 532–536.

(61) Morohashi, N.; Hattori, T.; Yokomakura, K.; Kabuto, C.; Miyano, S. *Tetrahedron Lett.* **2002**, *43*, 7769–7772.

(62) Morohashi, N.; Yokomakura, K.; Hattori, T.; Miyano, S. *Tetrahedron Lett.* **2006**, *47*, 1157–1161.

(63) Ozerov, O. V.; Patrick, B. O.; Ladipo, F. T. *J. Am. Chem. Soc.* **2000**, *122*, 6423–6431.

(64) Ladipo, F. T.; Sarveswaran, V.; Kingston, J. V.; Huyck, R. A.; Bylikin, S. Y.; Carr, S. D.; Watts, R.; Parkin, S. *J. Organomet. Chem.* **2004**, *689*, 502–514.

(65) Evans, D. A.; Carter, P. H.; Carreira, E. M.; Prunet, J. A.; Charette, A. B.; Lautens, M. *Angew. Chem. Int. Ed.* **1998**, *37*, 2354–2359.

(66) Evans, D. A.; Ripin, D. H. B.; Halstead, D. P.; Campos, K. R. *J. Am. Chem. Soc.* **1999**, *121*, 6816–6826.

(67) Soriente, A.; De; Rosa, M.; Apicella, A.; Scettri, A.; Sodano, G. *Tetrahedron: Asymmetry* **1999**, *10*, 4481–4484.

(68) Evans, D. A.; Hu, E.; Burch, J. D.; Jaeschke, G. *J. Am. Chem. Soc.* **2002**, *124*, 5654–5655.

(69) Soriente, A.; Fruilo, M.; Gregoli, L.; Neri, P. *Tetrahedron Lett.* **2003**, *44*, 6195–6198.

(70) Soriente, A.; De; Rosa, M.; Fruilo, M.; Lepore, L.; Gaeta, C.; Neri, P. *Adv. Synth. Catal.* **2005**, *347*, 816–824.

(71) Clegg, W.; Elsegood, M. R. J.; Teat, S. J.; Redshaw, C.; Gibson, V. C. *J. Chem. Soc., Dalton Trans.* **1998**, 3037–3039.

(72) Gaeta, C.; De; Rosa, M.; Fruilo, M.; Soriente, A.; Neri, P. *Tetrahedron: Asymmetry* **2005**, *16*, 2333–2340.

(73) Notestein, J. M.; Solovyov, A.; Andrini, L. R.; Requejo, F. G.; Katz, A.; Iglesia, E. *J. Am. Chem. Soc.* **2007**, *129*, 15585–15595.

(74) Notestein, J. M.; Iglesia, E.; Katz, A. *J. Am. Chem. Soc.* **2004**, *126*, 16478–16486.

(75) Notestein, J. M.; Andrini, L. R.; Kalchenko, V. I.; Requejo, F. G.; Katz, A.; Iglesia, E. *J. Am. Chem. Soc.* **2007**, *129*, 1122–1131.

(76) (a) Katz, A.; Da Costa, P.; Lam, A. C. P.; Notestein, J. M. *Chem. Mater.* **2002**, *14*, 3363–3368. (b) For calixarene immobilization, see also Katz, A.; Iglesia, E.; Notestein, J. M. Assignee: The Reagents of the University of California, Oakland, CA. U.S. Patent 6,951,690, 2005.

(77) Massa, A.; D'Ambrosi, A.; Proto, A.; Scettri, A. *Tetrahedron Lett.* **2001**, *42*, 1995–1998.

(78) (a) Jacob, S.; Majoros, I.; Kennedy, J. P. *Macromolecules* **1996**, *29*, 8631–8641. (b) Jacob, S.; Majoros, I.; Kennedy, J. P. The University of Akron. U.S. Patent 5,844,056, 1996.

(79) Jacob, S.; Majoros, I.; Kennedy, J. P. *Polym. Bull.* **1998**, *40*, 127–134.

(80) Zhu, C. J.; Yuan, C. Y.; Lv, Y. *Synlett* **2006**, 1221–1224.

(81) Casolari, S.; Cozzi, P. G.; Orioli, P.; Tagliavini, E.; Umani Ronchi, A. *Chem. Commun.* **1997**, 2123–2124.

(82) Hoppe, E.; Limberg, C. *Chem. Eur. J.* **2007**, *13*, 7006–7016.

(83) Hoppe, E.; Limberg, C.; Ziemer, B. *Inorg. Chem.* **2006**, *45*, 8308–8317.

(84) Hoppe, E.; Limberg, C.; Ziemer, B.; Mugge, C. *J. Mol. Catal. A: Chem.* **2006**, *251*, 34–40.

(85) Limberg, C. *Eur. J. Inorg. Chem.* **2007**, 3303–3314.

(86) Redshaw, C.; Rowan, M. A.; Warford, L.; Homden, D. M.; Arbaoui, A.; Elsegood, M. R. J.; Dale, S. H.; Yamato, T.; Casas, C. P.; Matsui, S.; Matsuura, S. *Chem. Eur. J.* **2007**, *13*, 1090–1107.

(87) Redshaw, C.; Gibson, V. C.; Elsegood, M. R. J. *J. Chem. Soc., Dalton Trans.* **2001**, 767–769.

(88) Redshaw, C.; Rowan, M. A.; Homden, D. M.; Elsegood, M. R. J.; Yamato, T.; Pérez-Casas, C. *Chem. Eur. J.* **2007**, *13*, 10129–10139.

(89) Huang, C. Z.; Ahn, J.; Kwon, S.; Kim, J.; Lee, J.; Han, Y. H.; Kim, H. *Appl. Catal., A* **2004**, *258*, 173–181.

(90) Castellano, B.; Solari, E.; Floriani, C.; Re, N.; Chiesi-Villa, A.; Rizzoli, C. *Chem. Eur. J.* **1999**, *5*, 722–737.

(91) Redshaw, C.; Homden, D. H.; Hughes, D. L.; Wright, J. A.; Elsegood, M. R. J. *Dalton Trans.* In press.

(92) Giannini, L.; Guillemot, G.; Solari, E.; Floriani, C.; Re, N.; Chiesi-Villa, A.; Rizzoli, C. *J. Am. Chem. Soc.* **1999**, *121*, 2797–2807.

(93) Amato, M. E.; Ballistreri, F. P.; Pappalardo, A.; Tomaselli, G. A.; Toscano, R. M.; Williams, D. J. *Eur. J. Org. Chem.* **2005**, 3562–3570.

(94) Aleykseeva, E. A.; Rajlyan, R. V.; Gren, A. I.; Bogatsky, A. V. Poster abstract of posters at the International Symposium Molecular Design

and Synthesis of Supramolecular Architechtures. *Chem. Comput. Simul. Butlerov Commun.*, **2000**, *1* (3), Appendix C-SA, poster 28.

(95) Ueda, J.; Kamigaito, M.; Sawamoto, M. *Macromolecules* **1998**, *31*, 6762–6768.

(96) Quintard, A.; Darbost, U.; Vocanson, F.; Pellet-Rostaing, S.; Lemaire, M. *Tetrahedron: Asymmetry* **2007**, *18*, 1926–1933.

(97) van Leeuwen, P. W. N. M., Claver, C., Eds. *Rhodium Catalyzed Hydroformylation*; Kluwer Academic Publishers: Dordrect, 2000; pp 203−231.

(98) (a) Wieser-Jeunesse, C.; Matt, D.; Yaftian, M. R.; Burgard, M.; Harrowfield, J. M. *C. R. Acad. Sci. Ser. II* **1998**, 479–502. (b) Antipin, I. S.; Kazakova, E. K.; Habicher, W. D.; Konovalov, A. I. *Russ. Chem. Rev.* **1998**, *67*, 905–922. (c) Neda, I.; Kaukorat, T.; Schmutzler, R. *Main Group Chem. News* **1998**, *6*, 4–27. (d) Armspach, D.; Engeldinger, B. E.; Jeunesse, C.; Harrowfield, J.; Lejeune, M.; Matt, D. *J. Iran. Chem. Soc.* **2004**, *1*, 10–19. (e) Jeunesse, C.; Armspach, D.; Matt, D. *Chem. Commun.* **2005**, 5603–5614. (f) Tsuji, Y.; Fujihara, T. *Chem. Lett.* **2007**, *11*, 1296–1301.

(99) Parlevliet, F. J.; Kiener, C.; Fraanje, J.; Goubitz, K.; Lutz, M.; Spek, A. L.; Kamer, P. C. J.; van Leeuwen, P. W. N. M. *J. Chem. Soc., Dalton Trans.* **2000**, *7*, 1113–1122.

(100) Steyer, S.; Jeunesse, C.; Matt, D.; Welter, R.; Wesolek, M. *J. Chem. Soc., Dalton Trans.* **2002**, 4264–4274.

(101) Cobley, C. J.; Ellis, D. D.; Orpen, A. G.; Pringle, P. G. *J. Chem. Soc., Dalton Trans.* **2000**, *7*, 1109–1112.

(102) Paciello, R.; Siggel, L.; Roper, M. *Angew. Chem. Int. Ed.* **1999**, *38*, 1920–1923.

(103) (a) Kunze, C.; Selent, D.; Neda, I.; Schmutzler, R.; Spannenberg, A.; Börner, A. *Heteroat. Chem.* **2001**, *12*, 577–585. (b) Schmutzler, R.; Neda, I.; Kunze, C.; Börner, A.; Selent, D.; Borgmann, C.; Hess, D.; Wiese, K.-D. European Patent 1417212, 2002. (c) Schmutzler, R.; Neda, I.; Kunze, C.; Börner, A.; Selent, D.; Borgmann, C.; Hess, D.; Wiese, K.-D. U.S. Patent 7,009,068, 2002.

(104) Kunze, C.; Selent, D.; Neda, I.; Freytag, M.; Jones, P. G.; Schmutzler, R.; Baumann, W.; Börner, A. *Z. Anorg. Allg. Chem.* **2002**, *628*, 779–787.

(105) Bagatin, I. A.; Matt, D.; Thonnessen, H.; Jones, P. G. *Inorg. Chem.* **1999**, *38*, 1585–1591.

(106) Plourde, F.; Gilbert, K.; Gagnon, J.; Harvey, P. D. *Organometallics* **2003**, *22*, 2862–2875.

(107) Shimizu, S.; Shirakawa, S.; Sasaki, Y.; Hirai, C. *Angew. Chem., Int. Ed.* **2000**, *39*, 1256–1259.

(108) Shirakawa, S.; Shimizu, S.; Sasaki, Y. *New J. Chem.* **2001**, *25*, 777–779.

(109) Wieser, C.; Matt, D.; Fischer, J.; Harriman, A. *J. Chem. Soc., Dalton Trans.* **1997**, 2391–2402.

(110) Steyer, E.; Jeunesse, C.; Harrowfield, J.; Matt, D. *Dalton Trans.* **2005**, 1301–1309.

(111) (a) Dieleman, C.; Steyer, S.; Jeunesse, C.; Matt, D. *J. Chem. Soc., Dalton Trans.* **2001**, 2508–2517. (b) Jeunesse, C.; Dieleman, C.; Steyer, S.; Matt, D. *J. Chem. Soc., Dalton Trans.* **2001**, 881–892.

(112) Loeber, C.; Weiser, C.; Matt, D.; De; Cian, A.; Fischer, J.; Toupet, L. *Bull. Soc. Chem. Fr.* **1995**, *132*, 166–171.

(113) (a) Semeril, D.; Jeunesse, C.; Matt, D.; Toupet, L. *Angew. Chem., Int. Ed.* **2006**, *45*, 5810–5814. (b) Sémeril, D.; Matt, D.; Toupet, L. *Chem. Eur. J.* **2008**, *14*, 7144–7155.

(114) Karakhanov, E. A.; Karapetyan, L. M.; Kardasheva, Y. S.; Maksimov, A. L.; Runova, E. A.; Skorkin, V. A.; Terenina, M. V. *Macromol. Symp.* **2006**, *235*, 39–51.

(115) Karakhanov, E. A.; Kardasheva, Y. S.; Runova, E. A.; Sakharov, D. A.; Terenina, M. V. *Pet. Chem.* **2006**, *46*, 264–268.

(116) Karakhanov, E. A.; Kardasheva, Y. S.; Runova, E. A.; Sakharov, D. A.; Ternina, M. V. *Neflekhimiya* **2006**, *46*, 290–295.

(117) Csók, Z.; Szalontai, G.; Czira, G.; Kollár, L. *J. Organomet. Chem.* **1998**, *570*, 23–29.

(118) Dieleman, C. B.; Matt, D.; Neda, I.; Schmutzler, R.; Harriman, A.; Yaftian, R. *Chem. Commun.* **1999**, 1911–1912.

(119) Marson, A.; Freixa, Z.; Kamer, P. C. J.; van Leeuwen, P. W. N. M. *Eur. J. Inorg. Chem.* **2007**, 4587–4591.

(120) Seitz, J.; Maas, G. *Chem. Commun.* **2002**, 338–339.

(121) Brodsky, B. H.; Du Bois, J. *Chem. Commun.* **2006**, 4715–4717.

(122) Lejeune, M.; Semeril, D.; Jeunesse, C.; Matt, D.; Peruch, F.; Lutz, P. L.; Ricard, L. *Chem. Eur. J.* **2004**, *10*, 5354–5360.

(123) Lejeune, M.; Sémeril, D.; Jeunesse, C.; Matt, D.; Lutz, P.; Toupet, L. *Adv. Synth. Catal.* **2006**, *348*, 881–886.

(124) Lejeune, M.; Jeunesse, C.; Matt, D.; Semeril, D.; Peruch, F.; Toupet, L.; Lutz, P. J. *Macromol. Rapid Commun.* **2006**, *27*, 865–870.

(125) Semeril, D.; Lejeune, M.; Matt, D. *New J. Chem.* **2007**, *31*, 502–505.

(126) Kuhn, P.; Jeunesse, C.; Sémeril, D.; Matt, D.; Lutz, P.; Welter, R. *Eur. J. Inorg. Chem.* **2004**, 4602–4607.

(127) Kuhn, P.; Semeril, D.; Jeunesse, C.; Matt, D.; Lutz, P. J.; Louis, R.; Neuburger, M. *Dalton Trans.* **2006**, 3647–3659.

(128) Maksimov, A. L.; Buchneva, T. S.; Karakhanov, E. A. *J. Mol. Catal. A: Chem.* **2004**, *217*, 59–67.

(129) Karakhanov, E. E.; Maksimov, A. L.; Runova, E. A.; Kardasheva, Y. S.; Terenina, M. V.; Buchneva, T. S.; Guchkova, A. Y. *Macromol. Symp.* **2003**, *204*, 159–173.

(130) Maksimov, A. L.; Sakharov, D. A.; Filippova, T. Y.; Zhuchkova, A. Y.; Karakhanov, E. A. *Ind. Eng. Chem. Res.* **2005**, *44*, 8644–8653.

(131) Karakhanov, E.; Buchneva, T.; Maximov, A.; Zavertyaeva, M. *J. Mol. Catal. A: Chem.* **2002**, *184*, 11–17.

(132) Karakhanov, E. A.; Buchneva, T. S.; Maksimov, A. L.; Runova, E. A. *Pet. Chem.* **2003**, *43*, 38–45.

(133) Karakhanov, E.; Buchneva, T. S.; Maksimov, A. L.; Runova, E. A. *Neflekhimiya* **2003**, *43*, 42–48.

(134) Maksimov, A. L.; Buchneva, T. S.; Karakhanov, E. A. *Pet. Chem.* **2003**, *43*, 154–158.

(135) Maksimov, A. L.; Buchneva, T. S.; Karakhanov, E. A. *Neflekhimiya* **2003**, *3*, 173–178.

(136) Shimizu, S.; Shimada, N.; Sasaki, Y. *Green Chem.* **2006**, *8*, 608–614.

(137) Parlevliet, F. J.; Zuideveld, M. A.; Kiener, C.; Kooijman, H.; Spek, A. L.; Kamer, P. C. J.; van Leeuwen, P. W. N. M. *Organometallics* **1999**, *18*, 3394–3405.

(138) Baur, M.; Markus, M.; Schatz, J.; Schildbach, F. *Tetrahedron* **2001**, *57*, 6985–6991.

(139) Frank, M.; Maas, G.; Schatz, J. *Eur. J. Org. Chem.* **2004**, 607–613.

(140) Brendgen, T.; Maas, G.; Schatz, J. *Eur. J. Org. Chem.* **2006**, 2378–2383.

(141) Dinares, I; Garcia de Miguel, C.; Font-Bardia, M.; Solans, X.; Alcalde, E. *Organometallics* **2007**, *26*, 5125.

(142) Hapiot, F.; Lyskawa, J.; Bricout, H.; Tilloy, S.; Monflier, E. *Adv. Synth. Catal.* **2004**, *346*, 83–86.

(143) Hu, X.; Tian, Z.; Lu, X.; Chen, Y. *Chin. J. Catal.* **1997**, *18* (3), 187–188.

(144) Chen, Y.; Zhou, Y.; Zhong, Z.; Lu, X. *Wuhan Univ. J. Nat. Sci.* **1999**, *43*, 350–354.

(145) Buhl, M.; Terstegen, F.; Löffler, F.; Meynhardt, B.; Kierse, S.; Muller, M.; Nather, C.; Lüning, U. *Eur. J. Org. Chem.* **2001**, 2151–2160.

(146) Löffler, F.; Hagen, M.; Lüning, U. *Synlett* **1999**, 1826–1828.

(147) Molenveld, P.; Engbersen, J. F. J.; Kooijman, H.; Spek, A. L.; Reinhoudt, D. N. *J. Am. Chem. Soc.* **1998**, *120*, 6726–6737.

(148) Molenveld, P.; Engbersen, J. F. J.; Reinhoudt, D. N. *J. Org. Chem.* **1999**, *64*, 6337–6341.

(149) For first generation, see (a) Blanchard, S.; Rager, M.-N.; Duprat, A. F.; Reinaud, O. *New J. Chem.* **1998**, 1143–1146. (b) Blanchard, S.; Le Clainche, L.; Rager, M.-N.; Chansou, B.; Tuchagues, J.-P.; Duprat, A. F.; Le; Mest, Y.; Reinaud, O. *Angew. Chem.* **1998**, *37*, 2732–2735. (c) Le Clainche, L.; Giorgi, M.; Reinaud, O. *Inorg. Chem.* **2000**, *39*, 3436–3437. (d) Rondelez, Y.; Sénèque, O.; Rager, M.-N.; Reinaud, O. *Chem. Eur. J.* **2000**, *6*, 4218–4226. (e) Rondelez, Y.; Rager, M.-N.; Duprat, A. F.; Reinaud, O. *J. Am. Chem. Soc.* **2002**, *124*, 1334–1340. (f) Le Poul, N.; Campion, M.; Izzet, G.; Douziech, B.; Reinaud, O.; Le Mest, Y. *J. Am. Chem. Soc.* **2005**, *127*, 5280–5281. For second generation, see (g) Sénèque, O.; Reinhaud, O. *Tetrahedron* **2003**, *59*, 5563–5568. (h) Rondelez, Y.; Li, Y.; Reinhaud, O. *Tetrahedron Lett.* **2004**, *45*, 4669–4672. (i) Sénèque, O.; Campion, M.; Douziech, B.; Giorgi, M.; Le Mest, Y.; Reinaud, O. *Dalton Trans.* **2003**, 4216–4218. For third generation, see (j) Jabin, I.; Reinhaud, O. *J. Org. Chem.* **2003**, *68*, 3416–3419. (k) Zeng, X.; Hucher, N.; Reinhaud, O.; Jabin, I. *J. Org. Chem.* **2004**, *69*, 6886–6889.

(150) Sénèque, O.; Campion, M.; Douziech, B.; Giorgi, M.; Rivière, Y.; Le Mest, Y.; Reinaud, O. *Eur. J. Inorg. Chem.* **2002**, 2007–2014.

(151) Sénèque, O.; Campion, M.; Douziech, B.; Giorgi, M.; Le Mest, Y.; Reinaud, O. *Dalton Trans.* **2003**, 4216–4218.

(152) Angot, S.; Murthy, K. S.; Taton, D.; Gnanou, Y. *Macromolecules* **1998**, *31*, 7218–7225.

(153) Angot, S.; Murthy, K. S.; Taton, D.; Gnanou, Y. *Macromolecules* **2000**, *33*, 7261–7274.

(154) Ueda, J.; Kamigaito, M.; Sawamoto, M. *Macromolecules* **1998**, *31*, 6762–6768.

(155) Bukhaltsev, E.; Frish, L.; Cohen, Y.; Vigalok, A. *Org. Lett.* **2005**, *7*, 5123–5126.

(156) Molenveld, P.; Kapsabelis, S.; Engbersen, J. F. J.; Reinhoudt, D. N. *J. Am. Chem. Soc.* **1997**, *119*, 2948–2949.

(157) Molenveld, P.; Engbersen, J. F. J.; Reinhoudt, D. N. *Eur. J. Org. Chem.* **1999**, 3269–3275.

(158) Cacciapaglia, R.; Casnati, A.; Mandolini, L.; Reinhoudt, D. N.; Salvio, R.; Sartori, A.; Ungaro, R. *J. Org. Chem.* **2005**, *70*, 624–630.

(159) Cacciapaglia, R.; Casnati, A.; Mandolini, L.; Reinhoudt, D. N.; Salvio, R.; Sartori, A.; Ungaro, R. *J. Org. Chem.* **2005**, *70*, 5398–5402.

(160) Molenveld, P.; Stikvoort, W. M. G.; Kooijman, H.; Spek, A. L.; Engbersen, J. F. J.; Reinhoudt, D. N. *J. Org. Chem.* **1999**, *64*, 3896–3906.

(161) Molenveld, P.; Engbersen, J. F. J.; Reinhoudt, D. N. *Angew. Chem., Int. Ed.* **1999**, *38*, 3189–3192.

(162) (a) Sénèque, O.; Rager, M.-N.; Giorgi, M.; Reinaud, O. *J. Am. Chem. Soc.* **2000**, *122*, 6183–6189. (b) Sénèque, O.; Rondelez, Y.; Le Clainche, L.; Inisan, C.; Rager, M.-N.; Giorgi, M.; Reinaud, O. *Eur. J. Inorg. Chem.* **2001**, 2597–2604. (c) Sénèque, O.; Giorgi, M.; Reinaud, O. *Chem. Commun.* **2001**, 984–985. (d) Sénèque, O.; Rager, M.-N.; Giorgi, M.; Reinaud, O. *J. Am. Chem. Soc.* **2001**, *123*, 8442–8443. (e) Sénèque, O.; Rager, M.-N.; Giorgi, M.; Prangé, T.; Tomas, A.; Reinaud, O. *J. Am. Chem. Soc.* **2005**, *127*, 14883–14840. (f) Coquière, D.; Marrot, J.; Reinaud, O. *Chem. Commun.* **2006**, 3924–3926. (g) Colasson, B.; Save, M.; Milko, P.; Roithová, J.; Schrôder, D.; Reinaud, O. *Org. Lett.* **2007**, *9*, 4987–4990.

(163) Zheng, Y. S.; Shen, Z. Q. *Eur. Polym. J.* **1999**, *35*, 1037–1042.

(164) Zheng, Y. S.; Shen, Z. Q. *Chem. J. Chin. Univ. Chin.* **2000**, *21*, 654–656.

(165) Zheng, Y. S.; Shen, Z. Q. *Chin. Chem. Lett.* **1999**, *10*, 597–600.

(166) Chen, Y. F.; Zhang, Y. F.; Shen, Z. Q. *Chin. J. Chem.* **2003**, *21*, 216–217.

(167) Gou, P. F.; Zu, W. P.; Shen, Z. Q. *Acta Polym. Sin.* **2007**, *10*, 967–973.

(168) Zheng, Y. S.; Shen, Z. Q. *Acta Polym. Sin.* **2005**, 629–632.

(169) Nie, J.; Zhang, Y. F.; Jiang, L. M.; Shen, Z. Q. *Acta Polym. Sin.* **2002**, 203–207.

(170) Shen, Z. Q. *Chin. J. Polym. Sci.* **2005**, *23*, 593–602.

(171) Ling, J.; Shen, Z. Q.; Zhu, W. P. *J. Polym. Sci., Part A: Polym. Chem.* **2003**, *41*, 1390–1399.

(172) Zhu, W. P.; Ling, J.; Xu, H.; Shen, Z. Q. *Polymer* **2005**, *46*, 8379–8385.

(173) Ge, L.; Huang, Q.; Zhang, Y.; Shen, Z. *Eur. Polym. J.* **2000**, *36*, 2699–2705.

(174) Zheng, Y. S.; Ying, L. Q.; Shen, Z. Q. *Polymer* **2000**, *41*, 1641–1643.

(175) Shen, Z. Q.; Chen, Y. F.; Zhang, Y. F.; Kou, R. Q.; Chen, L. S. *Chem. J. Chin. Univ. Chin.* **1999**, *20*, 1982–1984.

(176) Shen, Z. Q.; Chen, Y. F.; Zhang, Y. F.; Kou, R. Q.; Chen, L. S. *Eur. Polym. J.* **2001**, *37*, 1181–1184.

(177) Zhu, W.; Gou, P.; Shen, Z. *Macromol. Symp.* **2008**, *261*, 74–84.

(178) Zhu, W. P.; Ling, J.; Xu, H.; Shen, Z. Q. *Chin. J. Polym. Sci.* **2005**, *23*, 407–410.

(179) Ge, L.; Shen, Z. Q.; Zhang, Y. F.; Huang, Q. H. *Chin. J. Polym. Sci.* **2000**, *18*, 77–80.

(180) Group 4, Changchun Inst. Appl. Chem. Chin. Acad. Sci. *Collection of Papers for Synthetic Rubber with Rare Earth Metals*; Science Press: Beijing, 1980.

(181) Ni, X. F.; Zhang, Y. F.; Shen, C. H.; Tao, J. *Chem. J. Chin. Univ. Chin.* **2001**, *35*, 132–136.

(182) Ni, X.-F.; Li, W.-S.; Zhang, Y.-F.; Shen, Z.-Q; Zhang, T.-X. *Chem. J. Chin. Univ. Chin.* **2000**, *21*, 1938–1943.

(183) Chawla, H. M.; Hooda, U.; Singh, V. *J. Chem. Soc. Chem. Commun.* **1994**, 617–618.

(184) Kuran, W.; Listos, T.; Abramczyk, M.; Dawidek, A. *J. Macromol. Sci., Part A: Pure Appl. Chem.* **1998**, *A35*, 427–437.

CR8002196